รายงานวิจัยฉบับสมบูรณ์

โครงการ การประดิษฐ์แก้วเซรามิกเฟร์โรอิเล็กทริกที่ประกอบด้วยผลึกฐานไนโอเบต

โดย ดร.พลอยไพลิน ยงศิริ

เดือนมิถุนายน ปีพุทธศักราช 2563

สัญญาเลขที่ TRG6080016

รายงานวิจัยฉบับสมบูรณ์

โครงการ การประดิษฐ์แก้วเซรามิกเฟร์โรอิเล็กทริกที่ประกอบด้วยผลึกฐานไนโอเบต

ดร.พลอยไพลิน ยงศิริ
วิทยาลัยนวัตกรรมการผลิตขั้นสูง
สถาบันเทคโนโลยีพระจอมเกล้าเจ้าคุณทหารลาดกระบัง

สนับสนุนโดยสำนักงานกองทุนสนับสนุนการวิจัยและสถาบันเทคโนโลยีพระจอมเกล้าเจ้าคุณทหารลาดกระบัง

รูปแบบ **Abstract** (บทคัดย่อ)

Project Code : **TRG6080016**

Project Title : **The fabrication of ferroelectric glass-ceramics containing niobate-based crystals**

(ชื่อโครงการ) **การประดิษฐ์แก้วเซรามิกเฟร์โรอิเล็กทริกที่ประกอบด้วยผลึกฐานไนโอเบต**

Investigator : **ดร.พลอยไพลิน ยงศิริ**
สถาบันเทคโนโลยีพระจอมเกล้าเจ้าคุณทหารลาดกระบัง

E-mail Address : **pyongsiri@gmail.com**

Project Period : **2 Years**
(ระยะเวลาโครงการ) **2 ปี**

บทคัดย่อ:

แก้วเซรามิกเฟร์โรอิเล็กทริกชนิดโปร่งใส (transparent ferroelectric glass-ceramics, TFGCs) เป็นวัสดุกลุ่มใหม่ที่คาดว่าจะนำมาทดแทนการวัสดุโปร่งใสที่มีผลึกเดี่ยว (transparent single crystal) งานวิจัยหลายชิ้นระบุว่า TFGC มีข้อดีหลายประการ เช่น ความโปร่งใสสูง มีคุณสมบัติเชิงแสงแบบไม่เป็นเส้นตรง ได้แก่ second harmonic generation ความสามารถในการจัดเรียงผลึกที่ใช้งานอยู่ให้ตอบสนองต่อแสงเพื่อควบคุมคุณสมบัติทางไฟฟ้า และสุดท้ายคือความสามารถในการขึ้นรูปแบบฟิล์ม เส้นใย หรือรูปทรงอื่นๆ และเปลี่ยนโครงสร้างจุลภาคเป็นแก้วเซรามิกที่ต้องการได้ในภายหลัง งานวิจัยนี้มุ่งเน้นที่การผลิตแก้วเซรามิกไนโอเบตโปร่งใสขององค์ประกอบโพแทสเซียมโซเดียมไนโอเบต ($K_{0.5}Na_{0.5}NbO_3$, KNN) และโพแทสเซียมโซเดียมลิเทียมไนโอเบต ($(K_{0.5}Na_{0.5})_{1-x}Li_xNbO_3$, KNLN) ในระบบแก้วซิลิกา (SiO_2) และเทลลูเลี่ยม (TeO_2) ในงานวิจัยนี้ยังศึกษาอิทธิพลของการเจือสารกลุ่มแลนทาไนด์ เช่น Er_2O_3, Yb_2O_3, Eu_2O_3 และ Ho_2O_3 ต่อคุณสมบัติไฟฟ้าเชิงแสง โดยสารแลนทาไนด์มีคุณสมบัติในการเพิ่มชั้นของโครงสร้างอิเล็กโทรนิกส์ซึ่งเพิ่มโอกาสในการกระตุ้นอิเล็กตรอนได้ง่ายขึ้น สำหรับกระบวนการทดลองได้นำกระบวนการอินคอร์ปอเรชั่น (incorporation method) มาช่วยในการควบคุมการตกผลึก KNN, KNLN ในแก้วซึ่งจะช่วยลดการเกิดองค์ประกอบแปลกปลอมอื่นๆ ที่ไม่ต้องการให้เกิดในแก้วได้ ภายหลังการทดลอง กระบวนการวิเคราะห์แก้วเซรามิกที่ได้จะแบ่งเป็น 3 ขั้นตอนด้วยกัน ได้แก่ การวิเคราะห์เชิงความร้อน การวิเคราะห์โครงสร้างและองค์ประกอบเฟส และการตรวจสอบสมบัติเชิงแสงและไฟฟ้า ตามลำดับ

คำหลัก : ไนโอเบต, แก้วเซรามิกเฟร์โรอิเล็กทริกชนิดโปร่งใส, สารแลนทาไนด์, กระบวนการอินคอร์ปอเรชั่น

Abstract

Recently, much attention has been paid on the development of transparent ferroelectric glass-ceramics (TFGCs) to replaced transparent single crystal. Many research stated that TFGCs provide many advantages as high transparency, high optical nonlinearity including second harmonic generation, ability to rearrange active crystallites so that the optical response can be controlled electrically, and lastly, ability to make films, fibers or other shapes as a glass that can be subsequently transformed into desired glass-ceramic microstructure. This research focuses on the fabrication of niobate based transparent ferroelectric glass-ceramics (TFGC) in system of $K_{0.5}Na_{0.5}NbO_3$ (KNN) and $(K_{0.5}Na_{0.5})_{1-x}Li_xNbO_3$ (KNLN) in two glass systems including silicate (SiO_2) and tellurite (TeO_2). This study also doped lanthanide element consisting Er_2O_3, Yb_2O_3, Eu_2O_3 and Ho_2O_3 to increase opto-electrical efficiency. Such element can increase the level of electronic structure enhancing the opportunity of electron excitation. The incorporation method was introduced for controlling crystallization of KNN and KNLN single phase and reduce the chance of any unwanted second phase, which frequently co-precipitates in the conventional glass-ceramic method. The characterization is divided into 3 steps 1) thermal analysis, 2) structure and phase composition and 3) optical and electrical measurement.

Keywords : Niobate, Transparent ferroelectric glass-ceramics, Lanthanide, Incorporation method

1. Introduction to the research problem and its significance

Transparent ferroelectric glass-ceramics (TFGC) is one of glass-ceramic composites. These composites combine the remarkable features of ferroelectric crystals and transparent glass matrix, offering superior ferroelectric non-linear optical (NLO) , electro-optical properties and energy storage capacibility **[1-3]** . Those interesting properties are being use in various applications such as solid state device, optical communication, pulse power technology, solar cell etc **[3-6]**.

The goal of study TFGC is the attempt to find new material that replaces the former ferroelectric ceramics in which usually found many problems such as high dielectric loss, low electrical break down strength and low transmission **[6,7]** . Even though the ferroelectric ceramics provide high dielectric constant, high dielectric loss always limits in practical use. These limitations are caused by pore phase and defect formation inside ceramic, which brought about the raise of dielectric loss and lower the dielectric constant and the electric break down strength. Moreover, the grain size and grain boundary also increase the number of scattering light cause the decrease of transmission. The fabrication of ferroelectric single crystal was introduced, and it was found that most of them showed interesting opto-electrical property. Anyway, the preparation of single crystal as Czochralski process etc is difficult and involves high costs. Hence, the idea of combining ferroelectric ceramics crystal with glass was originated to overcome those problems. The addition of ferroelectric crystals in glass matrix is expected to reduce percent of porosity, to reduce dielectric loss and increase percent of transparency. However, there are some problems which further consider before study glass-ceramics. The ferroelectric crystal phase perceived a structural mismatch with the host glass which might effect to the mechanical strength of glass-ceramics. The ferroelectric crystal phase and glass phase are hugely different due to the interfacial polarization. Thus, it is necessary to find the suitable glass for precipitate the crystal phases. Furthermore, the glass-ceramic preparation process as melting-quenching and heat treatment are counted for solves those problems.

To fabricate glass-ceramics, glass is first prepared by melting-quenching technique and then is subjected to a carefully controlled heat-treatment process in order to convert original glasses to glass with small crystal phase inside. With selecting optimize glass compositions and controlling crystal nucleation and growth processes in the glass, glass ceramics with desired properties can be achieved. The development of practical glass ceramics is relatively recent. The advantage of glass preparation like melting-quenching technique is the ability in reproduce the large number of samples.

There are several groups of ferroelectric glass-ceramics that have been extensively studied, for example $BaTiO_3$ **[8,9]**, $LiNbO_3$ **[10-12]**, $BaSrTiO_3$ **[13,14]**, $NaNbO_3$ **[15,16]** and $KNbO_3$ **[17,18]** crystal in different based glass such as silicate, telluride, borosilicate, aluminosilicate and oxyfluoride glasses. All of these ferroelectric ceramics crystal show an interesting electrical and optical property due to their perovskite structure (ABO_3 structure). The perfect ideal perovskite has full cubic symmetry in which the body center position is occupied by B atoms, the edges by A atoms and the face centers by oxygen atoms in P_{m3m} space groups **[19]**. The anisotropic structure of perovskite depends on spontaneous polarization; P_s which is resulting from build-in electrical diploes in their crystal structure, giving rise to a host of non-linear optical properties such as the electro-optic effect (change in optical index with electric filed), harmonic generation (changing frequency of light), and photorefraction (index change in respond to light) **[1]**.Thus, it is important to perform an insight study for understanding important behaviors of these ferroelectric glass-ceramics.

The ferroelectric ceramic crystals used in this study are niobate based glass-ceramics in system of $K_{0.5}Na_{0.5}NbO_3$ (KNN), $(K_{0.5}Na_{0.5})_{1-x}Li_xNbO_3$ (KNLN) and $(K_{0.5}Na_{0.5})_{1-x}Ba_xNb_{1-x}Ti_xO_3$ (KNBNT) in three glass systems including silicate (SiO_2), tellurite (TeO_2) and borosilicate. Those systems are complex perovskite structure that show interesting dielectric property. The composition of KNN was firstly introduced in 1960 by Egerton and Dillon **[20]**. According to their report, KNN ceramics were prepared by solid state sintering, which offered many attractive properties especially piezoelectricity. It has been found that the piezoelectric constant (d_{33}) and coupling factor coefficient (k_p) are about 80 pC/N and 0.35, respectively. The increase of temperature caused structural changes. At room temperature, KNN has orthorhombic structure which transforms to tetragonal structure at 200°C. When the temperature increases to over 420°C, tetragonal KNN transforms to cubic structure. In this cubic form, the electrical property of KNN becomes paraelectric which is not appropriate for further electrical applications **[21-22]**. In 1971, Jaffe et al. **[23]** found the morphotropic phase boundary (MPB) of KNN which was shown in the of 50 mol% $KNbO_3$: 50 mol% $NaNbO_3$ composition. In this MBP area, the KNN ceramic gained high piezoelectric value, however, this value is still far from that found in lead-based materials (i.e. lead zirconatetitanate or PZT). Due to the need of environmental friendly materials to replace the toxic lead-based ceramics, this KNN phase has been subjected to intensive studies as a promising lead-free material. Moreover, KNN also showed non-linear optical property. The nature of the luminescent perovskite structure in the visible range

attributed to the disorder of perovskite structure like intrinsic defects occur inside. These defects as well as structural deformations in the disorder structure generate asymmetry in the crystal. This asymmetry can promote degeneracy in the atomic orbital, which in turn induces intermediary states inside the gap region and a reduction in the gap value. Such decrease in the gap value is explained by the modification in the splitting of the atomic orbitals, which can be associated to the structural deformation and symmetry change **[24]**.

Recently, there are some research stated that rare earth-doped perovskite structure has shown photoluminescence (PL) properties combining with piezoelectric properties, which may increase the possibility for using piezoelectric materials as a multifunctional device by integrating luminescent and piezoelectric property. The rare-earth doped materials are used to perform the energy conversion process of light photons to UV or IR photons **[25,26]**. To the best of our knowledge, the variation for the crystal structure of the host materials would bring about significant influence on the crystal field around the rare earth dopant ions, and consequently affect its optical properties. Lately, some reports have revealed that rare-earth elements are able to generate the energy states inside band gap, via 3 different processes; up-conversion, down-conversion and photoluminescence. Fig. 1 shows simple diagrams which describe the different between those 3 processes.

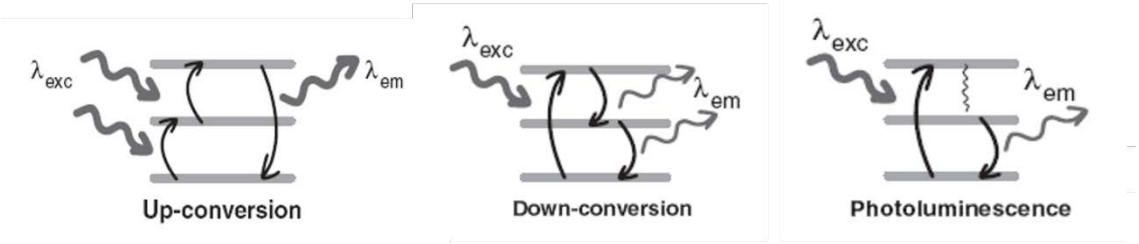

Fig. 1 Energy conversion process presented by energy level diagrams **[25]**.

These interesting materials have a special characteristic. Their triple charge ions could activated the energy level in unused range to release the visible light. The most well-known triple ions RE is erbium (Er^{3+}), europium (Eu^{3+}), terbium (Tb^{3+}) and cerium (Ce^{3+}), which can produce the intense visible light as red, green and blue colors **[26]**.

Many research also indicated that rare earth dopant also improve the ferroelectric and piezoelectric properties of the host materials, and show the multi-property coupling, such as electro-mechanical property and electro-optic property **[27-33]**. In the case of practical applications, rare earth doped piezoelectric materials are

already being used in white-emitting, temperature sensor, NIR sensor and so forth. Moreover, rare earth-doped lead-free ferroelectrics were found to exhibit conversion emissions, with the intensity that varied with the phase induced by the temperature change. As a result, the rare earth-doped ferroelectrics glass-ceramics are expected to be prominent in the next generation multifunctional devices.

Normally, it is difficult to produce single phase by using conventional glass-ceramic method **[10,34]** . To account for this, the incorporation method has been introduced. This proposing technique provides the fabrication process that reduces the second phase which usually occurred in conventional methods. In this method, the glass batch is prepared from desired single phase compound such as KNN and glass former, in which single phase as KNN and KNN with different additions are prepared from calcination method. After that, a batch was melted-quenched and then heat treated at optimized temperature. The successfully preparation of glass-ceramics with single phase was reported for many glass-ceramics systems such as KN-TeO_2 **[18,34]**, $LiNbO_3$-SiO_2 **[10]** and also in our previous work with KNN-SiO_2 **[35]**.

In this research, the fabrication of niobate based transparent ferroelectric glass-ceramics (TFGC) in system of $K_{0.5}Na_{0.5}NbO_3$ (KNN), $(K_{0.5}Na_{0.5})_{1-x}Li_xNbO_3$ (KNLN) and $(K_{0.5}Na_{0.5})_{1-x}Ba_xNb_{1-x}Ti_xO_3$ (KNBNT) in three glass systems including silicate (SiO_2), tellurite (TeO_2) and borosilicate. The incorporation method was used for preparing the glass-ceramics. The starting ferroelectric codoped with rare-earth element was firstly prepared by calcination method. These ferroelectric crystal powder were mixed with glass former. Then, melting-quenching techniques and heat treatment process were introduced to produce transparent glass-ceramic samples and engineer microstructure inside glass matrix. In this thesis, we report the physical feature, thermal behavior, electrical and optical properties of all glass-ceramic samples.

5. Literature review

Recently, much attention for lead-free ceramics has been paid to ferroelectric $(K_{0.5}Na_{0.5})NbO_3$: KNN ceramics because of their relatively high Curie temperature (T_c), strong piezoelectricity and ferroelectricity, high electromechanical coupling coefficient (K_p), especially near the equimolar composition and that it is environmentally friendly. To synthesize the solid solution of KNN, a classical solid-state reaction route was applied, starting from a powder mixture of K_2CO_3, Na_2CO_3, and Nb_2O_5, with calcination temperatures between 900°C and 950°C **[20-23,36]**.

In 1959, Egerton et al. **[20]** found that sintered KNN ceramic samples showed lower electrical properties (d_{33}=70 pC/N, k_p=25%) due to the difficulty in obtaining a high density by conventional preparation and sintering in air.

In 1962, Jaeger et al. **[22]** reported that hot pressing greatly increased the sintered density from 4.25 g/cm^3 to 4.46 g/cm^3 (about 99% of the theoretical density) and these KNN ceramics showed a high Curie temperatures ($\approx$ 420°C), a large piezoelectric responses ($d_{33}\approx$ 160 pC/N), and a high planar coupling coefficient ($k_p\approx$45%). Various techniques, such as cold-isostatic pressing, spark plasma sintering, texture ceramics and sintering aids, have been utilized to improve the electrical properties of KNN ceramics.

In 2007 Bomlai et al. **[37]** reported the effect of the calcination conditions and an excess of alkali carbonates on the phase formation and particle morphology of $(K_{0.5}Na_{0.5})NbO_3$ powders. From the study, the use of 5 mol% excess Na_2CO_3 and K_2CO_3 allowed lower calcination condition of 800°C for 2 h. XRD data showed that unreacted Nb_2O_5 disappeared from the mixture after calcination at 700°C for 2 h, which is 200°C lower than observed for the non-excess powder.

Ferroelectric glass-ceramic has been investigated and attracted much attention for ferroelectric properties since the 1970s. The relevant research works are now summarized as follows.

In 1969, Borrelli et al. **[38]** studied transparent ferroelectric glass-ceramic materials with compositions $BaTi0_3$, $Na_{0.4}K_{0.5}Nb0_3$, and $Na_{0.5}K_{0.5}Nb0_3$ and their properties as a function of crystallite size and found optical switching behavior. This glass type showed low light scattering because of the small crystallite size in order of 0.2 μm.

In 2000, Vernacotola et al. **[39]** reported that potassium niobate has been formed in potassium-niobium-silicate glasses containing $\leq$36 mol% silica. Solid solutions of $(K/Na)NbO_3$ have been obtained in heat treated sodium-potassium-niobium-silicate glasses containing 24 mol% silica. The dielectric behavior of these materials is controlled by the presence of non-ferroelectric phases and by the presence of a continuous, conductive glassy boundary phase.

In 2003, Petrovskii et al. **[40]** studied glass in the Na_2O–K_2O–Nb_2O_5–SiO_2 system with Nb_2O_5 content ranging from 5 to 39 mol %. They demonstrated that for glasses containing 15 mol% Nb_2O_5 and more, the metastable phase separation is the primary process responsible for the formation of a micro-inhomogeneous structure. With further heat treatment of these glasses, $NaNbO_3$ crystals precipitated in regions with a

high Nb_2O_5 content. In this case, each region has a heterogeneous structure and consists of $NaNbO_3$ microcrystals surrounded by layers of the high-silica matrix. This result was also reported by Zhilin et al. in 2004 [28].

In 2006, Jeong et al. **[41]** studied glass-ceramics with composition xK_2O-(14-x)Na_2O- $14Nb_2O_5$-$72TeO_2$ (x = 0-12 mol%) and found that refractive index and density of this glass-ceramics system 1.88-1.97, 4.22-4.64 g/cm^3, respectively . The measured optical energy band of the transmission cut-off wavelength, E_g (eV) = 3.17-3.14 and relative permittivity, ε_r, = 28-29.

In 2011, Kioka et al. **[42]** studied the crystallization behavior of glasses from (30-x) K_2O–xNa_2O–$25Nb_2O_5$–$45SiO_2$ (KNNS; x = 0, 5, 10, 20 and 30 mol%). The perovskite-type nonlinear optical (K, Na)NbO_3 (KNN) crystals were synthesized by using a conventional glass–ceramics method. Their research found that Na_2O amounts over around x = 10 mol% is necessary to form perovskite-type KNN crystals which showing second-harmonic generations.

The SHG microscope photograph for the powdered sample obtained by a heat-treatment at the crystallization temperature for KNNS; x = 10 glass is shown in Fig. 2, Clear SHGs were confirmed, demonstrating that (K, Na) NbO_3 crystals formed are nonlinear optical crystals. On the other hand, it was found that the KNNS; x = 0 and 5 heat-treated samples give no clear SHG, suggesting that the metastable phase formed might have a crystal structure with an inversion symmetry. X-ray diffraction (XRD) analysis in Fig. 2 also demonstrate that there are the substitution between K^+ and Na^+ ions.

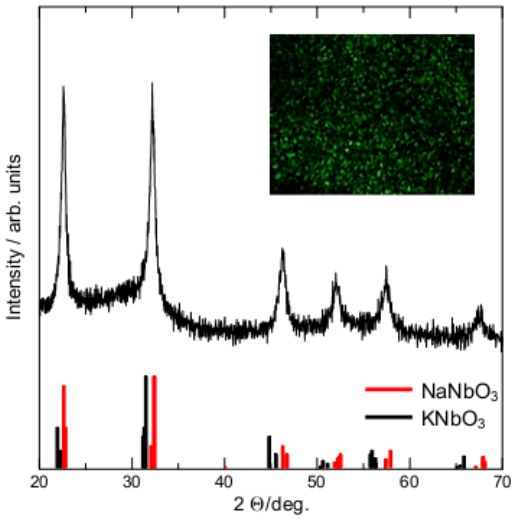

Fig. 2 XRD patterns at room temperature for the crystallized powder samples obtained by heat-treatments at 754°C for 5 h in air of KNNS; x = 10 glass. The photograph of second-harmonic generation microscope for the powdered samples is included **[42]**.

A continues-wave of Yb:YVO_4 fiber laser (wavelength: 1080 nm) was irradiated onto CuO doped KNNS; x = 10 (Cu–KNNS) surface. The absorption coefficient of this Cu–KNNS glass was determined to be α = 5.0 cm^{-1}. Perovskite-type KNN crystals were successfully patterned in the condition of the laser power of >1.20 W and the laser scanning speed of S =7 μm/s. The XRD result show in Fig. 3.

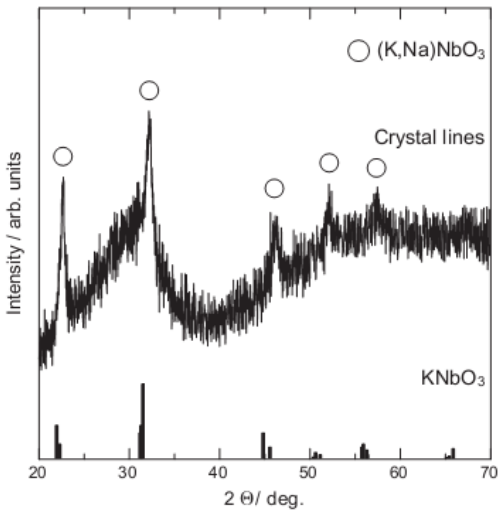

Fig. 3. XRD patterns at room temperature for the laser patterned (P = 1.20 W, S =7μm/s) crystal lines in the area of 4 mm x 4 mm in the Cu–KNNS glass **[42]**.

However, most KNN base glass researchers have found the same problem that for glass-ceramics it is difficult to maintain KNN as a single phase. Most attention has been paid to KN base glass-ceramics rather than KNN base glass-ceramics, but in 2009, Prapitpongwanich et al. **[10]** reported the successful preparation of single phase of $LiNbO_3$ in SiO_2 glass with nano-crystal $LiNbO_3$ in glass matrix by incorporation method. Dielectric constant was in the range 80 – 180 and it increased with increasing $LiNbO_3$ concentration. Then, in 2012, Yongsiri et al. **[35]** have reported the successful preparation of KNN single phase base SiO_2 glass-ceramics. The maximum room temperature dielectric constant (ε_r) was as high as 474 at 10 kHz with an acceptable low loss (tanδ) around 0.02 at 10 kHz.

In 2003, Hai lin et al. **[43]** studied the optical transition and up-conversion luminescence of Er^{3+} (1.0 wt%) doped Nb_2O_5-TeO_2 (NT) glass in order to develop optical fiber laser and amplifier. They found that the intense peak or IR fluorescence at 1.53 μm with full width at half maximum (FWHM) of 51 nm and visible up-conversion luminescence peak were observed under 975 nm and 798 nm (laser diode) excitation respectively. They also found that the up-conversion emitted light by using 2-photon

absorption. In addition, the researchers also summarized the energy level of Er^{3+} ions in NT glass as shown in Fig. 4.

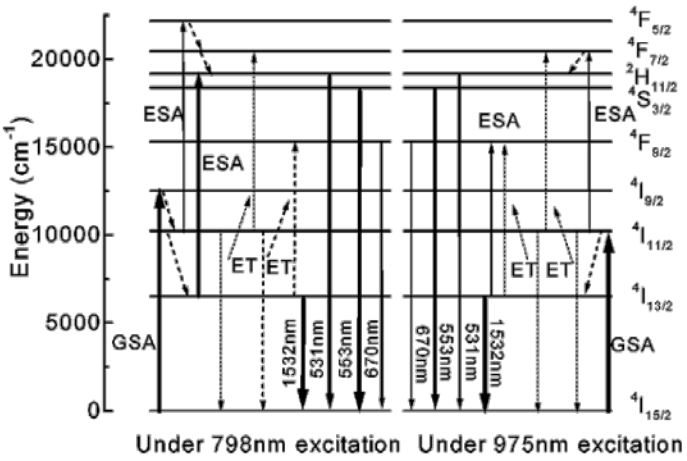

Fig. 4 Energy level of Er^{3+} ions in Nb_2O_5-TeO_2 glass after applied 975 nm and 798 nm excitation source. GSA is ground state absorption, ESA is excited state absorption and ET is energy transfer **[43]**.

Then, in 2005, Shixun Dai et al. **[44]** studied glass TeO_2-Nb_2O_5 system doped with 0.5 mol% Er_2O_3 ((100-x)TeO_2-xNb2O5, x=5-20) and summarized all data in Table 1.

Table 1 Density, refractive index, concentration of Er^{3+} inside glass, glass transition - crystallization temperature and glass stability **[44]**.

Glass composition	ρ (g/cm^3)	n_d (±0.02)	Er^{3+} concentration ($\times 10^{20}$ ion/cm^{-3})	T_g (°C)	T_x (°C)	$T_x - T_g$ (°C)
$95TeO_2$–$5Nb_2O_5$	5.290	2.04	2.01	374	466	92
$90TeO_2$–$10Nb_2O_5$	5.335	2.06	1.89	380	486	114
$85TeO_2$–$15Nb_2O_5$	5.416	2.07	1.81	405	544	139
$80TeO_2$–$20Nb_2O_5$	5.544	2.10	1.74	421	543	123
$70TeO_2$–25ZnO–$5Na_2O$	5.30	1.99	2.03	355	484	129

From their studies, the increase of Nb_2O_5 also increased density, refractive index and glass transition temperature in this glass system. It can be seen that the broad fluorescence spectrum was also found in telluride-niobic glass with higher amount of Nb_2O_5. The structural studies by XRD and Raman spectroscopy of glasses having more than 10 mol% Nb_2O_5revealed that the substitution of Nb^{5+} in niobium octahedral site [NbO_6], leads to the increase in the strength of the glass in this system. In addition, the fluorescence life time of the$^4I_{13/2}$ was decreased while the emission cross-section for Er^{3+}:$^4I_{13/2}$-$^4I_{15/2}$ was found to increase.

Recently, in 2013, Goncalo Monteiro et al. **[45]** had studied the structural of Er^{3+} in xGeO_2-(80-x)TeO_2-10Nb_2O_5-10K_2O glasses and glass-ceramics by using differential

scanning calorimeter (DSC) to optimize the heat treatment temperature. The DSC results are shown in Fig. 5. XRD data in Fig. 6 revealed that this glass system has show several crystalline phases such as α-TeO_2, δ-TeO_2, GeO_2 (α-quartz), together with$K(Nb_{1/3}Te_{2/3})_2O_{4.8}$. In addition, their work also reported the structural data from Raman spectroscopy and Fourier transform infrared (FTIR).

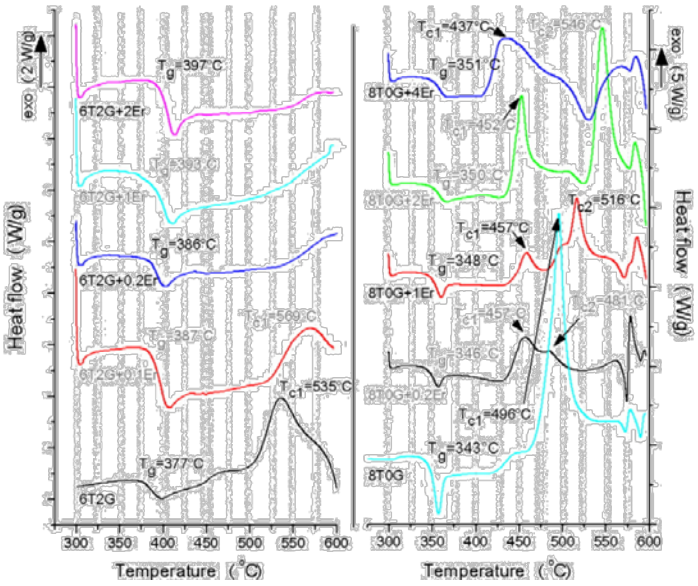

Fig. 5 Thermal profile of $60TeO_2$-$20GeO_2$-$10Nb_2O_5$-$10K_2O$ (6T2G) and $80TeO_2$-$10Nb_2O_5$-$10K_2O$ (8T0G) with different mol% of Er_2O_3. (T_g=glass transition temperature, T_{c1} and T_{c2}=crystallization temperature) **[45]**

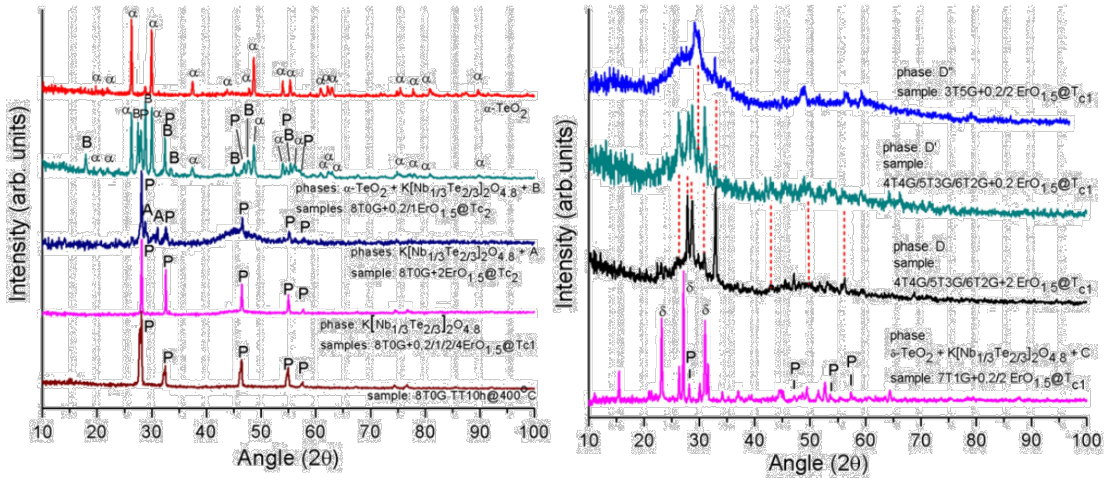

a. **b.**

Fig. 6 XRD patterns of heat treatment sample. **(a.)** glass 8T0G systems with different percent of Er_2O_3, **(b.)** glass TeO_2 systems with different composition ranging from 30 – 70 mol% TeO_2 **[45]**.

In 2004, Sheng-Yuan Chu et al. **[46]** reported the effect of poling process to photoluminescence of Er^{3+} doped $KNbO_3$ ceramics. In this work, the electric field in poling process, poling time and annealing process were controlled in order to study the relation of photoluminescence phenomenon with those mention factors. The XRD results confirmed that no erbium cluster found in this work, which mean, the poling process did not change the structure of ceramics. After poling the ceramic samples show electron transition of $^4S_{3/2}$-$^4I_{13/2}$. Moreover, this work also showed that the polarization and anneal process could modified the intensity of photoluminescence. In the other work, Cheng-Hung Wen et al. **[47-50]** had reported and discussed on the influent of Er^{3+} doped $KNbO_3$ ceramics. They found that erbium dopant has affected on sintering process **[46]**. The Er^{3+} dopants acted like sintering aid in which it is useful for $KNbO_3$ to form uniformity. However, the higher amount of Er^{3+} dopant (>2mol% Er_2O_3) could decrease the homogeneous of $KNbO_3$ form and create new phase transition **[50]**. After increasing sintering temperature, the Er^{3+} cluster that always occur in other ceramics was reduced. From SEM micrographs in Fig. 7 indicated that Er^{3+} dopant could inhibit the grain growth of $KNbO_3$ during sintering process. The optimize Er^{3+} doped $KNbO_3$ ceramics that activated the maximum intensity of photoluminescence is 1% of Er_2O_3. To improve the photoluminescence effect of $KNbO_3$ ceramics, the annealing treatment process was performed. From their report **[47]**, the intensity of luminescence was increased with increasing annealing temperature as shown in Fig. 8. This results occurrence as annealing process could reduce the imperfection in $KNbO_3$ structure, and annealing process decrease hydroxyl groups in samples.

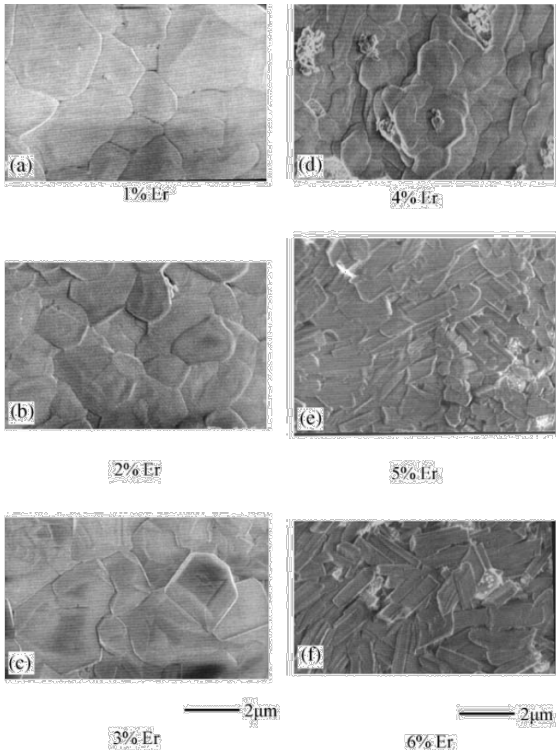

Fig.7 SEM micrograph $KNbO_3$ ceramic with different Er^{3+} percent dopants [46].

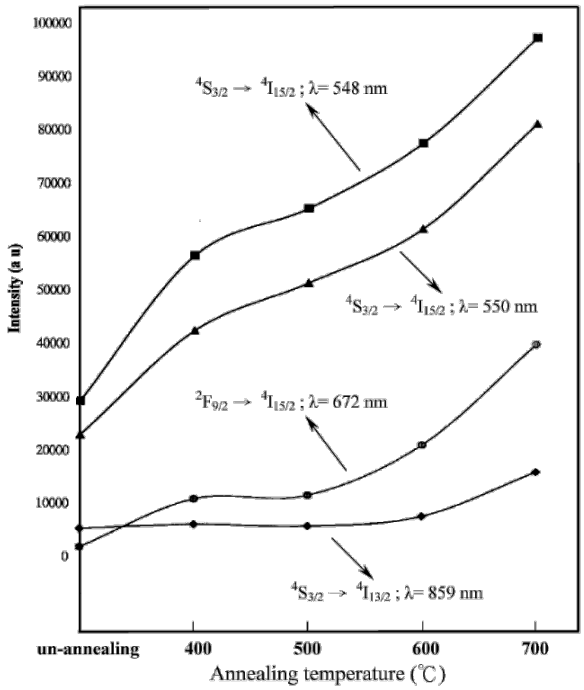

Fig. 8 The effect of annealing temperature on photoluminescence intensity [47].

2010, R. S. Chaliha et al. **[17]** had reported the effect of Er_2O_3 dopant on optical and dielectric properties of K_2O–Nb_2O_5–SiO_2 glasses by heated at 800˚C for 0 –100 h to obtain nanocrystals $KNbO_3$ in SiO_2 glass matrix. From XRD, SEM and TEM

observations in Fig. 9, it was found that the average crystalline size of $KNbO_3$ crystals were in range 7-23 nm.

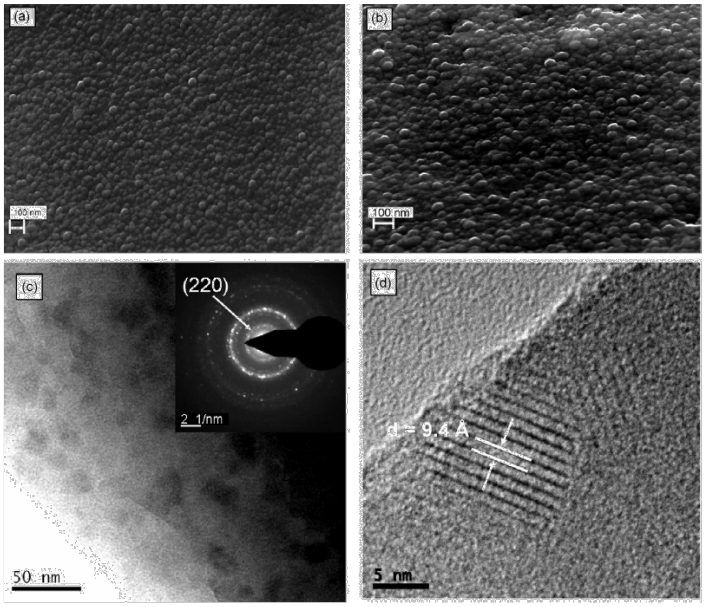

Fig. 9 FESEM and TEM image of heat-treated glasses at 800˚C. (a) and (b) FESEM observed of glass heat treated for 3h and 50 h,(c) and (d)SAED from TEM of glass heat treated for 50 h and HRTEM image of lattice fringe **[17]**.

The dielectric property measurement was found to increase with increasing heat treatment temperature (Fig. 10). The dielectric constant increase sharply (from ε =17 to ε = 31) in heat treated samples. It is indicated that heat treatment process could generate the crystallization of $KNbO_3$ in silica rich phase and the further prolong heat treatments could increase the crystal size with higher dielectric constant (at 100 h, ε = 137) and spontaneous polarization (Ps= 0.41 C/m^2).

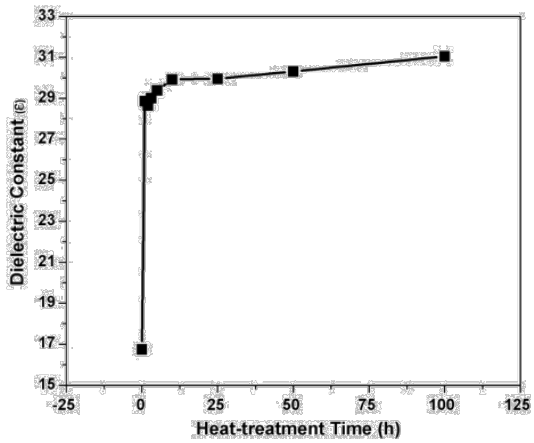

Fig. 10 Dielectric constant of as-received glass and heat treated glass **[17]**.

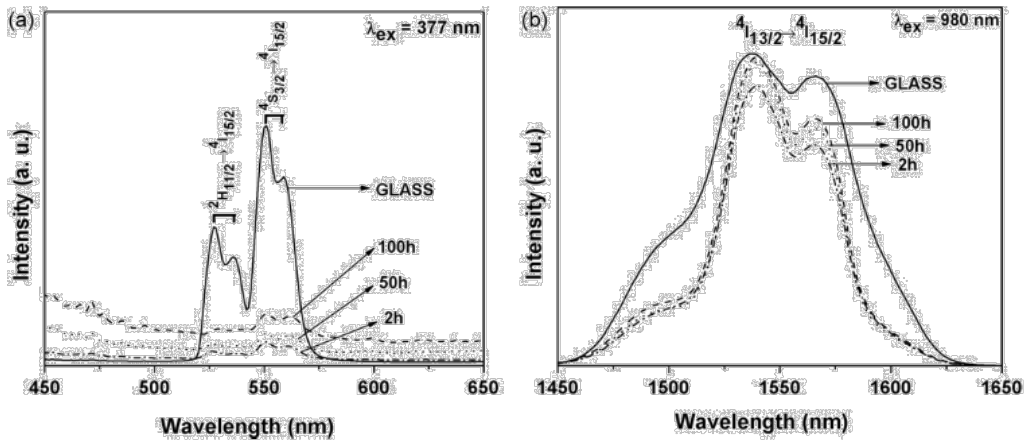

Fig. 11 Photoluminescence measurement with different excitation source (a) λ_{ex}= 377 nm and (b) λ_{ex}= 980 nm **[17]**.

In Fig. 11 (a), the obtained spectrum of the as-received glass which excited by 377 nm ($^4I_{15/2}$-$^4G_{11/2}$) showed the intense visible light emission around 500 nm. This green emission around 515-542 nm and 542-577 nm corresponded to the $^2H_{11/2}$-$^4I_{15/2}$ and $^4S_{3/2}$-$^4I_{15/2}$ transitions respectively. While in Fig. 11 (b), as-received and heat treated glasses show emission band around 1550 nm on excitation at 980 nm ($^4I_{15/2}$-$^4I_{11/2}$) which is an absorption bands of Er^{3+} ions. However, the study showed that the photoluminescence intensity gradually decreased with heat treatment time.

Then, in 2014, the up-conversion luminescence of $K_{0.5}Na_{0.5}NbO_3$ ceramics doped with Er_2O_3 via solid state sintering has been investigated by H. Sun et al. **[51]**. The composition ratio of Er_2O_3 was varied between 0 – 0.05 mol%. From XRD analysis, the lower concentration than 1mol% of Er_2O_3 dopant ceramics showed KNN single phase, after increasing Er_2O_3 concentration than 1 mol% , the second phase occurred. This indicated that the optimize Er_2O_3 contents should be less than 1 mol% Er_2O_3 due to the limit of diffusibility of this RE type. Thus, the excesses of Er^{3+} (at higher content of Er^{3+}) which would not directly diffuse in KNN structure could result in impurity phase as shown in Fig. 12.

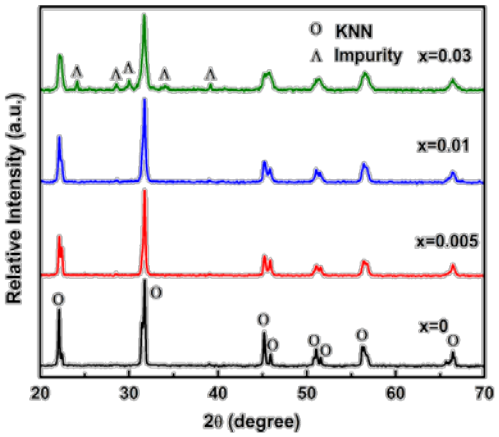

Fig. 12 The XRD results of KNN doped with various Er_2O_3 contents **[51]**.

The photoluminescence behavior of these ceramic systems after applying 980nm laser diode excitation source are shown in Fig. 13. It can be seen that the suitable Er_2O_3 concentration being able to activate the maximum intensity of up-conversion luminescence is 0.005 mol% Er_2O_3. From this figure, the luminescence consists of 2 emission band at around 510-590 nm (green light emission) and 645-695 nm (red light emission). Each emission band is associated with electron transition of 4f-4f level. In the first emission band (510-595 nm) is attributed to ($^2H_{11/2}$, $^4S_{3/2}$)-$^4I_{15/2}$ of Er^{3+} ions, while the second band (645-695 nm) is attributed to $^4F_{9/2}$-$^4I_{15/2}$, respectively. The mechanism of electronic transition in KNN ceramic doped Er_2O_3 is shown in Fig. 14.

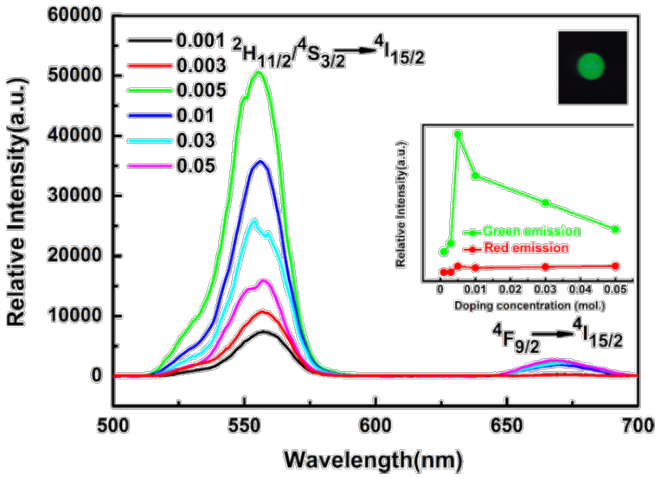

Fig. 13 The up-conversion luminescence spectra of KNN ceramics doped with various Er_2O_3 content **[51]**.

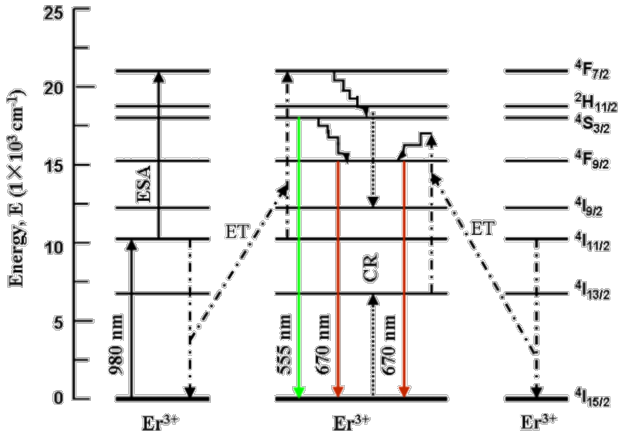

Fig. 14 Energy level of KNN ceramics doped with Er_2O_3 **[51]**.

In 2015, Xiao Wu et al. **[52]** reported the fabrication of Er^{3+}/Yb^{3+}-codoped $K_{0.5}Na_{0.5}NbO_3$ (KNN) ceramics via the solid state reaction method. Their research found that Er^{3+} ions exhibit visible up-conversion emissions as well as the near-infrared (NIR) and middle-infrared (MIR) emissions, under the excitation of 980 nm. Then, Yb^{3+} ions are added as the sensitizer to codope with Er^{3+} in the KNN host in the purpose of improving the emission efficiency and PL intensities, i.e. significantly enhancing the blue, green, red (Fig. 15) and MIR emissions of Er^{3+} (Fig. 16). The energy transfer processes between Er^{3+} and Yb^{3+} have been investigated with the relationship between the Yb^{3+} concentration and PL intensities. Due to the moderate ferroelectric and piezoelectric properties of the host, the ceramics show multifunctional performance and potential in the application of optoelectronic areas. Fig. 17 shows the P – E loops of the ceramics under an electric field of 4 kV/mm with the frequency of 100 Hz. The Er–KNN ceramic exhibits a well-saturated loop with the remanant polarizat ion (Pr) of ~12.1 mC/cm^2 and coercive electric field (Ec) of ~1 kV/mm. With increasing Yb^{3+} (x), the P– E loops become slant and flattened with Pr and Ec gradually decreasing.

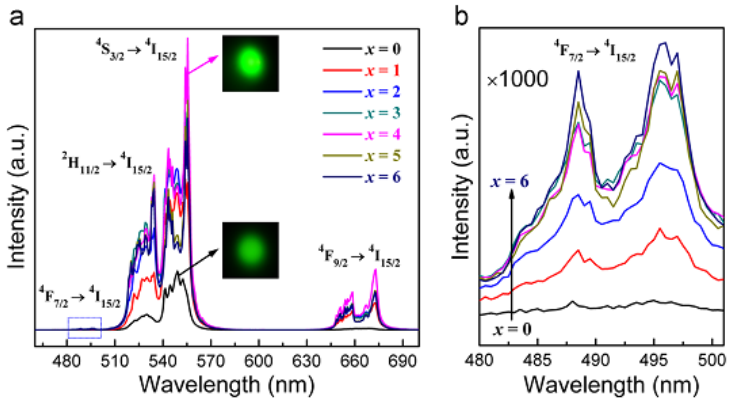

Fig. 15. (a) Vis up-conversion emissions of the Er–KNN–Yb-x ceramics under the excitation of 980 nm, (b) enlargement of the blue emissions **[52]**.

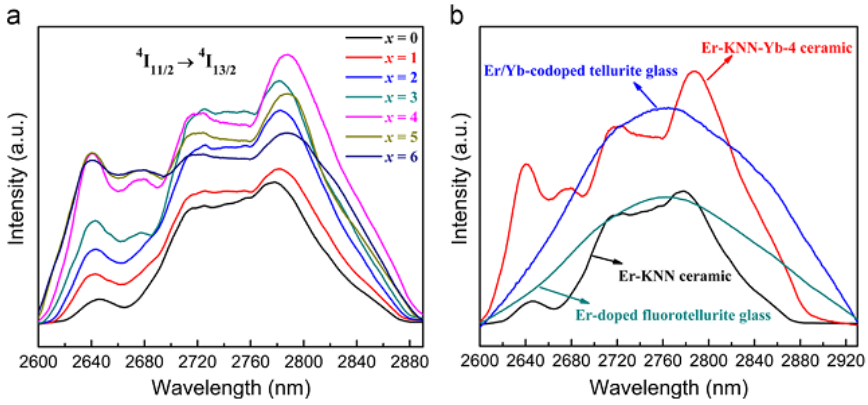

Fig. 16. (a) MIR emissions of the Er–KNN– Yb-x ceramics under the excitation of 980 nm, (b) MIR emissions of the Er –KNN ceramic, Er –KNN–Yb-4 ceramic, Er-doped fluorotellurite glass and Er/Yb-codoped tellurite glass **[52]**.

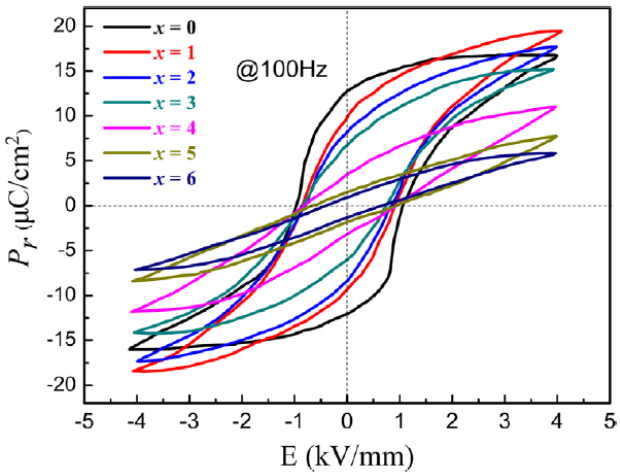

Fig. 17 P–E loops of the Er–KNN–Yb-x ceramics under an electric field of 4 kV/mm with the frequency of 100 Hz **[52]**.

Refference

1. H. Jain, "Transparent Ferroelectric Glass-Ceramics", Ferroelectrics, 306 (2004) 111–127.
2. V. Marghussian, Nano-Glass Ceramics; Processing, Properties and Applications, William Andrew publications, 1st ed., 2015, ISBN: 978-0-323-35386-1.
3. H. Zheng, Y. Pu, X. Liu, J. Wan, "Correlation between dielectric properties and crystallization treatment in potassium sodium niobate glass-ceramics for energy storage application", Journal of Alloys and Compounds 674 (2016) 272-276.
4. J. Feinberg, "Photorefractive Nonlinear Optics", Phys. Today, 41 (1988) 46-52.

5. C. R. Giuliano, “Applications of Optical Phase Conjugation”, Phys. Today, 34 (1981) 27-35.
6. W. Holand, G. H. Beall, Glass-ceramics technology, The American Ceramics Society, 2nd ed., 2002, ISBN: 978-1-118-26592-5.
7. Jiajia Huang,YongZhang,JichunChen,Anoverviewondielectric materials with high energy storage density, Mater. Rev. 23(14)(2009) 307–312.
8. T. Komatsu, H. Tawarayama, and K. Matusita, “Preparation and optical properties of transparent TeO_2-based glasses containing $BaTiO_3$ crystals: Optical materials and their applications”, J. Ceram. Soc. Jpn. 101 (1993) 48.
9. A. Narazaki, K. Tanaka, and K. Hirao, “Optical second-order nonlinearity of transparent glass-ceramics containing $BaTiO_3$ precipitated via surface crystallization”, J. Mater. Res. 14 (1999) 3640.
10. P. Prapitpongwanich, R. Harizanova, K. Pengpat, C. Rüssel, “Nanocrystallization of Ferroelectric Lithium Niobate in $LiNbO_3$-SiO_2 Glasses”, Mater. Lett., 63 (2009) 1027–1029.
11. T. Komatsu, H. Tawarayama, H. Mohri, and K. Matusita, “Properties and crystallization behaviors of TeO_2-$LiNbO_3$ glasses”, J. Non-Cryst. Solids., 135 (1991) 105.
12. M. V. Shankar, K. B. R. Varma, “Dielectric and optical properties of surface crystallized TeO_2-$LiNbO_3$ glasses”, J. Non Cryst. Solids., 243 (1999) 192-203.
13. J. Zheng, G.H. Chena, C.L. Yuan, C.R. Zhou, X. Chen, Q. Feng and M. Li, “Dielectric Characterization and Energy-Storage Performance of Lead-free Niobate Glass–ceramics Added with La_2O_3”, Ceramics International, 42 (2016) 1827–1832.
14. S. Xiu, S. Xiao, W. Zhang, S. Xue, B. Shen and J. Zhai “Effect of Rare-Earth Additions on The Structure and Dielectric Energy Storage Properties of Ba_xSr_{1-x}TiO-based Barium Boron Alumino Silicate Glass-Ceramics”, Journal of Alloys and Compounds 670 (2016) 217-221.
15. M. M. Layton and A. Herczog, “Nucleation and Crystallization of $NaNbO_3$ from Glasses in the Na_2O-Nb_2O_5-SiO_2 System”, J. Am. Ceram. Soc., 59 (1967) 369.
16. S. Pin, F. Piccinelli, K.U. Kumar, S. Enzo, P. Ghigna, C. Cannas, A. Musinu, G. Mariotto, M. Bettinelli and A. Speghini, “Structural Investigation and Luminescence of Nanocrystalline Lanthanide Doped $NaNbO_3$ and $Na_{0.5}K_{0.5}NbO_3$”, J. Solid State Chem. 196 (2012) 1–10.

17. R. S. Chaliha, K. Annapurna, A. Tarafder, P.K. Gupta, B. Karmakar, V.S. Tiwari, "Optical and Dielectric Properties of Isothermally Crystallized Nano-$KNbO_3$ in Er^{3+}-doped K_2O–Nb_2O_5–SiO_2 Glasses", Spectrochim. Acta A., 75 (2010) 243–250.
18. A. Tarafder, B. Karmakar, "Chapter 19: Nanostructured $LiTaO_3$ and $KNbO_3$ Ferroelectric Transparent Glass-Ceramics for Applications in Optoelectronics", Ferroelectrics - Material Aspects (2011) DOI: 10.5772/16455.
19. R. Whatmore, Ferroelectric Materials", Springer Handbook of Electronic and Photonic Materials, 2006, 597-623.
20. L. Egerton, D.M. Dillon, Piezoelectric and Dielectric Properties of Ceramics in The System Potassium-Sodium Niobate, J. Am. Ceram. Soc. 42 (1959) 438-442.
21. G. H. Haertling, " Properties of Hot-Pressed Ferroelectric Alkaliniobate Ceramics", J. Am. Ceram. Soc., 50 (1967) 329-330.
22. R. E. Jaeger, L. Egerton, "Hot Pressing of Potassium-Sodium Niobates", J. Am. Ceram. Soc., 45 (1962) 209-213.
23. B. Jaffe, W. R. Cook, and H. Jaffe, "Piezoelectric Ceramics", Academic Press Limited, London, 1971, ISBN: 0-12-379550-8.
24. M.F.C. Gurgel, M.L. Moreira, E.C. Paris, J.W.M. Espinosa, P.S. Pizani, J.A. Varela, E. Longo, "$BaZrO_3$ Photoluminescence Property: An ab Initio Analysis of Structural Deformation and Symmetry Changes, Int. J. Quantum Chem. 111 (2011) 694–701.
25. C. Strümpel, M. McCanna, G. Beaucarneb, V. Arkhipovb, A. Slaouic, V. Švrčekc, C. del Cañizod, I. Tobias, "Modifying The Solar Spectrum to Enhance Silicon Solar Cell Efficiency—An Overview of Available Materials", Sol. Energ. Mat. Sol. C., 91 (2007) 238-249.
26. A. J. Kenyon, " Recent Developments in Rare-Earth Doped Materials for Optoelectronics", Progress in Quantum Electronics, 26 (2002) 225–284.
27. Y. Zhao, Y. Ge, X. Yuan, Y. Zhao, H. Zhou, J. Li, H. Jin, "Effect of Phase Structure Changes on The Lead-Free Er^{3+}-Doped $(K_{0.52}Na_{0.48})_{1-x}Li_xNbO_3$ piezoelectric ceramics, Journal of Alloys and Compounds (2016), doi: 10.1016/j.jallcom.2016.04.098.
28. Y. Guo, K.-i. Kakimoto, and H. Ohsato, " Phase Transitional Behavior and Piezoelectric Properties of $(Na_{0.5}K_{0.5})NbO_3$–$LiNbO_3$ Ceramics", Appl. Phys. Lett., 85 (2004) 41214123.

29. K. Kakimoto, K. Akao, Y. P. Guo, and H. Ohsato, "Raman Scattering Study of Piezoelectric $(Na_{0.5}K_{0.5})NbO_3$–$LiNbO_3$ Ceramics", Jpn. J. Appl. Phys., 44 (2005) 7064-7067.
30. F. Tang, H. Du, Z. Li, W. Zhou, S. Qu, and Z. Pei, "Preparation and properties of $(Na_{0.5}K_{0.5})NbO_3$–$LiNbO_3$ ceramics", Trans. Nonferrous Met. SOC. China, 16, s446-s449 (2006).
31. H. Du, F. Tang, F. Luo, D. Zhu, S. Qu, Z. Pei, and W. Zhou, "Influence of sintering temperature on piezoelectric properties of $(Na_{0.5}K_{0.5})NbO_3$–$LiNbO_3$ lead-free piezoelectric ceramics", Mater. Res. Bull., 42 (2007) 1594-1601.
32. D. J. Liu, H. L. Du, F. S. Tang, F. Luo, D. M. Zhu, and W. C. Zhou, "Effect of Heating Rate on The Structure Evolution of $(Na_{0.5}K_{0.5})NbO_3$–$LiNbO_3$ Lead-Free Piezoelectric Ceramics", J. Electroceramics., 20 (2008) 107-111.
33. P. Yongsiri, S. Eitssayeam, U. Inthata, G. Rujijanagul, S. Sirisoonthorn, T. Tunkasiri, K. Pengpat, "Fabrication of Ferroelectric Glass Ceramics from $(K_{0.5}Na_{0.5})NbO_3$-SiO_2-Al_2O_3 Glass System", Ferroelectrics, 416 (2011) 144-150.
34. T. Komatsu, K. Shioya, K. Matusita, "Fabrication of Transparent Tellurite Glasses Containing Potassium Niobate Crystals by an Incorporation Method", J. Am. Ceram. Soc., 76 (1993) 2923–2926.
35. P. Yongsiri, S. Eitssayeam, G. Rujijanagul, S. Sirisoonthorn, T. Tunkasiri and K. Pengpat, "Fabrication of Transparent Lead-Free KNN Glass-ceramics by Incorporation Method", Nanoscale Res. Lett., 7 (2012) 136.
36. M. Kosec, B. Malic, A. Bencan and T. Rojac, "Piezoelectric and Acoustic Materials for Transducer Applications: KNN-Based Piezoelectric Ceramics", Springer Science+Business Media. LLC., 2008, 81-102.
37. P. Bomlai, P. Wichianrat, S. Muensit, S.J. Milne, "Effect of calcination and excess alkali carbonate on the phase formation and particle morphology of $K_{0.5}Na_{0.5}NbO_3$ powders", J. Am. Ceram. Soc., 90 (2007) 1650–1655.
38. N. F. Borrelli, M. M. Layton, "Electroopic Properties of Transparent Ferroelectric Glass-Ceramic System", Trans. Electron. Device, 6 (1969) 511-514.
39. D.E. Vernacotola, S. Chatlani, J.E. Shelby "Ferroelectric Sodium-Potassium-Niobium Silicate Glass Ceramics", proceedings of the 2000 12th IEEE international symposium on application of ferroelectrics, 2 (2000) 829.
40. G.T. Petrovskii, V.V. Golubkov, O.S. Dymshits, A.A. Zhilin and M.P. Shepilov, "Phase Separation and Crystallization in Glasses of The Na_2O–K_2O–Nb_2O_5–SiO_2 System", Glass Phys. Chem. 29 (2003) 243-253.

41. E.D. Jeong, M.G. Ha, H.K. Pak, B.K. Ryu, P.H. Borse, J.S. Lee, T. Komatsu, H.J. Kim, and H.G. Kim, Thermal Stabilities, Physical and Optical Properties of K_2O-Na_2O-Nb_2O_5-TeO_2 Glasses. J. Ind. Eng. Chem. 12 (2009) 926-931.
42. K. Kioka, T. Honma, T. Komatsu, "Fabrication of (K,Na)NbO_3 Glass–ceramics and Crystal Line Patterning on Glass Surface", Optical Materials 33 (2011) 1203–1209.
43. H. Lin, G. Meredith, S. Jiang, X. Peng, T. Luo, "Optical Transitions and Visible Upconversion in Er^{3+} Doped Niobic Tellurite Glass", J. Appl. Phys. 93 (2003) 186.
44. S. Dai, J. Wu, J. Zhang, G. Wang, Z. Jiang , "The Spectroscopic Properties of Er^{3+}-doped TeO_2–Nb_2O_5 Glasses with High Mechanical Strength Performance", Spectrochim. Acta A., 62 (2005) 431–437.
45. G. Monteiro, L. F. Santos, R. M. Almeida, F. D'Acapito, "Local Structure Around Er^{3+} in GeO_2–TeO_2–Nb_2O_5–KO_2 Glasses and Glass-ceramics", J. Non-Cryst. Solids, 377 (2013) 129–136.
46. C.-H. Wen, S.-Y. Chu, C.-K. Wen, "The Post-Annealing Effects on The Stokes Photoluminescence Spectra of Erbium-Doped $KNbO_3$ Polycrystalline", J. Cryst. Growth., 269 (2004) 479–483.
47. C.-H. Wen, S.-Y. Chu, S.-L. Tyan, Y.-D. Juang, "The Stokes Photoluminescence Spectra of Erbium-doped $KNbO_3$ Polycrystalline line", J. Cryst. Growth., 262 (2004) 225–230.
48. C.-H. Wen, S.-Y. Chu, C.-K. Wen, "The Post-Annealing Effects on The Stokes Photoluminescence Spectra of Erbium-doped $KNbO_3$ Polycrystalline", J. Cryst. Growth., 269 (2004) 479–483.
49. C.-H. Wen, S.-Y. Chu, C.-K. Wen, "Polarization Dependence of the Luminescence Properties of the Erbium Doped $KNbO_3$ Ferroelectric Ceramics", Intergr Ferroelectr., 69 (2005) 267-275.
50. C.-H. Wen, S.-Y. Chu, Y.-D. Juang, C.-K. Wen, "New Phase Transition of Erbium-doped $KNbO_3$ Polycrystalline", J. Cryst. Growth., 280 (2005) 179–184.
51. H. Sun, Q. Zhang, X. Wang, M. Gu, "Green and Red Upconversion Luminescence of Er^{3+}-doped $K_{0.5}Na_{0.5}NbO_3$ Ceramics", Ceram. Int. 40 (2014) 2581–2584.
52. Xiao Wu, Tat Hang Chung, K. W. Kwok, "Enhanced Visible and Mid-IR Emissions in Er/Yb-Codoped $K_{0.5}Na_{0.5}NbO_3$ Ferroelectric Ceramics", Ceramics International 41 (2015) 14041–14048.

2. Objectives

2.1. To develop transparent glass-ceramic containing ferroelectric crystal with rare-earth oxide.

2.2. To study the effects of processing parameters on phase formation, microstructural evolution, electrical and optical properties of the prepared glasses and glass-ceramics.

2.3. To find the optimum conditions for producing glass and glass-ceramic for opto-electrical property.

2.4. To publication in international journal with high impact factor at least 2 journals.

3. Methodology

The methodology in this project is divided into 5 steps and explained as follow;

3.1 Literature review and order for materials

Before start doing an experimental, it is necessary to carefully review all works which done recently. After that, purchase the essential materials as chemical reagent and laboratory equipment.

3.2 Preparation of glass-ceramic samples

1. $K_{0.5}Na_{0.5}NbO_3$ (KNN) doped rare-earth in different glasses based

In KNN glass-ceramics system, reagent grade starting oxide powders will be weight based on the stoichiometric formula $(1\text{-}x)\,K_{0.5}Na_{0.5}NbO_3$-xRE (RE= Er^{3+}/Yb^{3+}, Eu^{3+}, Ho^{3+}) and then calcine at optimize temperature. The well prepare (1-x)KNN-xRE powder will mix with glass former as SiO_2 and TeO_2 via ball milling technique. Next, melting-quenching technique and heat treatment process are used in order to growth (1-x)KNN-xRE inside glass matrix.

2. $(K_{0.5}Na_{0.5})_{1-x}Li_xNbO_3$ (KNLN) doped rare-earth in different glasses based

In KNLN glass-ceramics system, reagent grade starting oxide powders will be weight based on the stoichiometric formula $(1\text{-}x)\,(K_{0.5}Na_{0.5})_{1-x}Li_xNbO_3$-xRE and then calcine at optimize temperature. The well prepare (1-x)KNLN-xRE powder will mix with glass former as SiO_2 and TeO_2 via ball milling technique. Next, melting-quenching technique and heat treatment process are used in order to growth (1-x)KNLN-xRE inside glass matrix.

3.3 Characterization

Many characterization techniques of glass ceramic samples were introduced in order to investigate the glass and glass-ceramics samples, which can be divided into 4 ways;

Thermal analysis: The thermal kinetic of glass-ceramic will be study by differential thermal analysis (DTA trace)

Physical/ structural investigation: The densities of the obtained glass-ceramics will be measured using the Archimedes' method. Phase formation will be determined by the X-ray diffraction (XRD) technique, Raman spectroscopy and X-ray absorption spectroscopy. Lastly, Morphology will be observed by using field emission scanning electron microscope (FE-SEM) and transmission electron microscope (TEM). The oxidation will be determined by XANES and EXAFS, respectively.

Optical property: The transmission (%T) and absorption coefficient (α) will be measured by UV-Vis-IR spectrophotometer.

Electrical property: The dielectric constant (ε_r), dielectric loss (tan δ) and impedance were measured in a range of 10 kHz–1 MHz using a precision LCZ meter. To measure ferroelectric hysteresis curves, the Sawyer Tower circuits consisting of high voltage power amplifier were used at 1 to 100 kHz with applied voltage between 1kv to 3kv.

3.4 Data analysis and discussion / preparing for publication

All data will be analyzed with the aim of achieving a better understanding of their properties. Then, the results will be discussed and compared to the related previous work reported. After that, this research will be presented in conference and publication in international journal, for example; Material Research Bulletin (IF. 2.435) and Ceramics International (IF. 2.758).

3.5 Summary results / report for finally result

Lastly, all results will be summarized and reported to original affiliation (TRF and OHEC)

4. Scope of research

This research focuses on transparent ferroelectric glass-ceramics (TFGC) in system of $K_{0.5}Na_{0.5}NbO_3$ (KNN) and $(K_{0.5}Na_{0.5})_{1-x}Li_xNbO_3$ (KNLN) in two glass systems including silicate (SiO_2) and tellurite (TeO_2). These materials combine the remarkable features of ferroelectric crystals and transparent glass matrix, offering superior

ferroelectric non-linear optical (NLO) and electro-optical properties. The ferroelectric crystals presented in the glass-ceramics have non-centrosymmetric perovskite structure, which leads to non-linear optical properties. Moreover, the effect of lanthanide ions added perovskite structure are interested due to the possibility of increasing the photoluminescence property, which was expected for use as solar cell, pulse power technology and LED applications. To analyze transparent ferroelectric glass-ceramics, many techniques are used and divided into 3 categories. First, thermal analysis is studied by TG-DTA. Second, structure and phase composition are studied by FE-SEM, TEM, XRD, raman (or FTIR) and XANES. Finally, optical and electrical measurement are studied by UV-Vis techniques and LCR/LCZ meter.

5. Schedule for the entire project and expected outputs

First two year												
Activities	Month											
	2	4	6	8	10	12	14	16	18	20	22	24
1. Literature survey												
2. Preparation of law powders in system of ● $(1-x)K_{0.5}Na_{0.5}NbO_3$-xRE ● $(1-x)(K_{0.5}Na_{0.5})_{1-x}Li_xNbO_3$-xRE												
3. Fabrication silicate glass-ceramics from ● $(1-x)K_{0.5}Na_{0.5}NbO_3$-xRE ● $(1-x)(K_{0.5}Na_{0.5})_{1-x}Li_xNbO_3$-xRE												
4. Study the thermal property												
5. Study the physical/structural of glass-ceramics system												

Third Year												
Activities	Month											
	2	4	6	8	10	12	14	16	18	20	22	24
1. Study the physical/structural of glass-ceramics system												
2. Study the optical property of all glass-ceramics system												
3. Study the electrical property of glass-ceramics system												
4. Summary results / report finally result for TRF												

6. Results and Discussion

In this part, the discussion from the our journal publication will be exhibit. However, other results will be report in the next journal because some results will be carefully correct before publication.

6.1. Dielectric properties and Microstructural Studies of Er_2O_3 doped Potassium Sodium Niobate Silicate Glass-Ceramics

Abstract. In this work, electrical and structural properties of ferroelectric glasses and glass-ceramics from $K_{0.5}Na_{0.5}NbO_3$-SiO_2 doped with 0.5-1.0 mol%Er_2O_3 system have been investigated. The influent of Er_2O_3 dopant was also compared with the original glass. The $K_{0.5}Na_{0.5}NbO_3$ (KNN) powder was mixed with SiO_2 in composition of 75KNN-25SiO_2 and doped with Er_2O_3. Well-mixed powder was subsequently melted at 1300^{o}C for 15 min in a platinum crucible using an electric furnace. The quenched glasses were then subjected to heat treatment at various temperatures for 4 h. From the study, KNN single phase in transparent glass was successfully prepared via incorporation method. The maximum ε_r of about 360 at 10 kHz with a low tanδ of 0.07 could be obtained from the glass-ceramic sample of 75KNN–25SiO_2 doped 0.5 mol% Er_2O_3 and heat treated at 600˚C. It can be seen that the higher percent of Er_2O_3 can lower the dielectric loss of KNN glass-ceramics. This interesting value suggesting the opportunity of using them in electronic applications in the future.

Keywords: Glass-ceramics, Er_2O_3, KNN,

Introduction

Recently, perovskite materials with ABO_3 structure are subjected to intensively study due to their marvelous properties. The interesting properties are piezoelectric, pyroelectric and ferroelectric which used in widely applications such as transducer, actuator etc [1].

The ABO_3-type perovskite is another type of crystal structure which combined many important properties such as magnetic, electronic and transport property [2]. This perovskite structure shows anisotropic property due to the build-in electronic dipoles in their crystal structure that lead to magnificent non-linear optical properties such as the electro-optic effect, harmonic generation and photo-refraction. $K_{0.5}Na_{0.5}NbO_3$ (KNN) is one of a ferroelectric material which show high Curie temperature (T_c) of 420°C,

piezoelectric constant (d_{33}) of 80 pC/N, coupling factor coefficient (k_p) of 36-40% and dielectric constant (ε_r) of 290. The temperature play a significant role to KNN crystal structure when increase from room temperature to 200°C causes an orthorhombic to tetragonal phase transformation, and when the temperature is higher than 420°C, the tetragonal phase changes to a cubic phase. Furthermore, KNN is also friendly to environment [3-4]. many research works have been focused on phosphors of rare-earth (RE) ions doped perovskite structure. Rare-earth ions are used to dope perovskite-type oxide as a probe to investigate local centers and energy promoting change in optical behavior, or improve the capacitance response of these materials making possible use as high frequency ultrasonic transducer [8]. The lanthanide as Er_2O_3 is also one of most suitable active ions for several hosts. Thus, it is possible to increase the electrical property of glass-ceramics.

In this work, transparent glass-cermics 75KNN-25SiO_2 doped 0.5 and 1.0 mol%Er_2O_3 were sucessfully fabricated by incorporation technique. This technique was employ to prepare glass with a small crystal of desired phase embeded inside glass matrix. The experimental start with the calcination of oxide precursor and then mixing with glass former and rare-earth dopant as SiO_2 and Er_2O_3, respectively The crystallization of the KNN crystals in the glass was accomplished by heat treatment processes which were also used to control the KNN crystal shape and size. Here, we report the thermal, electrical and micro-structural properties of the prepared KNN glass-ceramics.

Experimental

Sample preparation : The glass of 75KNN-25SiO_2 (mol%) doped with 0.5-1.0mol% of Er_2O_3 was prepared using incorporation method. KNN powder was firstly prepared by conventional mixed oxide method according to our previous work [5,6]. For incorporation method, the prepared KNN ceramic powder was then mixed with SiO_2 to form transparent based glass. The components were mixed in a platinum crucible and subsequently melted at 1300ºC for 15 min and then quenched between stainless steel plates. The quenched glass was immediately annealed at 300ºC (in Er_2O_3 doped glass) and 450 ºC (no dopant) for 2 hours to release their stress. Thermal properties of as-received glass were measured to find the glass transition temperature (T_g) and crystallization temperature (T_c) by using DTA [Differential thermal analysis; Du Pont Instrument, USA]. Then, annealed glass was subjected to heat treatment (HT) at

temperatures ranging between 500 to 600°C, depending upon the T_g and T_c of each glass, for 4 hours.

Material characterization To analyze the glass and glass-ceramic properties, various techniques were employed. FE-SEM techniques [scanning electron microscope; JSM 6335F type, JEOL, JP] was used to investigate the composition and microstructure of the glass and glass-ceramic samples. The room temperature dielectric constant (ε_r) and dielectric loss ($\tan\delta$) of the glass-ceramics were measured in range of 10 kHz to 1 MHz using a precision LCZ meter [E4980A type, Agilent Technologies, Malaysia]. The density was measured by Archimedes method.

Results and Discussion

The DTA profile curve of KNN-SiO_2 glass and glass doped with Er_2O_3 are shown in figure 1. The DTA technique were used to understand the thermal behavior of resulting glasses which benefit for predicting the suitable temperatures for glass-ceramics samples. These DTA measurements were carried out in an air atmosphere at a heating rate of 5°C/min in the temperature range of 30°C - 800°C.

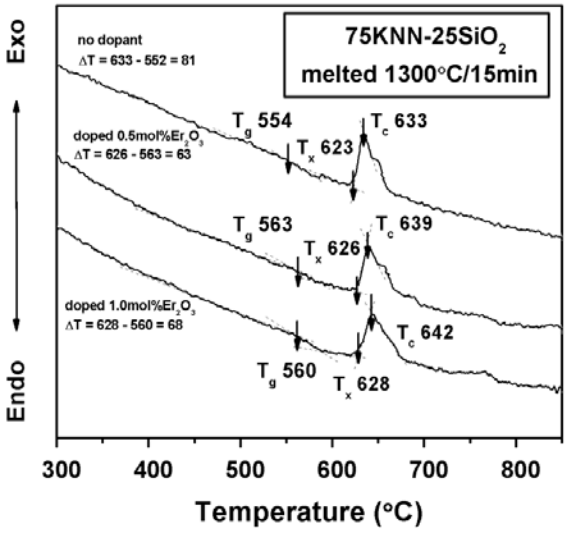

Figure 1 Thermal profile data of all glass samples by using DTA.

The intense exothermic peak of about 600°C of each composition related to crystallization temperature (T_c) of KNN crystal in glass. While, the noticeable endothermic peaks, representing by slight changes in slope of graphs as drawn by intersection point of two tangent lines at around 554°C, 563°C and 560°C, refer to the glass transition temperature (T_g) of no-dopant, 0.5mol% Er_2O_3 and 1.0mol% Er_2O_3 doped glasses, respectively. The 1.0 mol% doped 75KNN-25SiO_2 glass system has

higher T_g than those found in 0 mol% and 0.5 mol% Er_2O_3 doped 75KNN-25SiO_2 glass system. This slightly change in T_g of this glass system are the result from the entering of Er_2O_3 in KNN structure, which confirmed by our previous work [6]. The Er^{3+} ions incorporated to KNN structure lead to the distortion of crystal structure and bring about the change in glass transition temperature. This result also similarly to our previous work.

The estimation of the glass stability can be done by using Hruby's criterion [7].

$$\Delta T = T_x - T_g \quad (1)$$

where T_x is the onset point of crystallization temperature (T_c) peak. This term was used for determining the ability of glass in forming nanostructured glass-ceramics after applied energy from heat treatment process. From figure 1, the highest ΔT value was found in 75KNN-25SiO_2 without Er_2O_3 glass system. The lower ΔT value suggested that glass is easy to devitrify during melting-quenching process.

The heat treatment processes was employed at various temperatures depending on the observed thermal parameters from the DTA study in order to grow crystals inside the glass matrices. The appearances of the resulting glass-ceramics are shown in figure 2. It can be seen that glass-ceramics were all pink in color and the transparency of all glasses decreased with increasing heat treatment temperature. The density of all glass and glass-ceramic compositions are showed in figure 3. The density of the 1mol% Er_2O_3 doped glass-ceramics is slightly higher that found in the 0 and 0.5mol% Er_2O_3 doped glass-ceramics. It can be noticed that the density of the glass-ceramics increases with increasing heat treatment temperature. This may correspond to the decrease in molar volume of the glass-ceramic sample during crystallization.

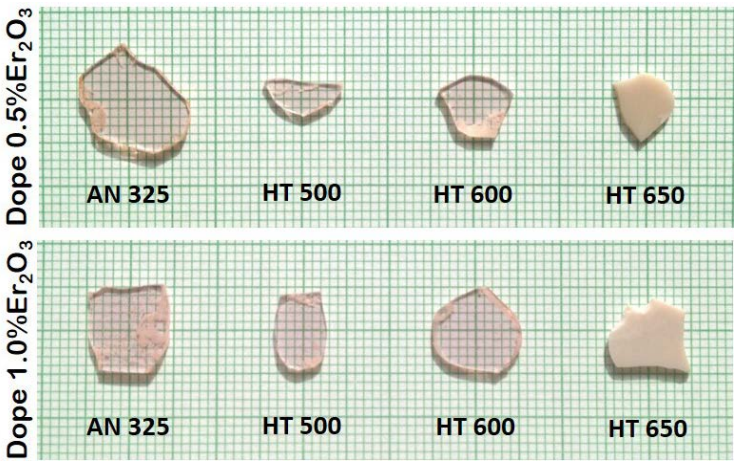

Figure 2 The appearance of glasses and glass-ceramics of 75KNN-25SiO_2 at various heat treatment temperatures. (a) doped 0.5mol% Er_2O_3, (b) doped 1.0mol% Er_2O_3

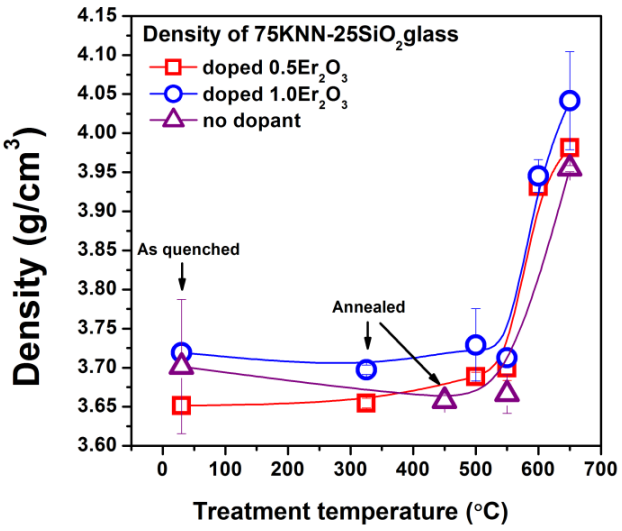

Figure 3 Glass and glass-ceramics density

SEM micrographs of the glass ceramics are shown in figure 4. These micrographs show a bulk crystallization of the KNN phase with a different shapes observed for the glass matrices of all heat-treated samples. At 550°C heat treated sample, the small spherical shape crystal of KNN solid solution was observed in 0%Er_2O_3. However, in 0.5 and 1.0mol% Er_2O_3 dopant samples found rectangular shape crystal different from 0%Er_2O_3 around 550°C. When increasing temperature to 650°C, the crystals of all systems are gradually changed to irregular shape. It can be seen that the glass-ceramics have crystallite size lower than 1 mm but larger than 200 nm, giving rise to the lower transparency in bulk glass-ceramics. To examine the element compound, EDS technique was used (figure 5). From EDS studied at bulk crystal, the embedded crystals in the glass matrix are identified as KNN solid solution. This confirm the exit of KNN crystal structure with small Erbium ions inside.

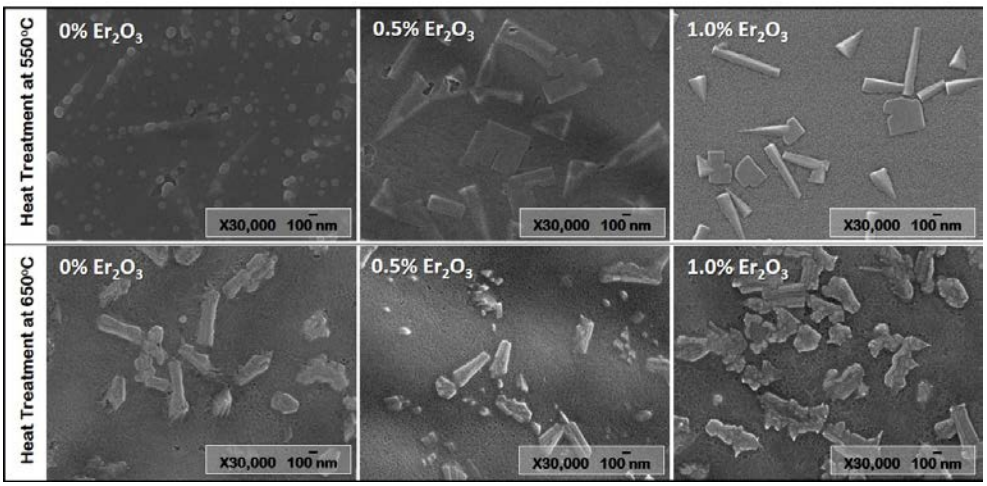

Figure 4 SEM micrograph of 75KNN-25SiO_2 doped Er_2O_3 glass-ceramics heat treated at 550 ˚C and 650 ˚C.

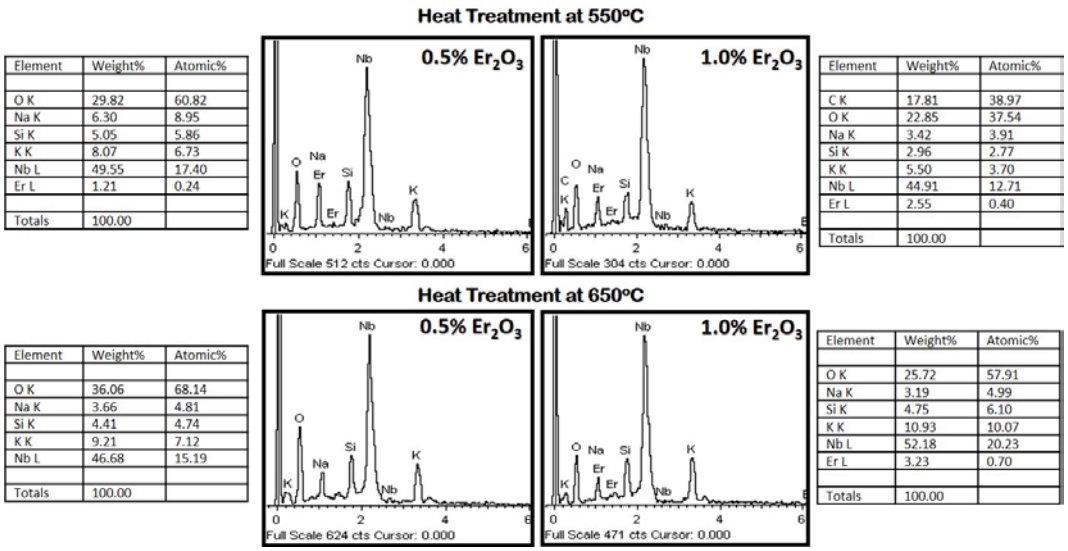

Element	Weight%	Atomic%
O K	29.82	60.82
Na K	6.30	8.95
Si K	5.05	5.86
K K	8.07	6.73
Nb L	49.55	17.40
Er L	1.21	0.24
Totals	100.00	

Element	Weight%	Atomic%
C K	17.81	38.97
O K	22.85	37.54
Na K	3.42	3.91
Si K	2.96	2.77
K K	5.50	3.70
Nb L	44.91	12.71
Er L	2.55	0.40
Totals	100.00	

Element	Weight%	Atomic%
O K	36.06	68.14
Na K	3.66	4.81
Si K	4.41	4.74
K K	9.21	7.12
Nb L	46.68	15.19
Totals	100.00	

Element	Weight%	Atomic%
O K	25.72	57.91
Na K	3.19	4.99
Si K	4.75	6.10
K K	10.93	10.07
Nb L	52.18	20.23
Er L	3.23	0.70
Totals	100.00	

Figure 5 EDS analysis of 75KNN-25SiO_2 doped Er_2O_3 glass-ceramics heat treated at 550 ˚C and 650 ˚C.

The dielectric constants (ε_r) and dielectric loss (tanδ) of heat treated glass-ceramics were measured at different freaquency from 10kHz to 1MHz and shown in figure 6. The maximum dielectric constant of about 360 at 10 kHz with rather low loss about 0.06 was found in the glass-ceramics from the glass-ceramics in composition of 75KNN-25SiO_2 doped 0.5Er_2O_3 and heat treatment at 600°C. R.S. Chaliha et al. [8] reported that glass-ceramics potassium niobate ($KNbO_3$) doped with Er^{3+} ions showed the average dielectric constant (ε_r) at about 17 which was higher than sodium silicate glasses (ε_r = 7 - 10) and borosilicate glasses (ε_r = 4.5 - 8). This might become from the ionic size of Nb^{5+} are too high. The Chaliha's report also showed that heat treatment time was

significant to dielectric constant due to the possibility to increase crystal size of $KNbO_3$. Thus, in this work, it can be seen that glass-ceramics KNN crystal doped Er^{3+} can raise the dielectric constant to nearly 90 in the as-quench glasses and can increased 350 in glass-ceramics with high heat treatment temperature. Moreover, the overall tanδ of the KNN–SiO_2 glass-ceramics is below 0.1 depending on each composition and heat treatment temperature. This may be useful in the applications in electro-optic, capacitors and microwave devices.

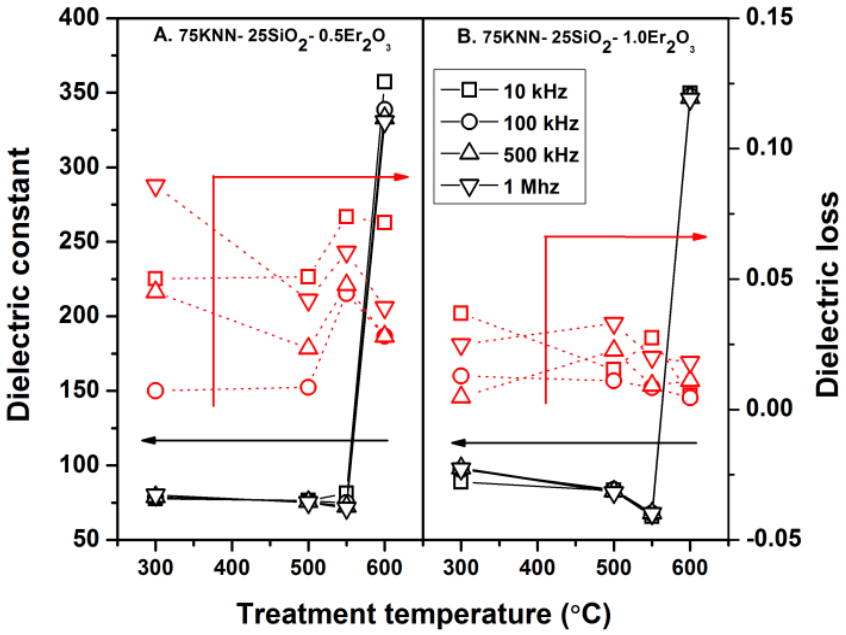

Figure 6 Dielectric constant of of 75KNN-25SiO_2 doped Er_2O_3 glass-ceramics. (A.) 0.5mol% doped Er_2O_3 and (B.) 1.0mol% doped Er_2O_3.

Conclusions

In this work, electrical and structural properties of ferroelectric glasses and glass-ceramics from $K_{0.5}Na_{0.5}NbO_3$-SiO_2 doped with 0.5-1.0 mol%Er_2O_3 system have been investigated. The influent of Er_2O_3 dopant was also compared with the original glass. From the study, KNN single phase in transparent glass was successfully prepared via incorporation method. It was indicated that heat treatment temperature plays a significant role in controlling the microstructure, crystallite sizes, and crystal quantity of the glass ceramics. The addition of Er_2O_3 can increase the dielectric constant of KNN glass-ceramic, which higher than those found in previous work. The maximum ε_r of about 360 at 10 kHz with a low tanδ of 0.07 could be obtained from the glass-ceramic sample of 75KNN–25SiO_2 doped 0.5 mol% Er_2O_3 and heat treated at 600˚C. From this

work, the higher percent of Er_2O_3 of about $1.0Er_2O_3$ can lower the dielectric loss of KNN glass-ceramics. This interesting value suggesting the opportunity of using them in electronic applications in the future. However, it is necessary to further study in effect of Er_2O_3 to KNN structure and optical property of this glass-ceramics system.

Acknowledgment

The authors would like to express their sincere gratitude to the Thailand Research Fund (TRF), Faculty of Science, Chiang Mai University for financial support. We wish to thank the Graduate School Chiang Mai University and The National Research University Project under Thailand's Office of the Higher Education Commission for financial support.

References

[1] G. H. Haerting, Ferroelectric Ceramics: History and Technology, J. Am. Ceram. Soc., 82 (1999) 797-818.

[2] B. Jaffe, W. R. Cook, H. Jaffe, Piezoelectric Ceramics, Academic Press Limited, London, 1971, ISBN: 0-12-379550-8.

[3] G. H. Haertling, Properties of Hot-Pressed Ferroelectric Alkaliniobate Ceramics, J. Am. Ceram. Soc., 50 (1967) 329-330.

[4] L. Egerton, D.M. Dillon, Piezoelectric and Dielectric Properties of Ceramics in The System Potassium-Sodium Niobate, J. Am. Ceram. Soc. 42 (1959) 438-442.

[5] P. Yongsiri, S. Eitssayeam, G. Rujijanagul, S. Sirisoonthorn, T. Tunkasiri, K. Pengpat, Fabrication of Transparent Lead-Free KNN Glass-ceramics by Incorporation Method, Nanoscale Res. Lett., 7 (2012) 136.

[6] P. Yongsiri, S. Sirisoonthorn, and K. Pengpat, Effect of Er_2O_3 Dopant on Electrical and Optical Properties of Potassium Sodium Niobate Silicate Glass-Ceramics, Mater. Res. Bull. 69 (2015) 84–91.

[7] A. Hruby, Evaluation of glass-forming tendency by means of DTA, Czech. J. Phys. B22 (1972) 1187.

[8] R. S. Chaliha, K. Annapurna, A. Tarafder, P.K. Gupta, B. Karmakar, V.S. Tiwari, Optical and dielectric properties of isothermally crystallized nano-$KNbO_3$ in Er^{3+}-doped K_2O–Nb_2O_5–SiO_2 glasses, Spectrochim. Acta A., 75 (2010) 243–250.

6.2. The electrical properties of Er_2O_3 doped potassium sodium lithium niobate based glass-ceramics

Abstract

In this work, the electrical properties of transparent ferroelectric glass-ceramics in the system of $((K_{0.5}Na_{0.5})_{0.994}Li_{0.006})_{1-x}Er_xNbO_3 - SiO_2$ system have been investigated. The lanthanide dopant as Er_2O_3 was found to promote the electrical property and optical property in many materials. The influent of Er_2O_3 dopant was also compared with the original glass. The $((K_{0.5}Na_{0.5})_{0.994}Li_{0.006})_{1-x}Er_xNbO_3$ (KNLNEr) powder, which x=0, 0.005 and 0.01 were mixed with SiO_2 in composition of 75KNLNEr-25SiO_2. Well-mixed powder was subsequently melted at 1300^oC for 15 min in a platinum crucible using an electric furnace. The quenched glasses were then subjected to heat treatment at various temperatures for 4 h depend on thermal profile from DTA. XRD results showed that the prepared glass ceramics contained crystals of KNLN solid solution and the crystallite size also increased when increasing heat treatment temperature which resulting in the reduction of transparency in the glass-ceramics. In contrary, dielectric constant (ε_r) and dielectric loss ($\tan\delta$) were found to increase with increasing heat treatment temperature. Moreover, it was found that temperature and frequency have significantly influenced on dielectric properties of the KNLNEr glass-ceramics.

Keywords : Ferroelectric glass-ceramics; complex perovskite; Er_2O_3; KNLNEr

I. Introduction

Recently, perovskite materials with ABO_3 structure are subjected to intensively study due to their marvelous properties. The interesting properties are piezoelectric, pyroelectric and ferroelectric which used in widely applications such as transducer, actuator etc [1]. The ABO_3-type perovskite crystals also showed unusual combination of their magnetic, electronic and transport properties [2].

Among the studied lead-free piezoceramics, only sodium, potassium and lithium niobate based materials $(K_{0.5-x/2}\ Na_{0.5-x/2}Li_x)NbO_3$—KNLN were considered proper candidates to substitute PZT [3-5]. In compositions next to the morphotropic phase boundary, NKLN systems present a d_{33} coefficient higher than 230 pC/N and a kp value of 0.42 [3], which were the best piezoelectric properties reported for a normal sintered lead-free piezoceramic [5]. Furthermore, the greatest advance was achieved via the texturization of these ceramics through a Reactive Templated Grain Growth process (RTGG),

wherein a promising material with properties similar to PZT4 was obtained (d_{33} = 416 pC/N and kp =0.61) [5]

In this work, $((K_{0.5}Na_{0.5})_{0.994}Li_{0.006})_{1-x}Er_xNbO_3$ – SiO_2 (KNLNEr-SiO_2) glass-ceramics which x=0, 0.005 and 0.01 were prepared by using incorporation method. The experimental start from a simple mixed-oxide technique for prepared KNLN and KNLNEr single phase powder before mixing with the glass former oxide of SiO_2 in coposition of 75KNLN-25SiO_2 and 75KNLNEr-25SiO_2. The crystallization of the KNN crystals in the glass was accomplished by heat treatment processes which were also used to control the KNN crystal shape and size. Here, we report the thermal, electrical and optical properties of the prepared glass-ceramics.

II. Experimental

Sample preparation : The glass of 75KNLN-25SiO_2 and 75KNLNEr-25SiO_2 was prepared using incorporation method. KNLN and KNLNEr powder was firstly prepared by conventional mixed oxide method according to our previous work [6]. For incorporation method, the prepared KNLN and KNLNEr ceramic powder were then mixed with SiO_2 in order to form transparent based glass. The components were mixed in a platinum crucible and subsequently melted at 1300ºC for 15 min and then quenched between stainless steel plates. The quenched glass was immediately annealed at 450ºC for 2 hours to release their stress. Thermal properties of as-received glass were measured to find the glass transition temperature (T_g) and crystallization temperature (T_c) by using DTA [Differential thermal analysis; Du Pont Instrument, USA]. Then, annealed glass was subjected to heat treatment (HT) at temperatures ranging between 500 to 600^{o}C, depending upon the T_g and T_c of each glass, for 4 hours.

Material characterization To analyze the glass and glass-ceramic properties, various techniques were employed. FE-SEM techniques [scanning electron microscope; JSM 6335F type, JEOL, JP] was used to investigate the composition and microstructure of the glass and glass-ceramic samples. The room temperature dielectric constant (ε_r) and dielectric loss ($\tan\delta$) of the glass-ceramics were measured in range of 10 kHz to 1 MHz using a precision LCZ meter [E4980A type, Agilent Technologies, Malaysia]. The transmission was measured by a UV–vis–NIR spectrophotometer (Varian Cary 50, USA; l = 190–1100 nm)

III. Results and Discussion

Phase composition of calcined powder

XRD patterns of KNLN and KNLNEr powder after calcination method at 900˚C for 5 hours are shown in figure 1. It can be seen that all of composition show ABO_3 perovskite structure with small trace of $K_3Li_2Nb_5O_{15}$ secondary phase (ICDD 52-0157). From this figure, the diffraction peaks of KNLN refer to orthorhombic structure mixed with tetragonal structure as reported in previous work [7-9]. The typical morphotropic phase boundary (MPB) of KNLN is found in the Li = 0.06 sample. The higher content of Li also suppressed the orthorhombic phase. Thus, the KNLN powder with Li = 0.006 are used as base composition in this work. In KNLNEr powder, the percent of Er_2O_3 are 0.005 and 0.01 mol% and represent by KNLN0.005Er and KNLN0.01Er respectively. From figure 1, KNLNEr powder was gradually change to tetragonal structure with increasing Er_2O_3 contents. This indicates that Er^{3+} ions are well incorporated in KNLN perovskite structure.

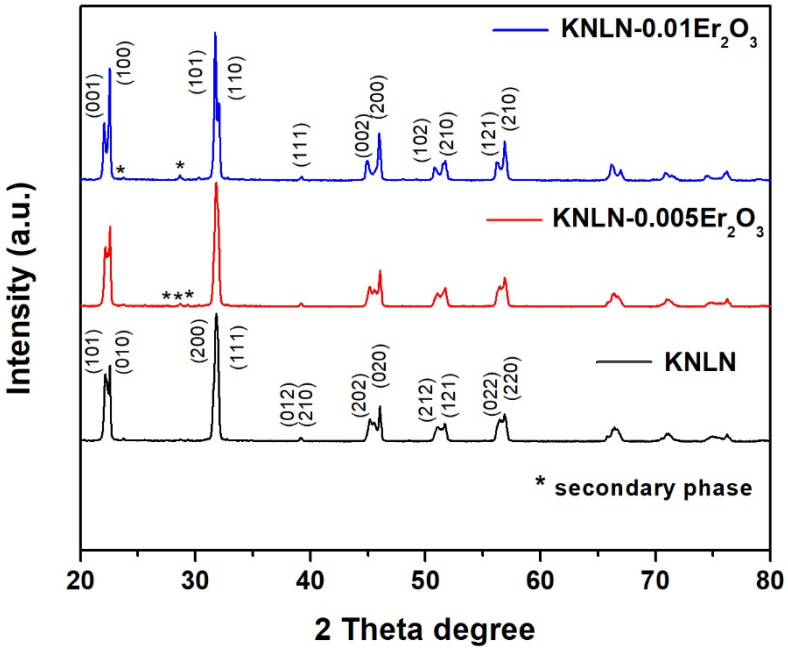

Figure 1 XRD patterns of $((K_{0.5}Na_{0.5})_{0.994}Li_{0.006})_{1-x}Er_xNbO_3$ powder, which x=0, 0.005 and 0.01, respectively.

Thermal study

After calcination process, these KNLN and KNLNEr starting powder were mixed with SiO_2 in composition of 75 : 25. Figure 2 showed the DTA profile curve of KNLN-SiO_2 glass and KNLNEr-SiO_2. The DTA technique was used to determine the thermal behavior of resulting glasses which benefit for estimate glass transition and crystallization temperatures for glass-ceramics samples. The DTA measurements were

carried out in an air atmosphere at a heating rate of 5°C/min in the temperature range of 30°C - 800°C. From figure 2, the intense exothermic peak of about 650°C of each composition related to crystallization temperature (T_c) of KNLN and KNLNEr crystals in glass. While, the noticeable endothermic peaks, representing by slight changes in slope of graphs as drawn by intersection point of two tangent lines are refer to the glass transition temperature (T_g) of each glass systems, respectively. The small shift of exothermic peak in higher Er_2O_3 content may be resulted from the higher content of Er_2O_3 oxide entered in KNLN perovskite structure, confirmed the XRD results as mention before.

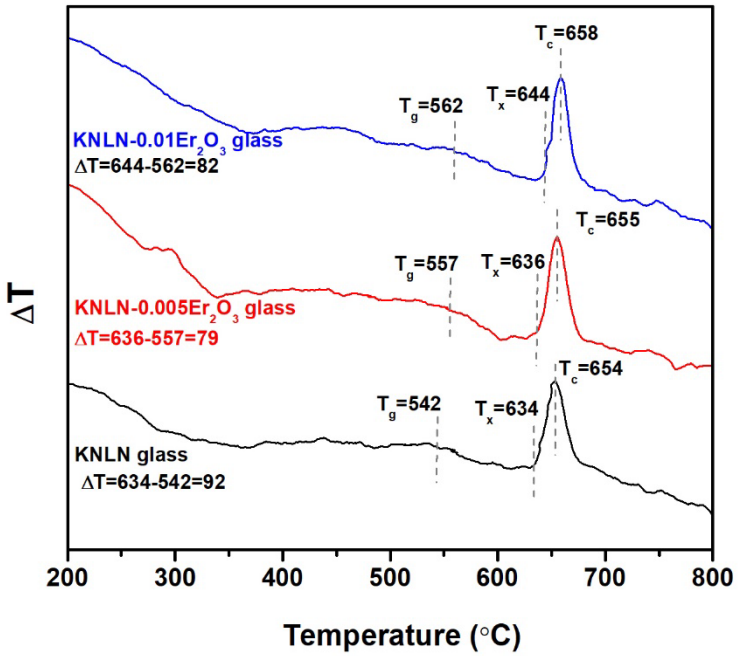

Figure 2 Thermal profile data of all glass samples by using DTA.

The stability of glass can be estimated by those thermal parameters. The estimation of the glass stability can be done by using Hruby's criterion [10].

$$\Delta T = T_x - T_g \quad (1)$$

where T_x is the onset point of crystallization temperature (T_c) peak. This term was used for determining the ability of glass in forming nanostructured glass-ceramics after applied energy from heat treatment process. From figure 2, the lowest ΔT value (ΔT=79) was found in 75KNLN-25SiO_2 with 0.005 mol% Er_2O_3 dopant system. The low ΔT value suggested that glass is easy to devitrify during melting-quenching process. Then, all glasses were heat treated at 550˚C and 650˚C depending on the observed thermal parameters from the DTA study in order to grow crystals inside the glass matrices. The appearance of all glass and glass-ceramics compositions are shown

in figure 3. It can be seen that the transparency of all glass system is decreased when heat treatment at 550˚C and 650˚C. This corresponds to the volume of crystallization during the heat treatment process.

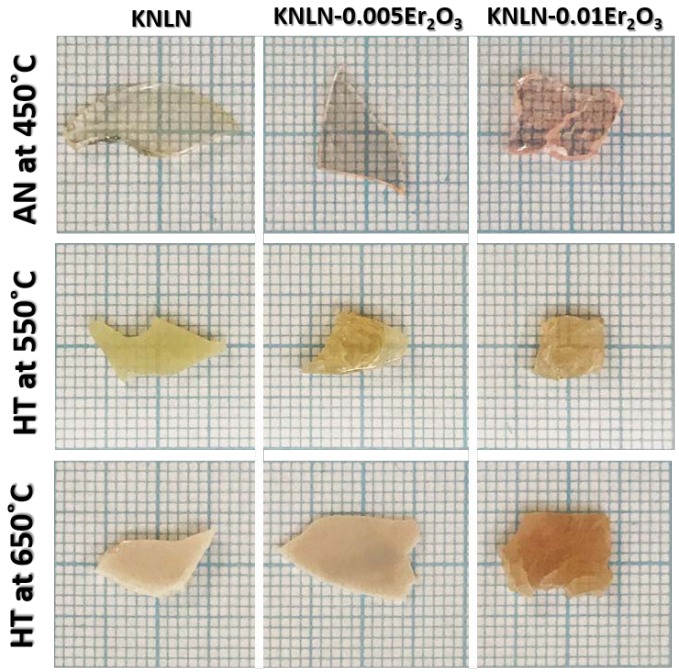

Figure 3 The appearance of glasses and glass-ceramics of 75KNLN-25SiO_2 doped and without doped Er_2O_3 at various heat treatment temperatures.

Dielectric property

The dielectric constants (ε_r) and dielectric loss ($\tan\delta$) of heat treated glass-ceramics were measured at different freaquency from 10kHz to 1MHz as shown in figure 4. From this figure, heat treatment temperature showed a significant role in increasing the dielectric constant. This results also confirmed by dielectric constant measurement as a function of frequency at room temperature comparing between glass compositions and heat treatment temperature in figure 5. The maximum dielectric constant of about 304 at 1 MHz with rather low dielectric loss than 0.01 was found in the glass-ceramics in composition of 75KNLN-25SiO_2 and heat treatment at 650^{o}C. Moreover, the addition of 0.005 mol%Er_2O_3 decrease the dielectric constant because of the entering of Er^{3+} ions into the KNLN perovskite structure distorted the orthorhombic phase to tetragonal phase. However, the increase amount of Er_2O_3 to 0.01 mol% can increase the dielectric constant due to appropriet amount of Er_2O_3 diffuse to KNLN site and brought to completely change to tetragonal perovskite structure. The overall $\tan\delta$ of the KNN–SiO_2

glass-ceramics is below 0.1 depending on each composition and heat treatment temperature. This may be useful in the applications in capacitors and microwave devices.

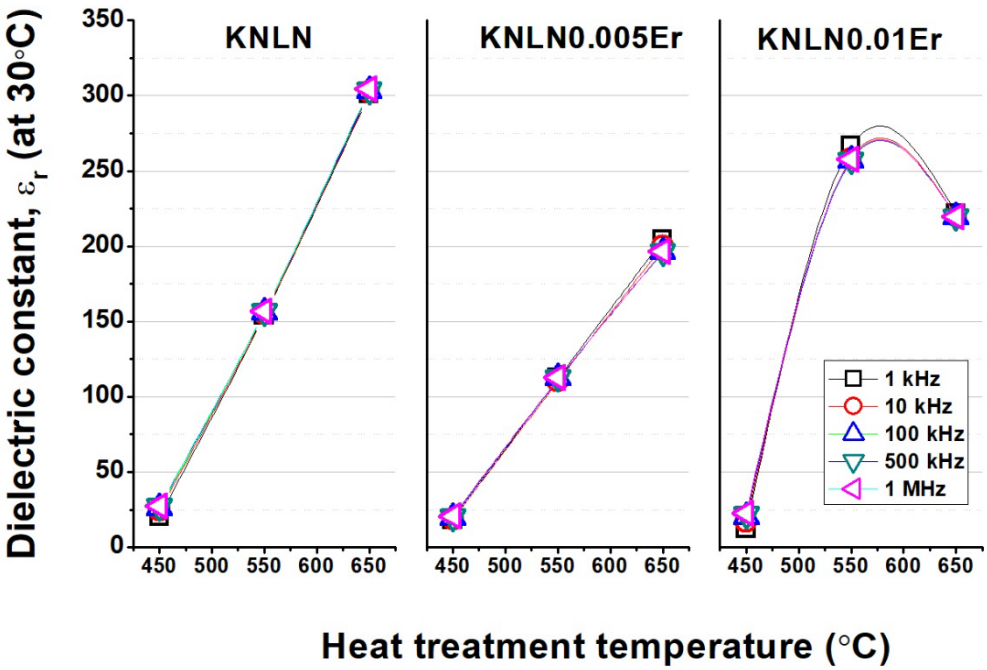

Figure 4 Dielectric constant 3 glass-ceramic systems with various temperature, annealed glass (450˚C), heat treated at 550˚C and heat treated at 650˚C.

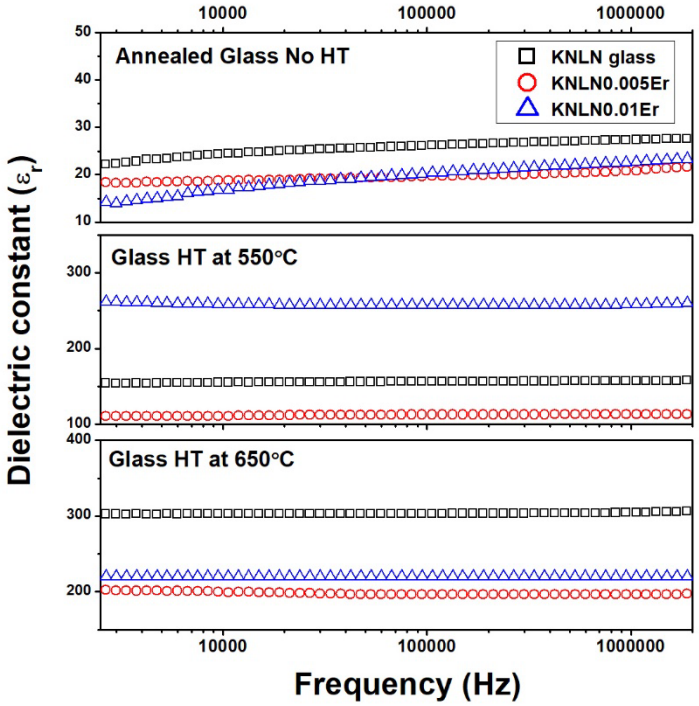

Figure 5 Dielectric constant (ε_r) measurement as a function of frequency at room temperature comparing between glass compositions and heat treatment temperature.

Optical property

UV-Vis absorption spectra (Abs%) of the prepared glasses and glass-ceramics were measured in the wavelength range of 200-1100 nm. This experiment was carried out on well polished with highly transparent sample with 2mm thickness. The Absoption spectra are shown in Figure 6. It can be seen that Abs% is increased with increasing heat treatment temperatures. The effect of heat treatment temperature on the transparency of glass originates from the type and size of crystals precipitated in the glass matrix. For visible light, samples containing crystals larger than 200 nm cause light scattering and hence the respective samples should be opaque. Transparent samples should contain crystals lower than 200 nm and also a small crystal size distribution. From figure 6, all of the absorption peaks are f-f transition of Er^{3+} ions reported by Carnall's conversion as $^4I_{15/2} \longrightarrow {}^2G_{9/2}$ (365 nm), $^4G_{11/2}$ (377 nm), $^2H_{9/2}$ (406 nm), $^4F_{5/2}+{}^4F_{3/2}$ (450 nm), $^4F_{7/2}$ (488 nm), $^2H_{11/2}$ (521 nm), $^4S_{3/2}$ (544 nm), $^4F_{9/2}$ (651 nm), $^4I_{9/2}$(799 nm) and $^4I_{11/2}$ (978 nm) [11,12]. Glass-ceramics display strong absorption edges below 350 nm. These absorption edges around 300 nm are transparent in all visible regions except intrinsic absorption lines due to Er^{3+} ions dopant [13,14]. However, the absorption edge at around 400 nm corresponded to nonlinear absorption via a two photon process which is an important mechanism of down-converting energy process.. This indicates that the

laser active Er^{3+} ions have entered into the (K,Na)NbO_3 crystalline phase. The optical band gap was obtained by plotting $(\alpha h\nu)^2$ versus $h\nu$ (where α is the absorption coefficient and $h\nu$ is the photon energy) as shown in Figure 7, which is described by equation 1.

$$\alpha h\nu=(h\nu-Eg)^{1/2} \quad (1)$$

Where α is the absorption coefficient, h is Planck's constant, ν is the photon frequency, and E_g is the band gap energy. The optical band gap, E_g of the selected transparent glass-ceramics was about 3.6 eV. It can also be noticed that the increase amount of Er_2O_3 dopant from 0.005 to 0.01 mol% has shown insignificant effect on modifying energy band gap of each glass series.

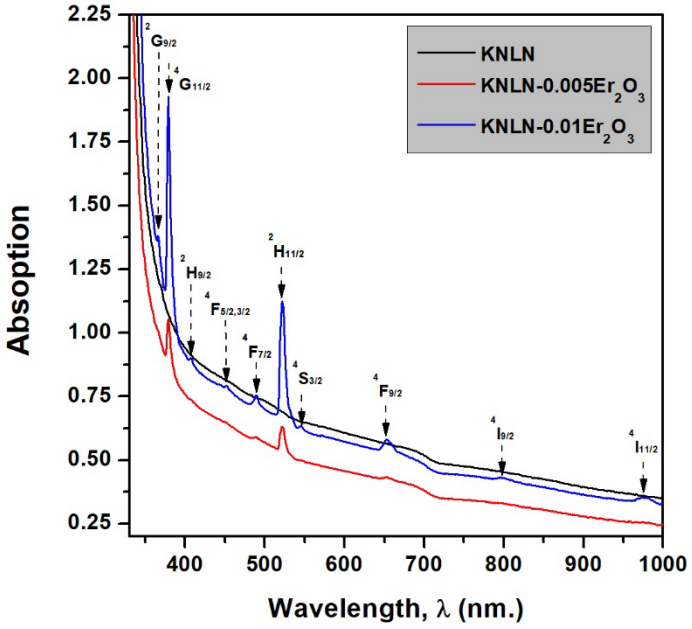

(a)

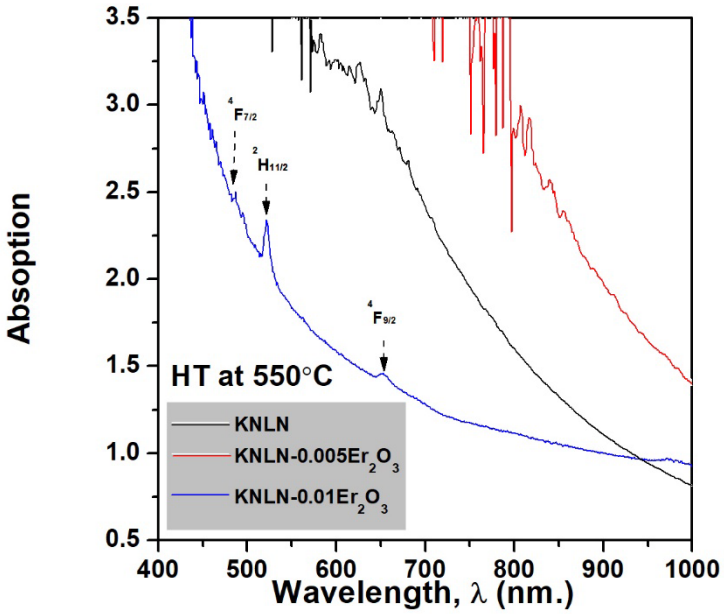

(b)

Figure 6 Absorption spectra of the KNLN and KNLNEr in SiO_2 glass (a) and glass-ceramics heat treated at 550˚C (b)

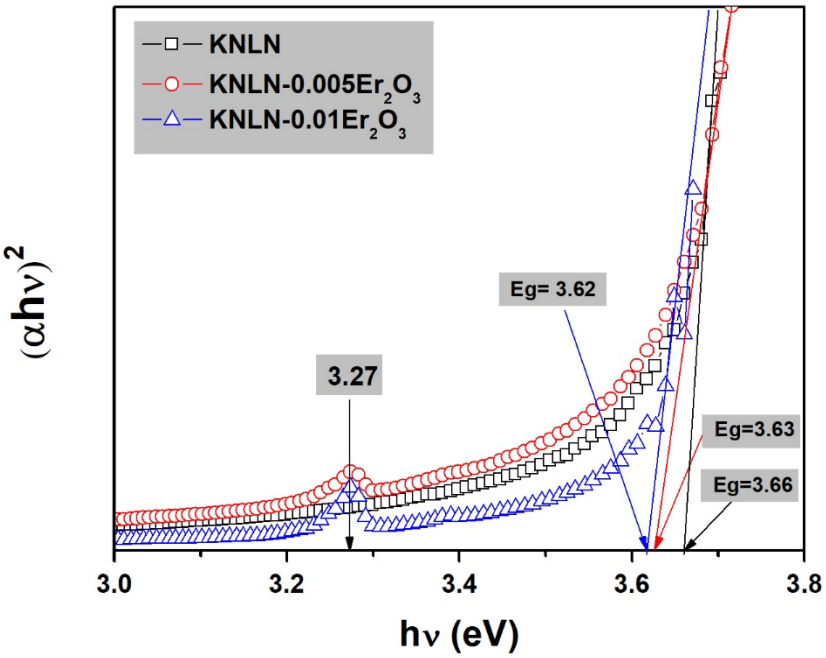

Figure 7 Plots of $(\alpha hV)^2$ versus hV of as-received KNLN and KNLNEr in SiO_2 glass

IV. Conclusions

In this work, electrical and structural properties of ferroelectric glasses and glass-ceramics from $75((K_{0.5}Na_{0.5})_{0.994}Li_{0.006})_{1-x}Er_xNbO_3 - 25SiO_2$ with x= 0, 0.005 and 0.01 system have been investigated. From the study, complex perovskite of KNLN phase was successfully prepared by using mixed oxide method or calcination at 900˚C for 5 hours. The transparent glass-ceramics was obtained by using incorporation method. It was indicated that heat treatment temperature plays a significant role in controlling the microstructure, crystallite sizes, and crystal quantity of the glass ceramics. The maximum ε_r of about 304 at 1MHz with a dielectric loss below of 0.01 could be obtained from the glass-ceramic sample of $75KNLN–25SiO_2$ and heat treated at 650˚C. From optical study, the transparency value dropped with an increase in the heat treatment temperature. It can be seen that the small amount of rare earth Er_2O_3 oxide play insignificant role in improving the energy state by increasing energy band gap in glass-ceramics. However, it is necessary to further study in effect of Er_2O_3 to KNN structure and optical property of this glass-ceramics system.

Acknowledgment

The authors would like to express their sincere gratitude to the Faculty of Science, Chiang Mai University for laboratory collaboration. P. Yongsiri would like to thank the Thailand Research Fund (TRG6080016) for financial support.

References

[1] G. H. Haerting, Ferroelectric Ceramics: History and Technology, J. Am. Ceram. Soc., 82 (1999) 797-818.

[2] B. Jaffe, W. R. Cook, H. Jaffe, Piezoelectric Ceramics, Academic Press Limited, London, 1971, ISBN: 0-12-379550-8.

[3] Y.P. Guo, K. Kakimoto, H. Ohsato, Appl. Phys. Lett. 85 (2004) 4121.

[4] E. Hollenstein, M. Davis, D. Damjanovic, N. Setter, Appl. Phys. Lett. 87 (2005) 182905.

[5] Y. Guo, K.-I. Kakimoto, H. Ohsato, Mater. Lett. 59 (2005) 241

[6] P. Yongsiri, S. Eitssayeam, G. Rujijanagul, S. Sirisoonthorn, T. Tunkasiri, K. Pengpat, Fabrication of Transparent Lead-Free KNN Glass-ceramics by Incorporation Method, Nanoscale Res. Lett., 7 (2012) 136.

[7] S.Wongsaenmai, S. Ananta, M.Unruan, R.Yimnirun, Effects of uniaxial stress on dielectric properties of lithium modified potassium sodium niobate ceramics, Physica B, 406 (2011) 2862-2864.

[8] Amauri J. Paula, Rodrigo Parra, Maria Aparecida Zaghete and Jose A. Varela, Study on the $K_3Li_2Nb_5O_{15}$ Formation During the Production of $(Na_{0.5}K_{0.5})_{(1-x)}Li_xNbO_3$ Lead-Free Piezoceramics at the Morphotropic Phase Boundary Solid State Communications 149(2009):1587–1590

[9] Ke Wang and Jing-Feng Li, Analysis of crystallographic evolution in (Na,K)NbO_3 (Na,K)NbO_3-based lead-free piezoceramics by x-ray diffraction, Appl. Phys. Lett. 91 (2007), 262902

[10] A. Hruby, Evaluation of glass-forming tendency by means of DTA, Czech. J. Phys. B22 (1972) 1187.

[11] A. Tarafder, B. Karmakar, Nanostructured $LiTaO_3$ and $KNbO_3$ ferroelectric transparent glass-ceramics for applications in optoelectronics, Ferroelectr. –Mater. A. (2011), doi:http://dx.doi.org/10.5772/16455 (Chapter 19)

[12] R. S. Chaliha, K. Annapurna, A. Tarafder, P.K. Gupta, B. Karmakar, V.S. Tiwari, Optical and dielectric properties of isothermally crystallized nano-$KNbO_3$ in Er^{3+}-doped K_2O–Nb_2O_5–SiO_2 glasses, Spectrochim. Acta A., 75 (2010) 243–250.

[13] W.T. Camall, P.R. Fields, K. Rajnak, Electronic energy levels in the trivalent lanthanide aquo ions. I. Pr^{3+}, Nd^{3+}, Pm^{3+}, Sm^{3+}, Dy^{3+}, Ho^{3+}, Er^{3+}, and Tm^{3+}, J. Chem. Phys. 49 (1968) 4424–4442

[14] M. Hayakawa, T. Hayakawa, X.T. Zhang, M. Nogami, Optical detection of near infrared femtosecond laser-heating of Er^{3+}-doped $ZnO–Nb_2O_5–TeO_2$ glass by green up-conversion fluorescence of Er^{3+} ions, J. Lumin. 131 (2011) 843–849

Output จากโครงการวิจัยที่ได้รับทุนจาก สกว.

1. ผลงานตีพิมพ์ในวารสารวิชาการนานาชาติ (ระบุชื่อผู้แต่ง ชื่อเรื่อง ชื่อวารสาร ปี เล่มที่ เลขที่ และหน้า) หรือผลงานตามที่คาดไว้ในสัญญาโครงการ

   1.1. ผลงานที่มีชื่อเป็นชื่อแรก

   1. **P. Yongsiri** and K. Pengpat, “Electrical Properties of Er_2O_3-Doped Potassium Sodium Niobate Based Silicate Glass”, *J. Nanosci. Nanotechnol.*: 17, 2979-2985 (2017). (WOS ; Q4, Impact factor 1.354)
   2. **P. Yongsiri,** W. Senanon, P. Intawin and K. Pengpat, “Dielectric Properties and Microstructural Studies of Er_2O_3 Doped Potassium Sodium Niobate Silicate Glass-Ceramics”, *Key Eng. Mater.*: 766, 258-263 (2018), (Scopus, SJR ; Q3)

   1.2. ผลงานที่มีชื่อร่วม

   1. W. Senanon, S. Eitssayeam, G. Rujijanagul, T. Tunkasiri, **P. Yongsiri** and K. Pengpat, *J. Nanosci. Nanotechnol*, : 18, 6195-6200 (2018). (WOS ; Q4, Impact factor 1.093)
   2. W. Senanon, T. Tunkasiri, S. Eitssayeam, G. Rujijanagul, **P. Yongsiri**, A. Niyompan and K. Pengpat, *Integr. Ferroelectr.* : 195, 11 – 18 (2019). (WOS ; Q4, Impact factor 0.486)
   3. W. Senanon, **P. Yongsiri**, S. Eitssayeam, G. Rujijanagul and K. Pengpat*, Mater. Lett.*, : 249, 160-164 (2019). (WOS ; Q2, Impact factor 3.019)

2. การนำผลงานวิจัยไปใช้ประโยชน์

   - เชิงพาณิชย์ (มีการนำไปผลิต/ขาย/ก่อให้เกิดรายได้ หรือมีการนำไปประยุกต์ใช้โดยภาคธุรกิจ/บุคคลทั่วไป)
     ไม่มี
   - เชิงนโยบาย (มีการกำหนดนโยบายอิงงานวิจัย/เกิดมาตรการใหม่/เปลี่ยนแปลงระเบียบข้อบังคับหรือวิธีทำงาน)
     ไม่มี
   - เชิงสาธารณะ (มีเครือข่ายความร่วมมือ/สร้างกระแสความสนใจในวงกว้าง)

ไม่มี

- เชิงวิชาการ (มีการพัฒนาการเรียนการสอน/สร้างนักวิจัยใหม่)
  ในงานวิจัยนี้ได้รับความร่วมมือให้ใช้อุปกรณ์ในการพัฒนาแก้วเซรามิกจากมหาวิทยาลัยเชียงใหม่ โดยได้รับความอนุเคราะห์จาก รศ.ดร.กมลพรรณ เพ็งพัด เป็นที่ปรึกษางานวิจัย ในระหว่างการทดลองนี้จึงมีนักศึกษาของท่านอาจารย์ทั้งในระดับปริญญาเอก ช่วยทำการทดลอง และตรวจสอบผลการทดลองบางอย่าง ทำให้นักศึกษาเป็นผู้ช่วยวิจัยร่วมในงานวิจัยนี้ ดังจะเห็นได้จากการที่มีชื่อร่วมในงานวิจัยที่ตีพิมพ์แล้ว

3. อื่นๆ (เช่น ผลงานตีพิมพ์ในวารสารวิชาการในประเทศ การเสนอผลงานในที่ประชุมวิชาการ หนังสือ การจดสิทธิบัตร)

1. **P. Yongsiri** and K. Pengpat, “Optical and Structural Studies of Er_2O_3 doped Potassium Sodium Niobate Silicate Glass-Ceramics” Poster presentation, International Conference on Traditional and Advanced Ceramics 2017 (ICTA2017), BITEC Bangna, Bangkok, Thailand	August 31 - September 1, 2017
2. **P. Yongsiri** and K. Pengpat, “The electrical properties of Er_2O_3 doped potassium sodium lithium niobate based glass-ceramics” Oral presentation, The First Materials Research Society of Thailand International Conference (1st MRS Thailand International Conference), Convention Center, The Empress Hotel, Chiang Mai, Thailand	October 31- November 3, 2017
3. **P. Yongsiri** and K. Pengpat, “Optical and Electrical Properties of Lanthanide Doped KNN-SiO_2 Glass-ceramics” Oral presentation, The First Materials Research Society of Thailand International Conference (2nd MRS Thailand International Conference), The Zign Hotel, Pattaya, Thailand	July 10-12, 2019

ภาคผนวก

ก 1 ผลงานที่มีชื่อเป็นชื่อแรก

1. P. Yongsiri and K. Pengpat, “Electrical Properties of Er_2O_3-Doped Potassium Sodium Niobate Based Silicate Glass”, J. Nanosci. Nanotechnol.: 17, 2979-2985 (2017)

2. P. Yongsiri, W. Senanon, P. Intawin and K. Pengpat, “Dielectric Properties and Microstructural Studies of Er_2O_3 Doped Potassium Sodium Niobate Silicate Glass-Ceramics”, Key Eng. Mater.: 766, 258-263 (2018)

ภาคผนวก

ข 1 ผลงานที่มีชื่อร่วม

1. W. Senanon, S. Eitssayeam, G. Rujijanagul, T. Tunkasiri, P. Yongsiri and K. Pengpat, J. Nanosci. Nanotechnol, : 18, 6195-6200 (2018). (WOS ; Q4, Impact factor 1.093)

2. W. Senanon, T. Tunkasiri, S. Eitssayeam, G. Rujijanagul, P. Yongsiri, A. Niyompan and K. Pengpat, Integr. Ferroelectr. : 195, 11 – 18 (2019). (WOS ; Q4, Impact factor 0.486)

3. W. Senanon, P. Yongsiri, S. Eitssayeam, G. Rujijanagul and K. Pengpat, Mater. Lett., : 249, 160-164 (2019). (WOS ; Q2, Impact factor 3.019)

Article

Journal of
Nanoscience and Nanotechnology
Vol. 17, 2979–2985, 2017
www.aspbs.com/jnn

Electrical Properties of Er_2O_3-Doped Potassium Sodium Niobate Based Silicate Glass

Ploypailin Yongsiri[1] and Kamonpan Pengpat[1, 2, *]

[1] Department of Physics and Materials Science, Faculty of Science, Chiang Mai University, Chiang Mai 50200, Thailand
[2] Materials Science Research Center, Faculty of Science, Chiang Mai University, Chiang Mai 50200, Thailand

In this study, the electrical properties of Er_2O_3 doped potassium sodium niobate (KNN) based silicate (SiO_2) glass has been investigated. This glass-ceramic system was successfully prepared via the incorporation method. The selected compositions used in this experiment were 70–80 mol% of KNN and 20–30 mol% of SiO_2, doped with 0.5 mol% Er_2O_3. From the study, the resulted KNN glass-ceramics greatly improved the dielectric constant at room temperature ($\varepsilon_r = 250$ at 10 kHz) above those found using a conventional glass-ceramic method, with a very low $\tan\delta$ below 0.1. It was found that temperature and frequency have significantly influenced on dielectric properties of the KNN glass-ceramics. The study of polarization mechanism via dielectric measurement found that this glass system had space-charge polarization and relaxation at low frequency. The results also showed that the electrical properties of the material arised mainly due to the bulk effects. *P–E* hysteresis loops of all glasses and glass-ceramic samples exhibited rugby ball-like loops which confirmed the high leakage current.

Keywords: Ferroelectric, Glass-Ceramics, $K_{0.5}Na_{0.5}NbO_3$.

1. INTRODUCTION

Ferroelectric glass-ceramics (FGCs) are polycrystalline materials containing perovskite crystals inside a glass matrix. FGC has superior properties as physical, electrical and optical from their parent glass. Recently, many researchers reported that FGCs exhibited high permittivity and high breakdown strength, which were useful for high energy density capacitors and memory devices.[1] Thus, glass-ceramics promote the new era of materials which combine the useful characteristic of glass and ceramic together. This involves the ability of engineering the crystal size and shape, giving rise to new hybrid materials with desired nano-crystal size in a pore-free bulk matrix.

$K_{0.5}Na_{0.5}NbO_3$ or KNN is a complex perovskite material which exhibits ferroelectric properties. KNN is one of the most promising alternative systems to the lead-based systems. KNN also shows interesting values such as high Curie temperature of 420 °C, piezoelectric constant (d_{33}) of 80 pC/N, coupling factor coefficient (k_p) of 36–40% and dielectric constant (ε_r) of 290 when it was prepared by the ordinary sintering process. The crystal structure of KNN is dependent on temperature where an increase from room temperature to 200 °C causes an orthorhombic to tetragonal phase transformation, and when the temperature is higher than 420 °C, the tetragonal phase changes to a cubic phase.[2, 3] Moreover, KNN is an environmental friendly material and also shows non-linear optical properties.

The dielectric properties of KNN based-glasses and glass-ceramics at high temperature have scarcely been studied due to the large dielectric loss, and only a few high temperature applications. However, the benefit of high temperature dielectric investigation is the ability to distinguish a material's space-charge and defect carrier contributions which are resolved in impedance measurements.[4] An ideal ferroelectric, such as KNN is a good electrical insulator and the dielectric constant should follow the Curie-Weiss law above the Curie temperature. The relaxation frequency may range from low frequency to high frequency depending on the type of chemical and physical constraints, which correspond to the behavior of the dipole moment.[4]

In this work, KNN-SiO_2 glass-ceramics containing KNN crystals with a small amount of 0.5 mol% Er_2O_3 were prepared using the incorporation method. In the

*Author to whom correspondence should be addressed.

incorporation method, a simple mixed-oxide technique was firstly employed to synthesize the KNN single-phase powder before mixing with the glass forming oxide and dopant of SiO_2 and Er_2O_3, respectively. The crystallization of the KNN crystals in the SiO_2 glass was accomplished by a heat treatment process which was also used to control the KNN crystal shape and size. Here, we report the electrical properties such as dielectric constant and loss, impedance and ferroelectric properties of the prepared KNN glass-ceramics.

2. EXPERIMENTAL DETAILS

2.1. Sample Preparation

The glasses of 70KNN-30SiO_2, 75KNN-25SiO_2 and 80KNN-20SiO_2 (mol%) doped with 0.5 mol% of Er_2O_3 were prepared using the incorporation method. KNN powder was firstly prepared by conventional mixed-oxide method according to our previous work.[5] For the incorporation method, the prepared KNN ceramic powder was then mixed with SiO_2 in order to form transparent based glass. The components were mixed in a platinum crucible and subsequently melted at 1300 °C for 15 min and then quenched between stainless steel plates which were heated at around 400–450 °C during quenching. The quenched glasses were immediately annealed at approximately 400–450 °C for 4 h to release their stresses.

2.2. Material Characterization

Thermal properties of as-received glasses were measured to find their glass transition temperature (T_g) and crystallization temperature (T_c) by using DTA (Differential thermal analysis; Du Pont Instrument, USA). Then, the annealed glass pieces were subjected to heat treatment (HT) at temperatures, depending on the T_g and T_c of each glass composition, for 4 h. To analyze the electrical properties of glasses and glass-ceramics, various techniques were employed. The dielectric constant (ε_r), dielectric loss ($\tan\delta$) and impedance were measured in the range of 10 kHz–1 MHz using a precision LCZ meter (E4980A type, Agilent Technologies). To measure the ferroelectric hysteresis curves, a Sawyer Tower circuit (Radiant Technologies, Inc.), powered by a high voltage power amplifier (Trek, model 609B) was used from 1 kHz to 100 kHz with applied voltages between 1 kV to 3 kV.

3. RESULTS AND DISCUSSION

3.1. Thermal Characterization

The DTA technique was used to determine the thermal properties of the prepared glasses. DTA measurements of the glass samples were carried out in an air atmosphere at a heating rate of 5 °C/min in the temperature range of 30 °C–1000 °C. From Figure 1, intense exothermic peaks can be observed in a range of 600 °C–700 °C for each glass composition. These peaks correspond to crystallization (T_c).

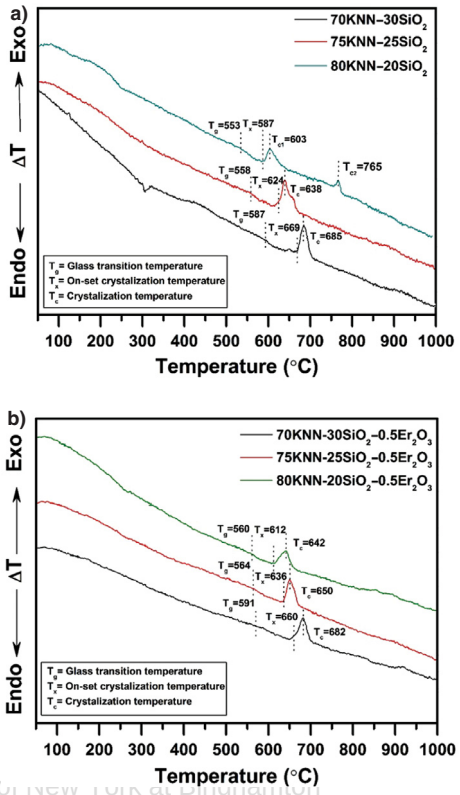

Figure 1. The thermal profiles of each glass studied by the DTA technique. (a) As-received glass without Er_2O_3 dopants. (b) As-received glass doped with 0.5 mol% Er_2O_3.

The noticeable endothermic peaks, represented by slight changes in slope of the graphs observed as the intersection point of two tangent lines in the range of 550 °C–600 °C, refer to the glass transition temperature (T_g). The T_g of these glasses gradually decreased with increasing KNN content, which may result from the lower content of SiO_2 glass forming oxide. Moreover, the addition of Er_2O_3 into this KNN-SiO_2 glass system caused an increase in T_c. The 80KNN-20SiO_2 glass system shows a second exothermic peak at T_{c2} indicating that this glass can form with erbium a secondary phase different from that formed at T_{c1}. However, the 80KNN-20SiO_2 doped 0.5 mol% glass showed no evidence of any secondary crystallization peak. These Er_2O_3 oxide may inhibite the growth of the secondary phase. The stability of each glass was measured by using the Hruby criteria[6] (Eq. (1)) in order to determine the ability of glass in forming nanostructured glass-ceramics after applying energy from the heat treatment process.

$$\Delta T = T_x - T_g \tag{1}$$

where T_x is the onset point of crystallization temperature (T_c) peak.

From Figure 2, the highest ΔT value was found in for the 70KNN-30SiO_2 glass system, and it is slightly

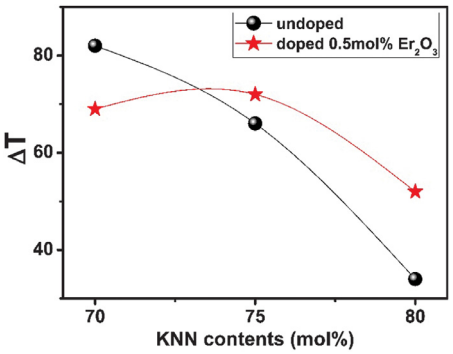

Figure 2. The stability of Er_2O_3-doped and undoped-glasses from their DTA curves.

decreased with increasing KNN content or reducing SiO_2 content. The lower ΔT value implied that glass is easy to devitrify during melting which is not suitable for controlled crystallization in further glass-ceramic process. It can be noticed that the Er_2O_3 dopant slightly increased the glass stability of the glasses with higher KNN content than 70 mol%. Here, in this work, the selected heat treatment condition was 600 °C for 4 h in order to allow the complete growth of crystal inside the glass matrix without residual stress, which often occurs if the glass is heated to near T_c. This stress can cause lower strength of the heat-treated glass-ceramic. Our resulting glass-ceramics were light yellow and the color changed to slight pink after doped with Er_2O_3. The transparency of all glasses decreased after heat treatment at 600 °C.

3.2. Composition Studies by XRD

The XRD patterns from Figure 3 show the amorphous-like structure for every composition. From XRD results, the crystalline phase was cleary observed in 80KNN-20SiO_2 doped 0.5 Er_2O_3 glass-ceramic heat treated at 600 °C, which corresponds to $K_{0.65}Na_{0.35}NbO_3$ (KNN)

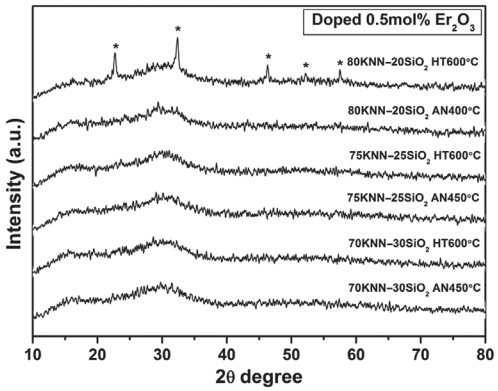

Figure 3. XRD pattern waveform spectra of Er_2O_3-doped glasses with comparison between annealed and heat treated glasses (*=$K_{0.35}Na_{0.65}NbO_3$).

phase (JCPDS 77–0038). The lower ΔT value of the 80KNN-20SiO_2 glass series can be explained as this glass system shows high tendency to devitrify during the heat treatment process. From our XRD pattern in Figure 3, the erbium cluster did not exist because no diffraction peak of Er_2O_3 at about $2\theta = 29.05$ (JCPDs no. 77-0464) was found, indicated that Er^{3+} had been incorporated well in the KNN-SiO_2 host lattice or the amount of Er^{3+} dopant was lower than the limit of XRD detection.

3.3. Dielectric Studies

The important characteristic of ferroelectric glass-ceramics is the dielectric constant (ε_r). The dependence of ε_r with temperature has been discussed in terms of the number of electrical dipoles and their mobility in the glass network. In this work, we measured the dielectric constant over a wide range of frequency and temperature (1 kHz to 1 MHz, 30 °C to 500 °C, respectively). Figure 4 shows the dielectric constant and dielectric loss at various frequencies for all compositions, at room temperature (of about 35 °C). It was found that the dielectric constant of every composition was between 150 and 300 and had a tendency to increase with increasing KNN content. The overall dielectric losses ($\tan\delta$) of all conditions are in a low range of about 0.01. The heat treatment at 600 °C caused an overall increase of dielectric constant of the KNN-SiO_2 glass-ceramics but oppositely decreased the dielectric constant of the glass-ceramics for the Er_2O_3 doped KNN-SiO_2 system. This may be due to the occurrence of an unknown secondary phase in the Er_2O_3 doped KNN-SiO_2 glass-ceramics, which was reported in our previous work.[5] However, the high dielectric constant with low loss behavior of this glass-ceramics system may be useful in the applications in capacitors and microwave devices. Figure 5 shows that the trends of dielectric constant versus temperature of the glasses and glass-ceramics heat treated at 600 °C for KNN-SiO_2 both with and without Er_2O_3 dopants are similar, except for the undoped 80KNN-20SiO_2 glass-ceramic sample heat treated at 600 °C, as the abrupt increase in dielectric constant occurred at lower temperature than for the others. As reported in our previous work[7] this sample contained a high amount of unknown secondary phase compared to other lower KNN content glass-ceramics.

As can be seen from Figure 5, the dielectric constant increased rapidly with increasing temperature especially at low frequency due to the generation of space charge polarization or ionic conduction, which is normally found in oxide glass. Therefore, in this study we have tried to observe the dielectric constant behavior at high frequency of the KNN-SiO_2 without Er_2O_3 dopants heated at 500 °C instead of 600 °C to avoid the possible precipitation of unwanted phase as shown in Figure 6. The trends are similar to the glass and glass-ceramics measured at 1 kHz, in which the high temperature stimulated the contributions from space charge polarization,

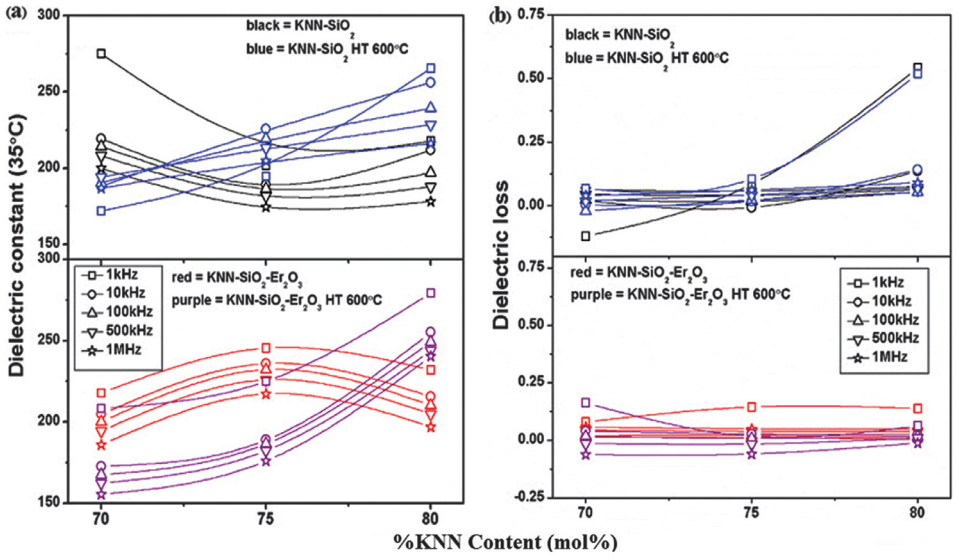

Figure 4. The room temperature dielectric constant (a) and dielectric loss (b) at various frequency of glasses with different percent of KNN. (black line = KNN-SiO_2, blue line = KNN-SiO_2 heat treatment at 600 °C, red line = KNN-SiO_2–Er_2O_3 and purple line = KNN-SiO_2–Er_2O_3 heat treatment at 600 °C).

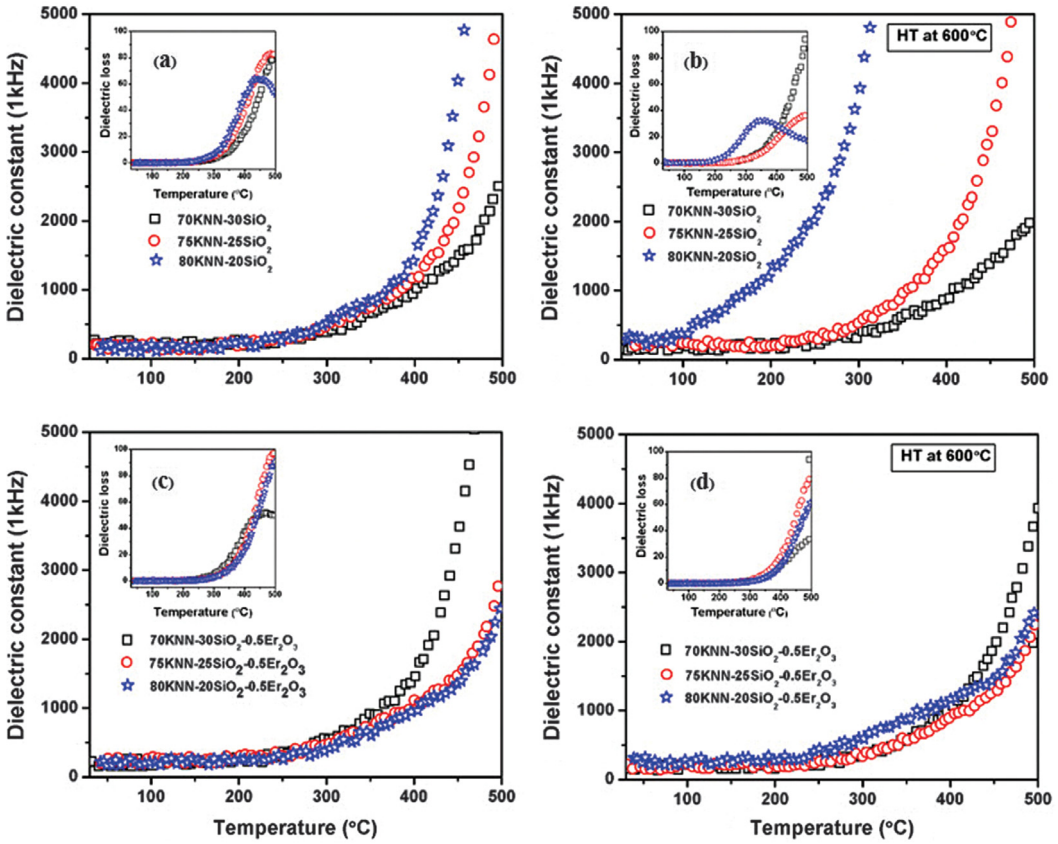

Figure 5. Dielectric constant and loss inset versus temperature at 1 kHz of different glass conditions. (a) KNN-SiO_2, (b) KNN-SiO_2 heat treatment at 600 °C, (c) KNN-SiO_2-Er_2O_3 and (d) KNN-SiO_2–Er_2O_3 heat treatment at 600 °C.

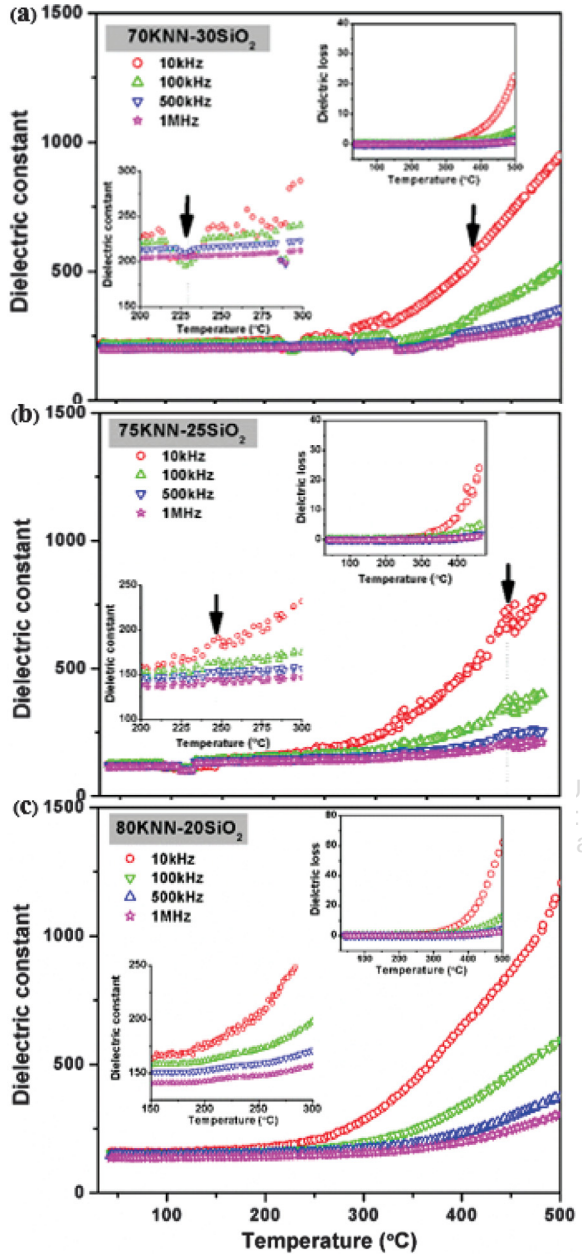

Figure 6. Dielectric constant and dielectric loss (inset) as a function of temperature at 10 kHz, 100 kHz, 500 kHz and 1 MHz. (a) 70KNN-30SiO_2, (b) 75KNN-25SiO_2 and (c) 80KNN-20SiO_2 glass conditions.

which come from the mobility of ions and imperfections in the material as mentioned before. In addition, small peaks were observed around 420 °C in 70KNN-30SiO_2 and 75KNN-25SiO_2 which may be related to the Curie temperature of KNN phase at 420 °C.[2,3] This temperature simply corresponds to the transformation of ferroelectric tetragonal/orthorhombic phase to paraelectric cubic phase. However, this dielectric anomaly was not found in the 80KNN-20SiO_2 glass-ceramic. This may be partly due to the occurrence of unknown secondary phase in this sample. However, this glass system offers the low loss and highly transparency glass-ceramics suggesting the opportunity for use in practical electronic applications.

3.4. Impedance Studies

The Maxwell-Wagner effect has been used to determine the contribution of ion movement by using the impedance complex plane plots (Z^* plots) at various temperatures. The study of the real part impedance (Z') plotted against the imaginary part (Z'') at 200 °C and 300 °C are shown in Figure 7 in order to understand the dielectric relaxation phenomena in the prepared glasses and glass-ceramics.

Figure 7 shows the Cole–cole plots of KNN-SiO_2 doped and undoped Er_2O_3 glasses heat treated at 600 °C in the frequency range of 100 Hz to 1 MHz. At 200 °C, there is a linear response in Z''. This trend indicates the insulation behavior of the samples.[8] The increase in the temperature up to 300 °C changed the linear dependence to a semicircle, showing conducting behavior in all glass and glass-ceramic samples. This indicates that the electrical properties of the materials are mainly due to bulk effects. The observed semi-arc centers of all KNN-SiO_2 glasses and glass-ceramics at 300 °C are under the Z' axis due to the distribution of relaxation times. This behavior is associated with the dielectric responses of the glass matrix, the ferroelectric phase and other dipoles arising from the free electron units.

Figure 8 shows the imaginary (Z'') parts of impedance as a function of frequency at various temperatures. It reveals that Z'' firstly increased with the increase in both frequency as well as temperature and reached a maximum (Z''_{max}) and then started to decrease at higher frequencies. The appearance of peak in Z'' versus frequency

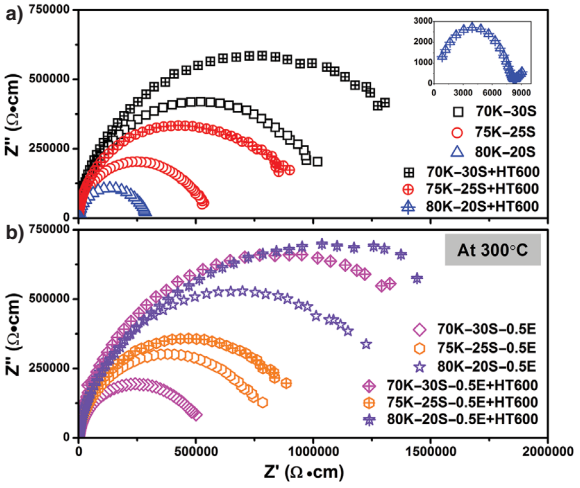

Figure 7. The Cole–cole plot (Z'' vs. Z') at 300 °C, compared between (a) based glass and (b) 0.5 mol% Er_2O_3 doped glass.

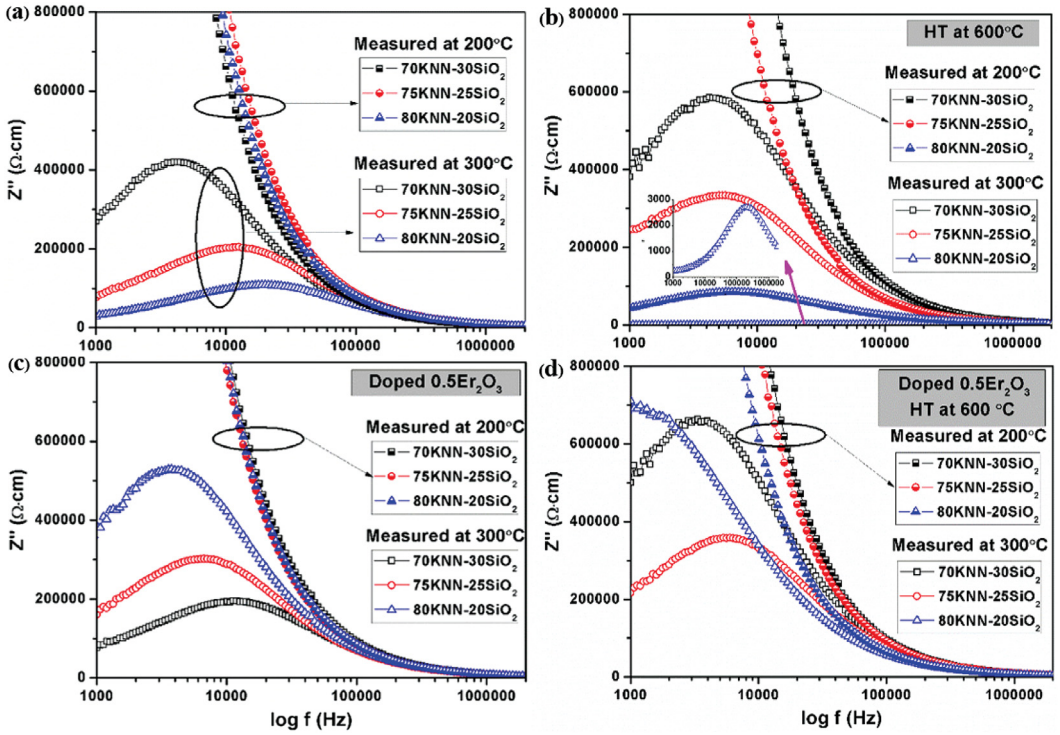

Figure 8. The imaginary (Z") parts of impedance as a function of frequency at 200 °C and 300 °C. (a) KNN-SiO_2, (b) KNN-SiO_2 heat treatment at 600 °C, (c) KNN-SiO_2–Er_2O_3 and (d) KNN-SiO_2–Er_2O_3 heat treatment at 600 °C.

at different temperatures suggests the presence of dielectric relaxation process in the material. It can also be seen that the Z'' peak of the plots are shifted toward higher frequencies with increasing temperature, indicating the presence of temperature dependent relaxation process in the system. The broadening of the peak increases with the increase in temperature, which suggests a spread of relaxation time. This may be due to the presence of defects at higher temperatures.

3.5. Ferroelectric Studies

Figure 9 shows the *P–E* hysteresis loops under an electric field of 1 kV/cm for the KNN-SiO_2 doped and undoped Er_2O_3 glasses annealed at 400–450 °C. All samples exhibited rugby ball-like loops, suggesting that these samples had large leakage currents. Moreover, undoped glass-ceramics and 0.5 mol% Er_2O_3 glass-ceramics also showed small pinched *P–E* hysteresis loops, which indicated the coexistence of antiferroelectric and ferroelectric phases of glass matrix and KNN phase, respectively. The inset of Figure 9 plots the dependence of KNN content on the ferroelectric remanent polarization (Pr) and shows the increasing trends of P_r with increasing KNN contents upto 80 mol% in both Er_2O_3 doped and undoped glasses. However, the addition of Er_2O_3 in the annealed KNN-SiO_2 glasses increased the remanent polarization which may be due to defects generated from oxygen vacancies in the glass structure.

In Figure 10, the ferroelectric hysteresis loops of the doped 0.5 mol% Er_2O_3 KNN-SiO_2 glasses and their corresponding glass-ceramics heat treated at 600 °C at 40 Hz are illustrated. The inset of Figure 9. plots the dependence of KNN content on the ferroelectric remanent

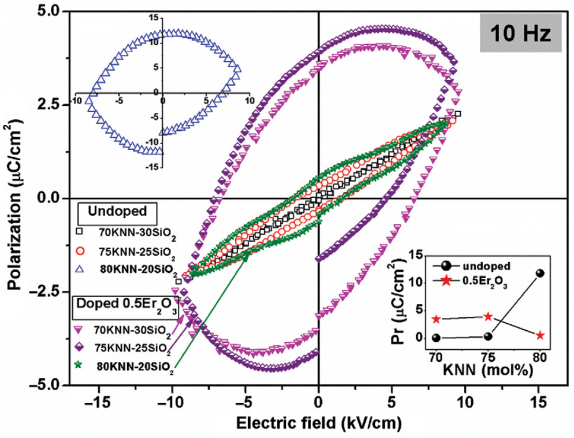

Figure 9. *P–E* hysteresis loops under an electric field at of 1 kV/cm (10 Hz), compared between KNN-SiO_2 and KNN-SiO_2–Er_2O_3 glass conditions.

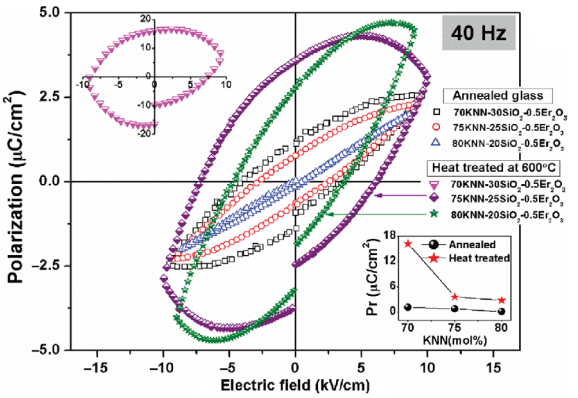

Figure 10. *P–E* hysteresis loops under an electric field of 1 kV/cm (40 Hz) of the KNN-SiO_2-Er_2O_3 glasses compared with KNN-SiO_2–Er_2O_3 heat treated at 600 °C glass-ceramics.

polarization (P_r). It can be seen that the heat treatment enhanced P_r values of all samples, which may be due to the growth of KNN crystals in the glass matrices. However, the rugby ball-like loops were still obtained, which confirmed the high leakage currents in these glasses and glass-ceramics.

4. CONCLUSION

Undoped and doped Er_2O_3 glasses and glass-ceramics from the KNN-SiO_2 system prepared by the incorporation method have been investigated in terms of their dielectric and ferroelectric properties. It was found that Er_2O_3 of about 0.5 mol% dopant was well incorporated in the KNN-SiO_2 glass matrix and increased the stability of the glass. From the dielectric study, the ε_r at room temperature of all samples showed higher values than those found in another types of glass-ceramics with $\tan\delta$ below 0.1.[9, 10] The study of polarization mechanism via dielectric measurement found that this glass system had space-charge polarization and relaxation at low frequencies (1 Hz–10 kHz). The Cole–cole plots showed linear response of Z'' in the temperature range of 30 °C–200 °C. This trend indicated the good insulation behavior of the samples. With increase of the temperature to 300 °C, the linear response gradually changed to a semicircle which confirmed the conducting behavior in the samples at higher temperature. This indicated that the electrical properties of the material arose mainly due to bulk effects. *P–E* hysteresis loops of all glass and glass-ceramic samples exhibited rugby ball-like loops, which confirmed the high leakage currents. However, this glass system still offers low loss and highly transparent bulk glasses and glass-ceramics, suggesting opportunity of using then in electronic applications in future.

Acknowledgment: The authors would like to thank Chiang Mai University, the Thailand Research Fund (TRF), and the National Research University (NRU) for financial support. We would like to express our thanks to financial support from the Graduate School, Chiang Mai University Thailand.

References and Notes

1. J. Chen, Y. Zhang, C. Deng, and X. Dai, *Mater. Chem. Phys.* 121, 109 (**2010**).
2. L. Egerton and D. M. Dillon, *J. Am. Ceram. Soc.* 42, 438 (**1959**).
3. B. Jaffe, W. R. Cook, and H. Jaffe, Piezoelectric Ceramics, Academic Press, London (**1971**). JCPDS 71-2171.
4. L. Liu, Y. Huang, C. Su, L. Fang, M. Wu, C. Hu, and H. Fan, *Appl. Phys. A* 104, 1045 (**2011**).
5. P. Yongsiri, S. Sirisoonthorn, and K. Pengpat, *Mater. Res. Bull.* 69, 84 (**2015**).
6. A. Hruby, *J. Phys. B* 22, 1187 (**1972**).
7. P. Yongsiri, S. Eitssayeam, S. Sirisoonthorn, and K. Pengpat, *Electron. Mater. Lett.* 9, 825 (**2013**).
8. P. Palei and P. Kumar, *J. Adv. Dielectr.* 1, 351 (**2011**).
9. R. S. Chaliha, K. Annapurna, A. Tarafder, V. S. Tiwari, P. K. Gupta, and B. Karmakar, *Spectrochim. Acta A Mol. Biomol. Spectrosc.* 75, 243 (**2010**).
10. M. P. F. Graça, M. A. Valente, and M. G. Ferreira Da Silva, *J. Mater. Sci.* 41, 1137 (**2006**).

Received: 30 January 2016. Accepted: 29 July 2016.

Key Engineering Materials
ISSN: 1662-9795, Vol. 766, pp 258-263
doi:10.4028/www.scientific.net/KEM.766.258

Submitted: 2017-09-15
Revised: 2018-01-18
Accepted: 2018-01-27
Online: 2018-04-13

Dielectric Properties and Microstructural Studies of Er_2O_3 Doped Potassium Sodium Niobate Silicate Glass-Ceramics

Ploypailin Yongsiri[1,a*], Wipada Senanon[1,b], Pratthana Intawin[1,c] and Kamonpan Pengpat[1,2,d]

[1]Department of Physics and Materials Science, Faculty of Science, Chiang Mai University, Chiang Mai, 50200, Thailand

[2]Materials Science Research Center, Faculty of Science, Chiang Mai, 50200, Thailand

[a]pyongsiri@gmail.com, [b]wipada_senanon@hotmail.com, [c]buai_sakura@hotmail.com, [d]kpengpat@gmail.com

Keywords: Glass-ceramics, Er_2O_3, KNN,

Abstract. In this work, electrical and structural properties of ferroelectric glasses and glass-ceramics from $K_{0.5}Na_{0.5}NbO_3$-SiO_2 doped with 0.5-1.0 mol%Er_2O_3 system have been investigated. The influent of Er_2O_3 dopant was also compared with the original glass. The $K_{0.5}Na_{0.5}NbO_3$ (KNN) powder was mixed with SiO_2 in composition of 75KNN-25SiO_2 and doped with Er_2O_3. Well-mixed powder was subsequently melted at 1300°C for 15 min in a platinum crucible using an electric furnace. The quenched glasses were then subjected to heat treatment at various temperatures for 4 h. From the study, KNN single phase in transparent glass was successfully prepared via incorporation method. The maximum ε_r of about 360 at 10 kHz with a low tanδ of 0.07 could be obtained from the glass-ceramic sample of 75KNN–25SiO_2 doped 0.5 mol% Er_2O_3 and heat treated at 600˚C. It can be seen that the higher percent of Er_2O_3 can lower the dielectric loss of KNN glass-ceramics. This interesting value suggesting the opportunity of using them in electronic applications in the future.

Introduction

Recently, perovskite materials with ABO_3 structure are subjected to intensively study due to their marvelous properties. The interesting properties are piezoelectric, pyroelectric and ferroelectric which used in widely applications such as transducer, actuator etc [1].

The ABO_3-type perovskite is another type of crystal structure which combined many important properties such as magnetic, electronic and transport property [2]. This perovskite structure shows anisotropic property due to the build-in electronic dipoles in their crystal structure that lead to magnificent non-linear optical properties such as the electro-optic effect, harmonic generation and photo-refraction. $K_{0.5}Na_{0.5}NbO_3$ (KNN) is one of a ferroelectric material which show high Curie temperature (T_c) of 420˚C, piezoelectric constant (d_{33}) of 80 pC/N, coupling factor coefficient (k_p) of 36-40% and dielectric constant (ε_r) of 290. The temperature play a significant role to KNN crystal structure when increase from room temperature to 200˚C causes an orthorhombic to tetragonal phase transformation, and when the temperature is higher than 420˚C, the tetragonal phase changes to a cubic phase. Furthermore, KNN is also friendly to environment [3-4]. many research works have been focused on phosphors of rare-earth (RE) ions doped perovskite structure. Rare-earth ions are used to dope perovskite-type oxide as a probe to investigate local centers and energy promoting change in optical behavior, or improve the capacitance response of these materials making possible use as high frequency ultrasonic transducer [8]. The lanthanide as Er_2O_3 is also one of most suitable active ions for several hosts. Thus, it is possible to increase the electrical property of glass-ceramics.

In this work, transparent glass-cermics 75KNN-25SiO_2 doped 0.5 and 1.0 mol%Er_2O_3 were sucessfully fabricated by incorporation technique. This technique was employ to prepare glass with a small crystal of desired phase embeded inside glass matrix. The experimental start with the calcination of oxide precursor and then mixing with glass former and rare-earth dopant as SiO_2 and

Er_2O_3, respectively The crystallization of the KNN crystals in the glass was accomplished by heat treatment processes which were also used to control the KNN crystal shape and size. Here, we report the thermal, electrical and micro-structural properties of the prepared KNN glass-ceramics.

Experimental

Sample preparation: The glass of 75KNN-25SiO_2 (mol%) doped with 0.5-1.0mol% of Er_2O_3 was prepared using incorporation method. KNN powder was firstly prepared by conventional mixed oxide method according to our previous work [5,6]. For incorporation method, the prepared KNN ceramic powder was then mixed with SiO_2 to form transparent based glass. The components were mixed in a platinum crucible and subsequently melted at 1300ºC for 15 min and then quenched between stainless steel plates. The quenched glass was immediately annealed at 300ºC (in Er_2O_3 doped glass) and 450 ºC (no dopant) for 2 hours to release their stress. Thermal properties of as-received glass were measured to find the glass transition temperature (T_g) and crystallization temperature (T_c) by using DTA [Differential thermal analysis; Du Pont Instrument, USA]. Then, annealed glass was subjected to heat treatment (HT) at temperatures ranging between 500 to 600^{o}C, depending upon the T_g and T_c of each glass, for 4 hours.

Material characterization: To analyze the glass and glass-ceramic properties, various techniques were employed. FE-SEM techniques [scanning electron microscope; JSM 6335F type, JEOL, JP] was used to investigate the composition and microstructure of the glass and glass-ceramic samples. The room temperature dielectric constant (ε_r) and dielectric loss (tanδ) of the glass-ceramics were measured in range of 10 kHz to 1 MHz using a precision LCZ meter [E4980A type, Agilent Technologies, Malaysia]. The density was measured by Archimedes method.

Results and Discussion

The DTA profile curve of KNN-SiO_2 glass and glass doped with Er_2O_3 are shown in figure 1. The DTA technique were used to understand the thermal behavior of resulting glasses which benefit for predicting the suitable temperatures for glass-ceramics samples. These DTA measurements were carried out in an air atmosphere at a heating rate of 5°C/min in the temperature range of 30°C - 800°C.

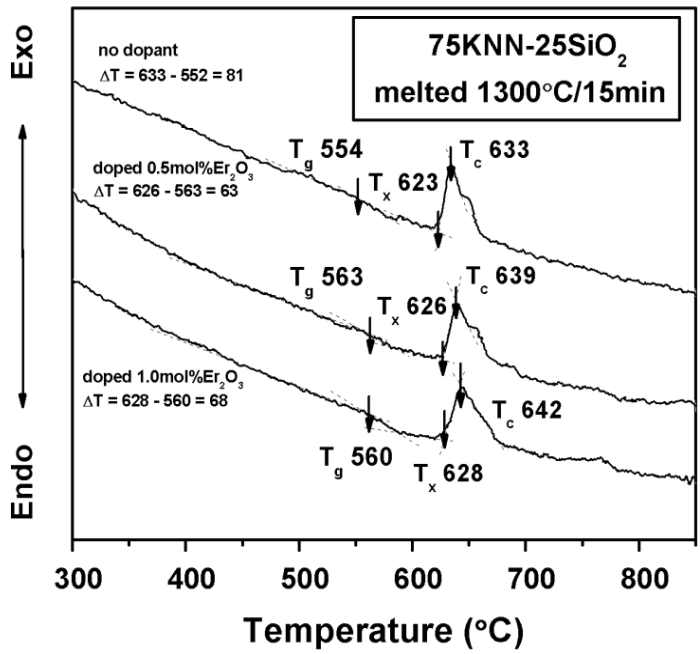

Figure 1 Thermal profile data of all glass samples by using DTA.

The intense exothermic peak of about 600°C of each composition related to crystallization temperature (T_c) of KNN crystal in glass. While, the noticeable endothermic peaks, representing by slight changes in slope of graphs as drawn by intersection point of two tangent lines at around 554°C, 563°C and 560°C, refer to the glass transition temperature (T_g) of no-dopant, 0.5mol% Er_2O_3 and 1.0mol% Er_2O_3 doped glasses, respectively. The 1.0 mol% doped 75KNN-25SiO_2 glass system has higher T_g than those found in 0 mol% and 0.5 mol% Er_2O_3 doped 75KNN-25SiO_2 glass system. This slightly change in T_g of this glass system are the result from the entering of Er_2O_3 in KNN structure, which confirmed by our previous work [6]. The Er^{3+} ions incorporated to KNN structure lead to the distortion of crystal structure and bring about the change in glass transition temperature. This result also similarly to our previous work.

The estimation of the glass stability can be done by using Hruby's criterion [7].

$$\Delta T=T_x-T_g \quad (1)$$

where T_x is the onset point of crystallization temperature (T_c) peak. This term was used for determining the ability of glass in forming nanostructured glass-ceramics after applied energy from heat treatment process. From figure 1, the highest ΔT value was found in 75KNN-25SiO_2 without Er_2O_3 glass system. The lower ΔT value suggested that glass is easy to devitrify during melting-quenching process.

The heat treatment processes was employed at various temperatures depending on the observed thermal parameters from the DTA study in order to grow crystals inside the glass matrices. The appearances of the resulting glass-ceramics are shown in figure 2. It can be seen that glass-ceramics were all pink in color and the transparency of all glasses decreased with increasing heat treatment temperature. The density of all glass and glass-ceramic compositions are showed in figure 3. The density of the 1mol% Er_2O_3 doped glass-ceramics is slightly higher that found in the 0 and 0.5mol% Er_2O_3 doped glass-ceramics. It can be noticed that the density of the glass-ceramics increases with increasing heat treatment temperature. This may correspond to the decrease in molar volume of the glass-ceramic sample during crystallization.

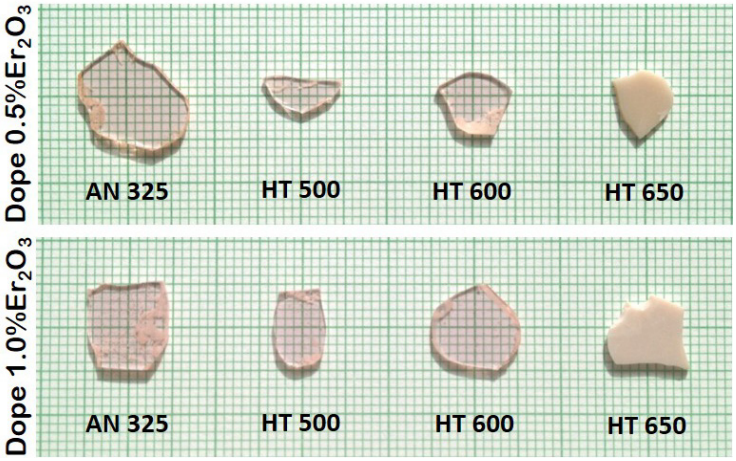

Figure 2 The appearance of glasses and glass-ceramics of 75KNN-25SiO_2 at various heat treatment temperatures. (a) doped 0.5mol% Er_2O_3, (b) doped 1.0mol% Er_2O_3

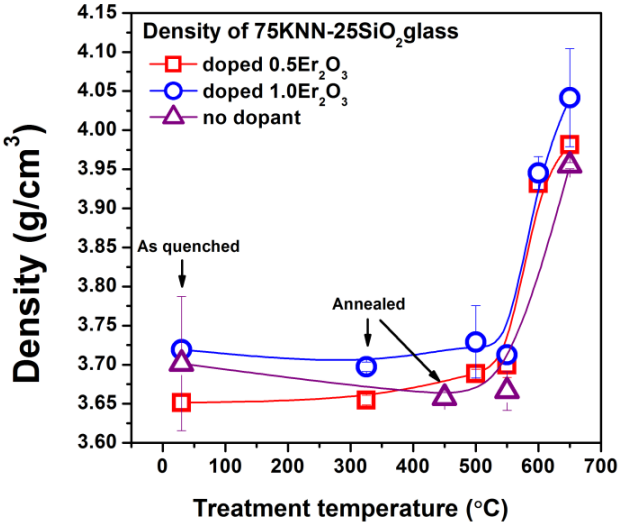

Figure 3 Glass and glass-ceramics density.

SEM micrographs of the glass ceramics are shown in figure 4. These micrographs show a bulk crystallization of the KNN phase with a different shapes observed for the glass matrices of all heat-treated samples. At 550°C heat treated sample, the small spherical shape crystal of KNN solid solution was observed in 0%Er_2O_3. However, in 0.5 and 1.0mol% Er_2O_3 dopant samples found rectangular shape crystal different from 0%Er_2O_3 around 550°C. When increasing temperature to 650°C, the crystals of all systems are gradually changed to irregular shape. It can be seen that the glass-ceramics have crystallite size lower than 1 mm but larger than 200 nm, giving rise to the lower transparency in bulk glass-ceramics. To examine the element compound, EDS technique was used (figure 5). From EDS studied at bulk crystal, the embedded crystals in the glass matrix are identified as KNN solid solution. This confirm the exit of KNN crystal structure with small Erbium ions inside.

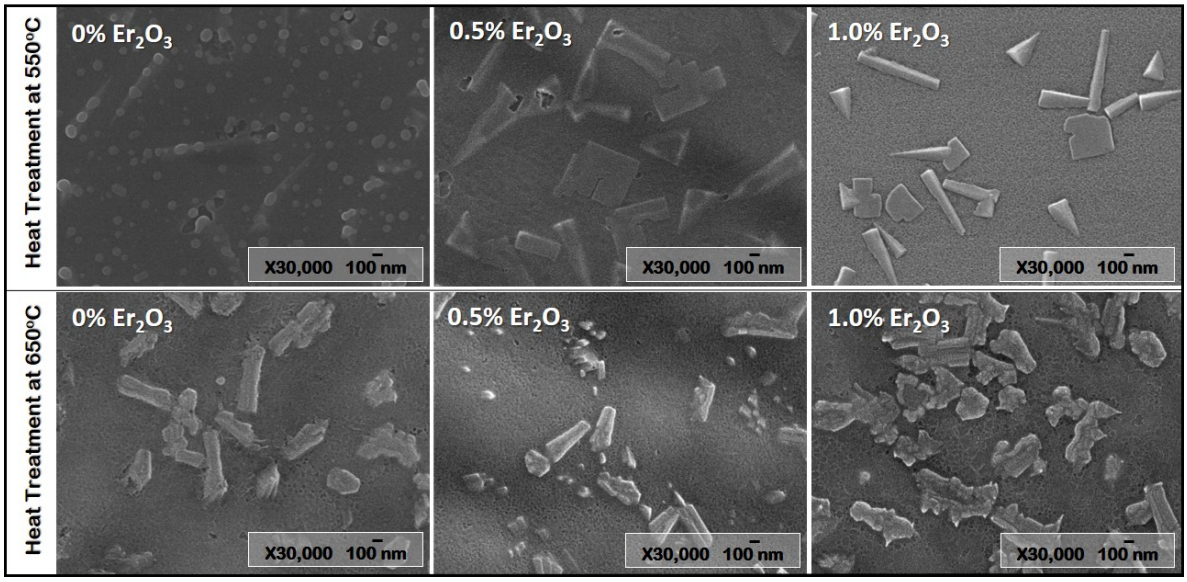

Figure 4 SEM micrograph of 75KNN-25SiO_2 doped Er_2O_3 glass-ceramics heat treated at 550˚C and 650˚C.

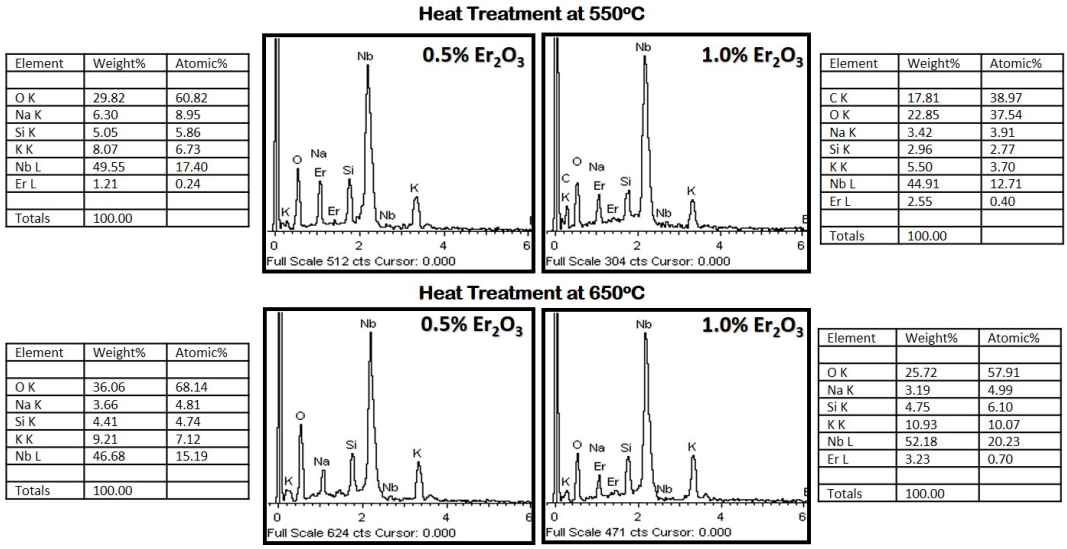

Element	Weight%	Atomic%
O K	29.82	60.82
Na K	6.30	8.95
Si K	5.05	5.86
K K	8.07	6.73
Nb L	49.55	17.40
Er L	1.21	0.24
Totals	100.00	

Element	Weight%	Atomic%
C K	17.81	38.97
O K	22.85	37.54
Na K	3.42	3.91
Si K	2.96	2.77
K K	5.50	3.70
Nb L	44.91	12.71
Er L	2.55	0.40
Totals	100.00	

Element	Weight%	Atomic%
O K	36.06	68.14
Na K	3.66	4.81
Si K	4.41	4.74
K K	9.21	7.12
Nb L	46.68	15.19
Totals	100.00	

Element	Weight%	Atomic%
O K	25.72	57.91
Na K	3.19	4.99
Si K	4.75	6.10
K K	10.93	10.07
Nb L	52.18	20.23
Er L	3.23	0.70
Totals	100.00	

Figure 5 EDS analysis of 75KNN-25SiO_2 doped Er_2O_3 glass-ceramics heat treated at 550˚C and 650˚C.

The dielectric constants (ε_r) and dielectric loss (tanδ) of heat treated glass-ceramics were measured at different freaquency from 10kHz to 1MHz and shown in figure 6. The maximum dielectric constant of about 360 at 10 kHz with rather low loss about 0.06 was found in the glass-ceramics from the glass-ceramics in composition of 75KNN-25SiO_2 doped 0.5Er_2O_3 and heat treatment at 600°C. R.S. Chaliha et al. [8] reported that glass-ceramics potassium niobate ($KNbO_3$) doped with Er^{3+} ions showed the average dielectric constant (ε_r) at about 17 which was higher than sodium silicate glasses (ε_r = 7 - 10) and borosilicate glasses (ε_r = 4.5 - 8). This might become from the ionic size of Nb^{5+} are too high. The Chaliha's report also showed that heat treatment time was significant to dielectric constant due to the possibility to increase crystal size of $KNbO_3$. Thus, in this work, it can be seen that glass-ceramics KNN crystal doped Er^{3+} can raise the dielectric constant to nearly 90 in the as-quench glasses and can increased 350 in glass-ceramics with high heat treatment temperature. Moreover, the overall tanδ of the KNN–SiO_2 glass-ceramics is below 0.1 depending on each composition and heat treatment temperature. This may be useful in the applications in electro-optic, capacitors and microwave devices.

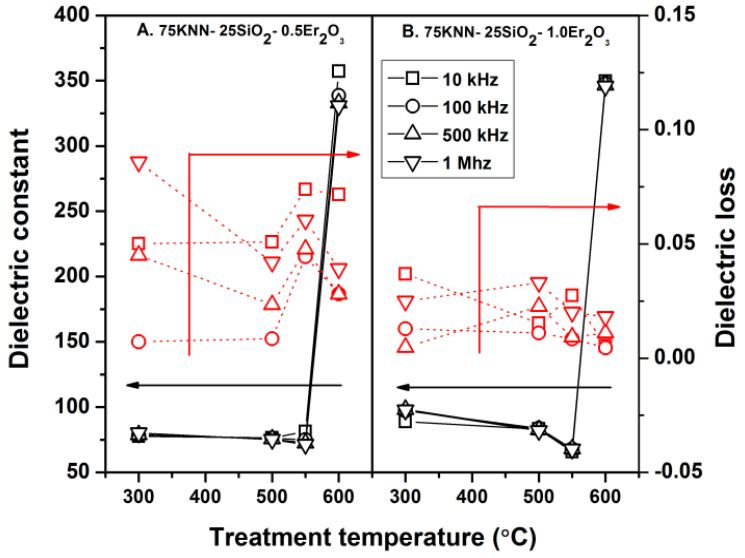

Figure 6 Dielectric constant of of 75KNN-25SiO_2 doped Er_2O_3 glass-ceramics. (A.) 0.5mol% doped Er_2O_3 and (B.) 1.0mol% doped Er_2O_3.

Conclusions

In this work, electrical and structural properties of ferroelectric glasses and glass-ceramics from $K_{0.5}Na_{0.5}NbO_3$-SiO_2 doped with 0.5-1.0 mol%Er_2O_3 system have been investigated. The influent of Er_2O_3 dopant was also compared with the original glass. From the study, KNN single phase in transparent glass was successfully prepared via incorporation method. It was indicated that heat treatment temperature plays a significant role in controlling the microstructure, crystallite sizes, and crystal quantity of the glass ceramics. The addition of Er_2O_3 can increase the dielectric constant of KNN glass-ceramic, which higher than those found in previous work. The maximum ε_r of about 360 at 10 kHz with a low tanδ of 0.07 could be obtained from the glass-ceramic sample of 75KNN–25SiO_2 doped 0.5 mol% Er_2O_3 and heat treated at 600˚C. From this work, the higher percent of Er_2O_3 of about 1.0Er_2O_3 can lower the dielectric loss of KNN glass-ceramics. This interesting value suggesting the opportunity of using them in electronic applications in the future. However, it is necessary to further study in effect of Er_2O_3 to KNN structure and optical property of this glass-ceramics system.

Acknowledgment

The authors would like to express their sincere gratitude to the Thailand Research Fund (TRF), Faculty of Science, Chiang Mai University for financial support. We wish to thank the Graduate School Chiang Mai University and The National Research University Project under Thailand's Office of the Higher Education Commission for financial support.

References

[1] G. H. Haerting, Ferroelectric Ceramics: History and Technology, J. Am. Ceram. Soc., 82 (1999) 797-818.

[2] B. Jaffe, W. R. Cook, H. Jaffe, Piezoelectric Ceramics, Academic Press Limited, London, 1971, ISBN: 0-12-379550-8.

[3] G. H. Haertling, Properties of Hot-Pressed Ferroelectric Alkaliniobate Ceramics, J. Am. Ceram. Soc., 50 (1967) 329-330.

[4] L. Egerton, D.M. Dillon, Piezoelectric and Dielectric Properties of Ceramics in The System Potassium-Sodium Niobate, J. Am. Ceram. Soc. 42 (1959) 438-442.

[5] P. Yongsiri, S. Eitssayeam, G. Rujijanagul, S. Sirisoonthorn, T. Tunkasiri, K. Pengpat, Fabrication of Transparent Lead-Free KNN Glass-ceramics by Incorporation Method, Nanoscale Res. Lett., 7 (2012) 136.

[6] P. Yongsiri, S. Sirisoonthorn, and K. Pengpat, Effect of Er_2O_3 Dopant on Electrical and Optical Properties of Potassium Sodium Niobate Silicate Glass-Ceramics, Mater. Res. Bull. 69 (2015) 84–91.

[7] A. Hruby, Evaluation of glass-forming tendency by means of DTA, Czech. J. Phys. B22 (1972) 1187.

[8] R. S. Chaliha, K. Annapurna, A. Tarafder, P.K. Gupta, B. Karmakar, V.S. Tiwari, Optical and dielectric properties of isothermally crystallized nano-$KNbO_3$ in Er^{3+}-doped K_2O–Nb_2O_5–SiO_2 glasses, Spectrochim. Acta A., 75 (2010) 243–250.

Article

Journal of
Nanoscience and Nanotechnology
Vol. 18, 6195–6200, 2018
www.aspbs.com/jnn

Non-Isothermal Crystallization Kinetics of Transparent Glass-Ceramic Phosphors Containing Calcium Magnesium Aluminosilicate Nanocrystals

Wipada Senanon[1,2], Sukum Eitssayeam[1], Gobwute Rujijanagul[1], Tawee Tunkasiri[1], Ploypailin Yongsiri[3], and Kamonpan Pengpat[1,*]

[1] *Department of Physics and Materials Science, Faculty of Science, Chiang Mai University, Chiang Mai 50200, Thailand*
[2] *Graduate School, Chiang Mai University, Chiang Mai 50200, Thailand*
[3] *Faculty of Industrial Technology, Valaya Alongkorn Rajabhat University Under Rayal Patronage, Pathumthani 13180, Thailand*

Glass-ceramic phosphors from CaO–MgO–SiO_2–Al_2O_3–ZnO co-doped with 0.5Eu^{3+}:0.1Sm^{3+} (mole%) were prepared by conventional melt-quenching method. Non-isothermal crystallization kinetics were performed by differential thermal analysis at various heating rates of 5, 10, 15 and 20 °C/min. The parent glasses were investigated by X-ray diffraction technique. From the heating rate dependence of crystallization temperature, the activation energy (E_a) of crystallization and Avrami parameter (n) were calculated by Kissinger equation and Ozawa equation, respectively. The results indicated that continuous nucleation and three-dimensional crystal growth were the dominating mechanisms in the crystallization process that was confirmed by scanning electronic microscopy and transmission electron microscopy. The luminescence properties were also determined by fluorescence spectroscopy in rang of 550–750 nm under 402 nm excitation. The results of XRD studies revealed the occurrence of diopside ($Ca_{0.8}Mg_{1.2}Si_2O_6$) phases and no other phase is observed. The emission spectra exhibited a strong red luminescence composed of 576, 599, 613 and 702 nm when excited at 402 nm.

Keywords: Crystallization Kinetics, Glass-Ceramic, Luminescence.

1. INTRODUCTION

In the past, luminescent materials were one of the important keys of technological development. Nowadays, many electronic lighting devices used in daily life are light emitting diodes (LED), which frequently contain one or more phosphor materials.[1] The properties of these phosphors materials results from the luminescence properties of the rare earth ions doped within the selected host materials. Examples of host materials that have been used in industry are SiO_2, GeO_2, B_2O_3 and P_2O_5, which are known as good glass network formers. These glass formers can generate three-dimensional random networks and form a glass structure by themselves.[2] Previously, single crystal materials with a wide variety of crystal structures were intensively studied and used in LED applications.

These phosphors showed excellent characteristics in both optical and mechanical properties. However, the single crystal growth method is rather complicated and costly. Therefore, other alternative materials such as glass-ceramic have become the best choice for the development of new generation LEDs.

Silicate glass-ceramics doped with rare earth ions and embedded with diopside ($CaMgSi_2O_6$) crystals have attracted great interest due to their special structure features, excellent physical and chemical stability, high transparency, low melting temperature, excellent thermal stability and good rare earth ion solubility.[3] Moreover, they can be produced at a low cost[4] and have been utilized in many applications for optical devices,[5,6] due to the luminescence properties such as the long afterglow phenomenon of glasses.

Guo et al.[7] reported that the diopside glass-ceramic prepared by conventional method always presented two-dimensional crystal growth. Yang et al.,[8] found that surface crystallization and irregular distribution of crystals growth occurred in their glass-ceramics. In addition,

*Author to whom correspondence should be addressed.

Zhang et al.[9] studied crystallization kinetics of diopside crystals from the $CaO–MgO–SiO_2–Al_2O_3–Fe_2O_3–Na_2O–CaF_2–SO_8$ glass system with different heating rates of 10, 20, 30 and 40 °C/min. The Avrami parameter (n) and the activation energy (E_a) were calculated as 4.39 and 152.79 kJ/mol, respectively. These parameter values indicated continuous nucleation and three-dimensional crystal growth. Transparency of such a glass-ceramic having surface crystallization tends to drop, giving rise to a decrease in optical properties, while bulk crystallization enhances the optical properties of glass-ceramic materials.[10]

Therefore, the bulk crystallization of suitable size and homogeneously distributed diopside crystals in the glass-matrix is required. It is essential to obtain control of processing parameters and understanding of the crystallization mechanism of diopside crystals in glasses. This is beneficial for morphology and microstructure of diopside glass-ceramic designed for use as a host material of rare earth ions. Measuring crystallization kinetics is a useful method for understanding the nucleation and crystal growth in materials especially glasses. The nucleation and growth rates are important keys in the crystallization process and evaluated in terms of the Kissinger modified by Matusita and Ozawa equation which can be applied to calculate the crystallizations activation energy (E_a) and Avrami parameter (n). These two constants can be used to understand the crystallization mechanisms in any glass system.[11]

Hence, in this study, the glass-ceramic system of $20CaO–15MgO–50SiO_2–10Al_2O_3–5ZnO$ co-doped with $0.5Eu^{3+}/0.1Sm^{3+}$ was prepared using conventional methods and the crystallization kinetics of this glass system were investigated. The crystallization kinetics were carried out by differential thermal analysis (DTA) under non-isothermal conditions. The activation energy of crystallization process were determined by the modified Kissinger's equation. The phase formations in the glass-ceramics were investigated by X-ray diffraction (XRD) technique. The continuous nucleation and crystal growth were confirmed by scanning electron microscopy (SEM) and transmission electron microscopy (TEM) of the glass. The luminescence properties were determined by using a fluorescence spectrometer (FL).

2. EXPERIMENTAL DETAILS

Samples of the parent glass of $20CaO–15MgO–10Al_2O_3–50SiO_2–5ZnO$ co-doped with $0.5Eu_2O_3/0.1Sm_2O_3$ (mol%) composition were prepared with weight of about 30 g. The nominal composition of the parent glass was $20CaCO_3$, 15MgO, $10Al_2O_3$, $50SiO_2$, 5ZnO, $0.5Eu_2O_3$, and $0.1Sm_2O_3$ (mol%). All starting materials were mixed and melted in a platinum crucible using an electric furnace at 1500 °C for 4 h. The melt was quenched by pouring onto a stainless steel plate. Small pieces of the quenched glass were ground into a fine powder.

The study of crystallization kinetics was carried out by differential thermal analysis (DTA) under non-isothermals conduction with various heating rates of 5, 10, 15 and 20 °C/min. The furnace temperature was ramped from room temperature to 1200 °C. To study the mechanism of crystal growth in glasses, the obtained glasses were subjected to heat treatment at various temperatures from 850–950 °C for 1 h. This rang was chosen from crystallization temperature peaks. The heating rate and cooling rate used were 5 °C/min (chosen from optimized DTA result). To determine the phase formation of the prepared glass-ceramic samples, X-ray diffraction analysis (XRD) was performed.

The continuous nucleation and crystal growth were confirmed by scanning electron microscopy (SEM). Scanning electron microscopy was employed for microstructure observation on the thermally-etched surfaces of the glass-ceramic samples. The TEM images of glass-ceramics powder were acquired by transmission electron microscopy (TEM: JEM2010). Emission spectra were measured in the range of 550–750 nm under 402 nm excitation by a Fluoro Max-4 spectrofluorometer (HORIBA JOBIN YVON) with a 450 W xenon lamp at room temperature.

3. RESULTS AND DISCUSSION

The DTA curves of the parent glass using different heating rates of 5, 10, 15 and 20 °C/min are illustrated in Figure 1. The glass transition and crystallization peak temperatures (T_g and T_p) were deduced from the DTA curves as shown and listed in Table I.

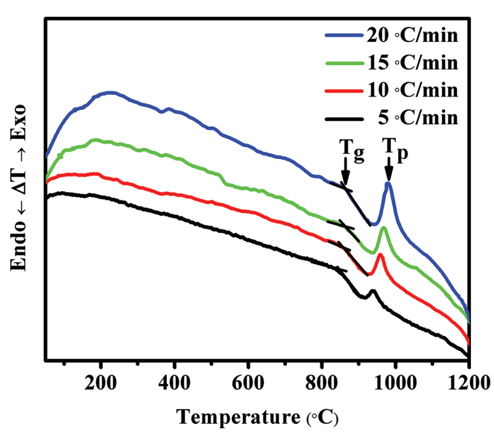

Figure 1. DTA curves of the $CaO–MgO–Al_2O_3–SiO_2–ZnO$ glass at different heating rates (α) of 5, 10, 15 and 20 °C/min.

Table I. Glass transition temperature (T_g) and crystallization peak temperature (T_p) of the parent glass at different heating rates.

Rate (°C/min)	T_g	T_p	ΔT
5	847.8	937.8	26.9
10	859.6	958.1	29.9
15	862.5	967.2	33.1
20	864.1	979.2	39.0

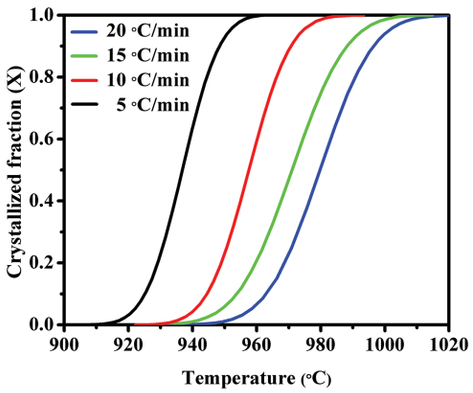

Figure 2. Crystallization fraction (X) as a function of temperature at different heating rates for crystallization curve.

The glass transition temperature (T_g) and crystallization peak temperature (T_p) were found in the ranges of 847.87–864.12 °C and 937.54–979.63 °C, respectively. It can also be noticed that these T_g and T_p increased with increasing heating rates. The difference temperature between T_p and T_g ($\Delta T = T_p - T_g$) can also describe the glass stability. From Table I, the increase in glass stability value can be related to the reduced tendency to form crystallization.

The crystallization fraction ($X(T)$), was determined from the T_p peaks. These peaks are strongly related to the heat generated from the crystal growth process of the diopside crystals in the glass-matrix. The crystallization fraction can be determined by using the relationship as in Eq. (1):[12]

$$X(T) = \frac{S_t}{S} \tag{1}$$

where $X(T)$ is a crystal fraction at any temperature, S_t is a partial area of the exothermic peak up to the temperature (t) and S is a total area of the exothermic peaks. Figure 2 shows $X(T)$ against temperature for the crystallization peaks of parent glass at heating rates of 5–20 °C/min. The S-type curve can be attributed to the growing of the saturated nuclei until the final stage of the complete crystallization of diopside crystals. These

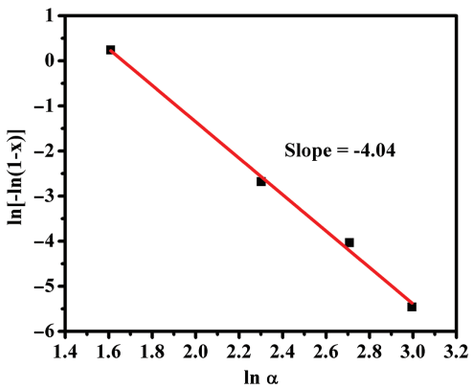

Figure 3. Ozawa plot for determining the Avrami parameter (n).

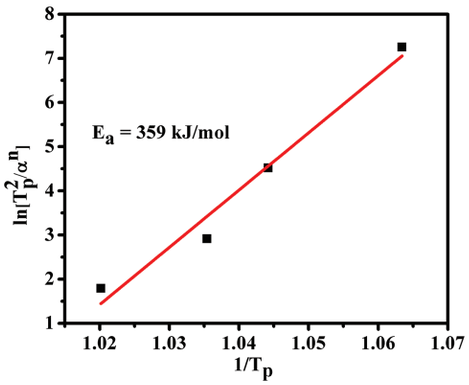

Figure 4. Modified Kissinger's equation plot for determining (E_a).

S-type curves shifted to higher temperature with increasing heating rate. Moreover, it may be assumed that at slow heating rate, nucleation increased in the sample, due to the increase in energy storage time. At high heating rate, the energy required for nucleation transfer was very fast. Therefore, energy needed for nucleation was provided at higher temperature. For non-isothermal measurements, a constant heating rate is used until complete crystallization. It is usually applied to learn the devitrification of different glasses and the rapidity with which this thermonalytical technique can be performed. The value of the Avrami parameter (n) was calculated by linear fit to the experimental data based on Ozawa equation as shown in Eq. (2).

$$\ln[-\ln(1-x)] = -n \ln \alpha \tag{2}$$

Figure 3 shows the plot of $\ln[-\ln(1-x)]$ against $\ln \alpha$ where x is the volume fraction of crystals and α is heating rate. The n value was calculated as 4.04 for $20CaO–15MgO–10Al_2O_3–50SiO_2–5ZnO$ co-doped with $0.5Eu_2O_3/0.1Sm_2O_3$ glasses. This obtained n value of about 4 can be used to determine the crystallization mechanism in the glass-ceramic. In this case bulk crystallization was the dominating mechanism during the crystallization process.[13]

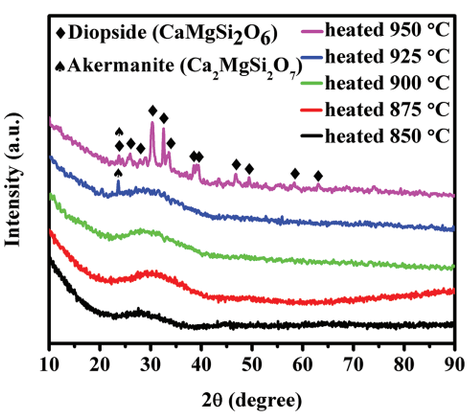

Figure 5. XRD patterns of glass-ceramic samples heat treated at 850, 875, 900, 925 and 950 °C for 1 h.

These results also verified that continuous nucleation also occurred during the crystallization process of the parent glass, which can be confirmed by SEM results.

The activation energy E_a value is associated with an energy barrier when the glass matrix transforms into the crystalline phase. It is easier for the glass to crystallize if the energy is low.[14, 15] The activation energy (E_a) of $20CaO–15MgO–10Al_2O_3–50SiO_2–5ZnO$ co-doped with $0.5Eu^{3+}/0.1Sm^{3+}$ glasses was calculated the by modified Kissinger equation in Eq. (3):

$$\ln\left(\frac{T_p^2}{\alpha^n}\right) = \frac{mE_a}{RT_p} + \text{const.} \quad (3)$$

where T_p is the crystallization peak temperature for a heating rate (α), E_a is an activation energy, R is a gas constant (8.314 J/mol · K), n is the Avrami parameter and m is a crystallization mechanism. The activation energy, (E_a) was determined from a linear fit of $\ln(T_p^2/\alpha^n)$ against $1/T_p$ plot as shown in Figure 4.

The value of activation energy was obtained as 359 kJ/mol. These results were higher than the activation energy of the crystallization process of $CaO–MgO–SiO_2–Al_2O_3–Fe_2O_3Na_2O–CaF_2–SO_8$ glass system (152 kJ/mol) as reported by Zhang,[16] which implies that the phase transition of diopside trace crystals in our glass trace system was more difficult than for the previous glass system.

Figure 5 shows the XRD patterns of the glass-ceramic samples obtained by different heat treatment temperatures where the heating rate was fixed at 5 °C/min because this at heating rate nucleation will increase in the sample, due to the increase in energy storage time.[17] It can be seen that the glass-ceramic samples heat treated at 850, 875 and 900 °C for 1 h consisted of only a broad peak centered at around $2\theta \approx 28$ degree confirming the amorphous phase in these samples. The XRD patterns of the glass-ceramics subjected to heat treatment at higher temperatures from 925 °C to 950 °C for 1 h contained well-pronounced diffraction peaks which were attributed

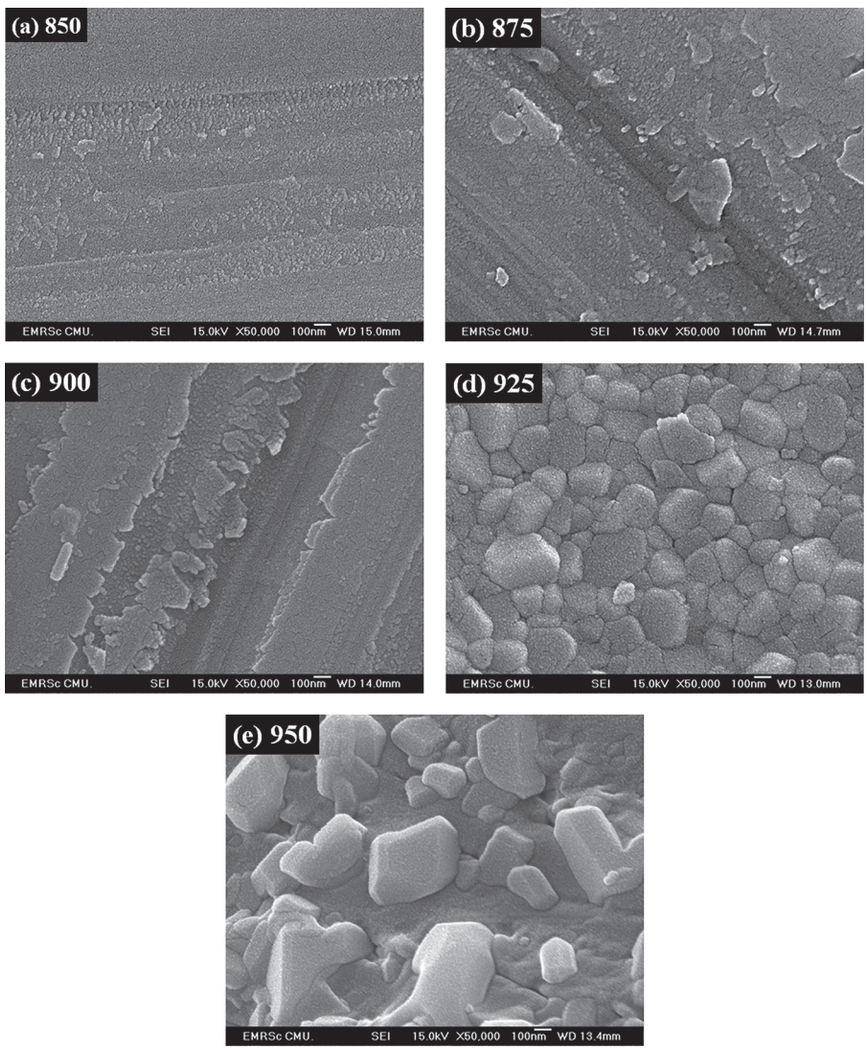

Figure 6. SEM images of glass-ceramic samples were heat treatment at (a) 850, (b) 875, (c) 900, (d) 925 and (e) 950 °C for 1 h.

to the better crystallinity in these glass-ceramic. It can be assumed that all of the glass-ceramics samples contain the diopside ($Ca_{0.8}Mg_{1.2}Si_2O_6$) phase (JCPDS file no. 76-0238) and akermanite ($Ca_2MgSi_2O_7$) phase (JCPDS file no. 35-0592) was observed.

SEM micrographs of glass-ceramic samples are shown in Figure 6. From the micrographs of samples heat treated at 850 °C to 900 °C for 1 h, no crystallization particles were observed which corresponded to the XRD result with heat treatment at higher temperatures, bulk crystallization occurred above 925 °C as can be seen in Figures 6(d)–(e). The clusters of diopside crystals were clearly observed for high temperatures and the crystallite size tended to increase with increasing heat treatment temperature. The XRD and SEM results confirmed the three-dimensional crystal growth of diopside crystals which agrees well with the crystallization kinetics as previously mentioned. Even though the diopside crystals seemed to be the dominant phase in these glass-ceramics, transmission electron micrographs of the glass-ceramic heat treated at 925 °C, as shown in Figure 7(a), revealed bulk crystals of tetragonal $Ca_2MgSi_2O_7$ (Akermanite) with crystal size of approximately 214 ± 38 nm together with monoclinic $Ca_{0.8}Mg_{1.2}Si_2O_6$ (diopside) and in Figure 7(b) (950 °C) with a slightly increase size of about 301 ± 99 nm.

The corresponding XRD patterns in Figure 5 showed no trace of $Ca_2MgSi_2O_7$ phase which may be due to the very small amount of this secondary phase which occurred in the glass-matrix. However, the work by Tulyagonov[18] reported that some $Ca_2MgSi_2O_7$ phase could be co-precipitated with diopside phase in the CaO–MgO–SiO_2 glass system with B_2O_3, P_2O_5, Na_2O and CaF_2 additives.

The luminescence properties of glass-ceramic co-doped with Eu^{3+}/Sm^{3+} were investigated by excitation and emission spectra. The emission spectra of the glass-ceramic system co-doped with Eu^{3+}/Sm^{3+} with different heat treatment temperatures from 850–950 °C for 1 h under 402 nm excitation are shown in Figure 8. The emission spectra of Eu^{3+} ions exhibited four emission transitions of $^5D_0 \rightarrow {}^7F_0$ (576 nm), $^5D_0 \rightarrow {}^7F_1$ (599 nm), $^5D_0 \rightarrow {}^7F_2$ (613 nm), $^5D_0 \rightarrow {}^7F_4$ (702 nm), while Sm^{3+} ions emitted $^4G_{5/2} \rightarrow {}^6H_{5/2}$ (563 nm), $^4G_{5/2} \rightarrow {}^6H_{7/2}$ (598 nm) and $^4G_{5/2} \rightarrow {}^6H_{9/2}$ (645 nm). These correspond to transition

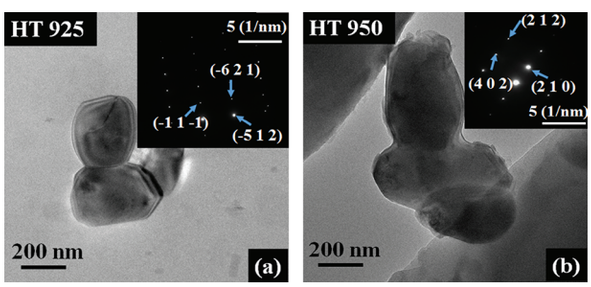

Figure 7. TEM images of glass-ceramic samples heat treated at (a) 925 °C and (b) 950 °C for 1 h.

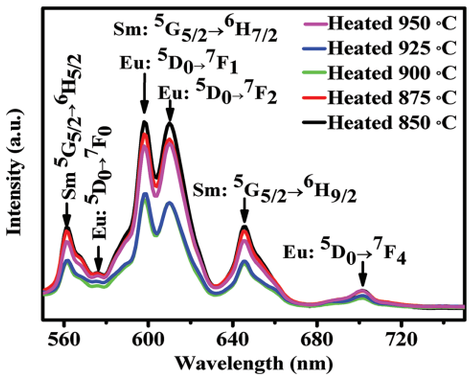

Figure 8. The emission spectra of $0.5Eu^{3+}/0.1Sm^{3+}$ co-doped glass-ceramics samples heat treated at 850, 875, 900, 925 and 950 °C for 1 h excited at 402 nm.

found in related works.[19] The emission spectra at 599 nm exhibited the mixing of Sm^{3+} and Eu^{3+} electronic transitions of $^4G_{5/2} \rightarrow {}^6H_{7/2}$ and $^5D_0 \rightarrow {}^7F_2$.

The emission spectra show similar line shapes for all heat treatment temperatures. It can be noticed that the highest emission intensity of samarium $^4G_{5/2} \rightarrow {}^6H_{7/2}$ (599 nm) transition is similar to that of the europium $^5D_0 \rightarrow {}^7F_2$ (613 nm) transition. Moreover, the presence and raising of Eu^{3+} (activator) emission intensity in the Sm^{3+} ion (sensitizer) co-doped glass-ceramic system could imply the possible energy transfer from Sm^{3+} ion to Eu^{3+} ion. Usually, Sm^{3+} emission intensity should decrease while Eu^{3+} emission intensity increase if energy transfer has occurred from sensitizer to activator in a co-doped glass-ceramic system.[20] In this work we found that Sm^{3+} and Eu^{3+} emission intensity at 599 nm and 613 nm were closely similar. This behavior of 599 nm emission intensity may be caused by the mixed effect of magnetic dipole transition of $^4G_{5/2} \rightarrow {}^6H_{7/2}$ of Sm^{3+} and $^5D_0 \rightarrow {}^7F_1$ (599 nm) of Eu^{3+}. The increasing heat treatment temperatures caused a huge crystallite volume fraction as confirmed by the XRD result. Even though the crystallinity of the glass-ceramics tended to increase with increasing heat treatment temperature, the intensity of emission spectra did not follow the same trend at 850, 875 and 950 °C which exhibited high emission intensity while glass-ceramics heat treated at 900 and 925 °C exhibited low emission intensity. This may be caused by crystallite size, crystallite distribution and the fluctuation in transparency in the measured glass-ceramic samples. Further studies should be carried out to clearly understand this problem.

4. CONCLUSIONS

Glass-ceramics in the system of CaO–MgO–SiO_2–Al_2O_3–ZnO co-doped with europium and samarium were successfully prepared via melt quenching methods. The DTA result showed that the glass transition temperature (T_g), the crystalline temperature (T_p) and ΔT shifted to higher temperature with increasing heating rates, which increased

glass stability and reduced tendency to form crystallization. The avrami parameter of the parent glass was determined as 4, indicating the bulk crystallization during crystallization process. The activation energy was calculated as 359.3 kJ/mol. The XRD result confirmed that the diopside ($Ca_{0.8}Mg_{1.2}Si_2O_6$) phase and akermanite ($Ca_2MgSi_2O_7$) was observed. The SEM micrographs exhibited the bulk crystallization of diopside crystals distributed in the glass matrices. The increase in heat treatment temperature caused an increase in crystallite size. The TEM images showed bulk crystals of tetragonal ($Ca_2MgSi_2O_7$: Akermanite) with the size of approximately 301 ± 99 nm together with monoclinic ($Ca_{0.8}Mg_{1.2}Si_2O_6$: diopside) with a slightly smaller size of about 213 ± 37 nm. The luminescence spectra showed several emission peaks were under excitation at 402 nm. The main emission peaks were located at 599 nm for Sm^{3+} and 612 nm for Eu^{3+} transitions. The obtained glass-ceramic samples could be classified as orange-red phosphors.

Acknowledgment: The authors would like to express their sincere gratitude to Faculty of Science, and the Graduate School, Chiang Mai University for financial support. Wipada Senanon also expresses her thanks to the Science Achievement Scholarship of Thailand (SAST).

References and Notes

1. W. Senanon, R. Tipakontitikul, and A. Niyompan, *Ceram. Int.* 41, S421 (**2015**).
2. M. Çelikbilek, A. E. Ersundu, and S. Aydın, Crystallization kinetics of amorphous materials, Advances in Crystallization Processes, edited by Y. Mastai, InTech (**2012**), DOI: 10.5772/35347. Available from: https://www.intechopen.com/books/advances-in-crystallization-processes/crystallization-kinetics-of-amorphous-materials.
3. F. Kuei-Chih, Ch. Chen-Chia, Ch. Li-Wen, and Ch. Haydn, *Meter. Res. Bull.* 47, 2851 (**2012**).
4. Y. Fuqian and C. M. James, *Mater. Sci. Eng. R: Rep.* 74, 233 (**2012**).
5. T. Peijing, H. Jinshu, Z. Gaoke, and Y. Qin, *Key En. Mat.* 509, 303 (**2012**).
6. J. Fu, *J. Am. Ceram.* 83, 2613 (**2000**).
7. X. Guo, X. Cai, J. Song, G. Yang, and H. Yang, *J. Non-Cryst. Solids* 405, 63 (**2014**).
8. J. Yang, B. Liu, S. Zhang, and A. A. Volinsky, *J. Alloy Comp.* 688, 709 (**2016**).
9. S. Zhang, J. Yang, B. Liu, D. Pan, C. Wu, and A. Volinsky, *J. Iron and Steel Res. Int.* 23, 220 (**2016**).
10. T. Toya, Y. Tamura, Y. Kameshima, and K. Okada, *Ceram. Int.* 30, 983 (**2004**).
11. L. Jiang, C. Chang, D. Mao, and C. Feng, *J. Alloy and Comp.* 377, 211 (**2004**).
12. J. Cheng, P. Tian, W. Zheng, J. Xie, and Z. Chen, *J. Alloy Comp.* 471, 470 (**2009**).
13. P. Tian, J. Cheng, W. Zheng, and H. Li, *Thermochim. Acta* 494, 30 (**2009**).
14. M. Marinovic-Cincovic, B. Jankovic, B. Milicevic, Z. Antic, R. K. Whiffen, and M. D. Dramicanin, *Powder Technol.* 249, 497 (**2013**).
15. C. Wu, Y. Ramaswaswamy, and H. Zreiqat, *Acta Biomater.* 6, 2237 (**2010**).
16. H. Shao, K. Liang, and F. Peng, *Ceram. Int.* 30, 927 (**2004**).
17. K. Oguri, N. Funamori, F. Sakai, T. Kondo, T. Uchida, and T. Yagi, *Earth Planet. Int.* 104, 363 (**1997**).
18. D. U. Tulyaganov, S. Agathopoulos, J. M. Ventura, M. A. Karakassides, O. Fabrichnaya, and J. M. F. Ferreira, *J. Eur. Ceram. Soc.* 26, 1463 (**2006**).
19. A. N. Meza-Rocha, A. Speghini, M. Bettinelli, and U. Caldino, *J. Lumin.* 167, 305 (**2015**).
20. Z. Cui, R. Ye, D. Deng, Y. Hua, S. Zhao, G. Jia, C. Li, and S. Xu, *J. Alloy Compd.* 509, 3553 (**2011**).

Received: 6 July 2017. Accepted: 8 January 2018.

Integrated Ferroelectrics
An International Journal

ISSN: 1058-4587 (Print) 1607-8489 (Online) Journal homepage: https://www.tandfonline.com/loi/ginf20

The effect of heat treatment temperature on phase formation and luminescence properties of calcium magnesium silicate glass-ceramics doped with Sm_2O_3

Wipada Senanon, Tawee Tunkasiri, Sukum Eitssayeam, Gobwute Rujijanagul, Ploypailin Yongsiri, Anuson Niyompan & Kamonpan Pengpat

To cite this article: Wipada Senanon, Tawee Tunkasiri, Sukum Eitssayeam, Gobwute Rujijanagul, Ploypailin Yongsiri, Anuson Niyompan & Kamonpan Pengpat (2019) The effect of heat treatment temperature on phase formation and luminescence properties of calcium magnesium silicate glass-ceramics doped with Sm_2O_3, Integrated Ferroelectrics, 195:1, 11-18, DOI: 10.1080/10584587.2019.1570040

To link to this article: https://doi.org/10.1080/10584587.2019.1570040

Published online: 07 May 2019.

INTEGRATED FERROELECTRICS
2019, VOL. 195, 11–18
https://doi.org/10.1080/10584587.2019.1570040

Taylor & Francis
Taylor & Francis Group

The effect of heat treatment temperature on phase formation and luminescence properties of calcium magnesium silicate glass-ceramics doped with Sm_2O_3

Wipada Senanon[a,b], Tawee Tunkasiri[a], Sukum Eitssayeam[a], Gobwute Rujijanagul[a], Ploypailin Yongsiri[a], Anuson Niyompan[c], and Kamonpan Pengpat[a]

[a]Department of Physics and Materials, Faculty of Science, Chiang Mai University, Chiang Mai, Thailand; [b]Graduate School, Chiang Mai University, Chiang Mai, Thailand; [c]Department of Physics, Faculty of science, Ubon Ratchathani University, Ubon Ratchathani, Thailand

ABSTRACT

The transparent glasses of CaO-MgO-Al_2O_3-SiO_2-ZnO system doped with Sm_2O_3 was prepared by conventional melt-quenching method. The obtained glasses were heat treated at a suitable temperature (875 °C–920 °C for 2 h) identified by differential thermal analysis (DTA). Phase formation and microstructure of glass-ceramics were characterized by X-ray diffraction and scanning electron microscopy, respectively. The optical transmission spectra were recorded by UV-Vis spectrophotometer in the wavelength range between 350 and 1000 nm. It was found that the increase in heat treatment temperature reduced the transparency of the glass-ceramics. The luminescence properties were identified by fluorescence spectroscopy. The excitation spectra of Sm_2O_3 doped CaO-MgO-Al_2O_3-SiO_2-ZnO glass-ceramic samples are in wavelength range of 550–750 nm and the emission spectra exhibited a strong orange-red luminescence composed of 562, 599 and 654 nm under excited at 402 nm. The results of XRD studies revealed the occurrence of diopside ($CaMgSi_2O_6$) and akermanite ($Ca_2MgSi_2O_7$) phases. The increasing of heat treatment temperature has no effect on the shift of emission spectra.

ARTICLE HISTORY
Received 31 October 2017
Accepted 22 June 2018

KEYWORDS
Glass-Ceramics;
Luminescence;
Heat Treatment

1. Introduction

In the part decades, many researchers are interested in the luminescence glass doped with rare earth ions. The glasses doped with rare earth ions exhibit fluorescence characteristic, high conversion efficiency, stable physical and chemical properties, which are assigned to the electron transition of ^4f_n electron configuration [1]. The luminescence glasses doped with rare earth ions are considered as good candidates for laser and optical devices [2,3]. Among rare earth ions, samarium (III) ion doped glasses gained great attention due to their technological application and optical properties [4]. It can be used in high density optical storage, color displays, absorbed in UV-visible and it is emitted by electron transition from in $^4G_{5/2}$ luminescence level exhibiting high quantum

CONTACT Kamonpan Pengpat kpengpat@gmail.com Department of Physics and Materials, Faculty of Science, Chiang Mai University, Chiang Mai 50200, Thailand
Color versions of one or more figures in the article can be found online at www.tandfonline.com/ginf.

efficiency. Moreover, it can be used in the color convention and the tepid of white light emitting diode.

Glass matrix materials are very important for improving optical devices doped with rare earth ions. These require excellent respond in both optical and mechanical properties. The silicate material is of particular interest as it has potential application in luminescence materials matrix, due to its excellent uniformity, good thermal stability and low-cost production [5].

Most common crystal phases for doping Sm^{3+} are $Ca_2MgSi_2O_7$ and $LiLa_2O_2BO_3$ as they exhibit good luminescence properties [6–8]. They are both suitable host materials for red emitting phosphor. For $LiLa_2O_2BO_3$, oxyborate group ($O_2BO_3^{-7}$) can act as a good Eu^{3+} site without concentration quenching, while Sm^{3+} ions prefer to situate in the six coordinated Ca^{2+} site of $Ca_2MgSi_2O_7$ crystals.

In this study, glass-ceramics based on CaO-MgO-SiO_2-Al_2O_3-ZnO doped with $0.5Sm^{3+}$ system were prepared by conventional melt-quenching method. Then, we emphasized on the discussion of the effect of heat treatment temperature on phase formation and luminescence properties. The obtained information will be useful for more series works of an attempt to improve the glass-ceramic phosphor suggesting to new optical devices.

2. Experiment

Glass with composition of 20CaO-15MgO-50SiO_2-10Al_2O_3-5ZnO doped with $0.5Sm^{3+}$ (mol %) were prepared by melt quenching method. All starting materials were mixed and melted in alumina crucible in an electric furnace at 1500 °C for 4 h. The melt was subsequently quenched by pouring into stainless steel plates and cooled to room temperature. Some portions of the obtained glasses were grounded to fine powder and subjected to differential thermal analysis (DTA) as to investigate thermal properties. The obtained glass sample was then subjected to heat treatment with heating rate of 5 °C/min. The phase formation and microstructure of glass and glass-ceramics were identified by X-ray diffraction analysis (XRD-CuK_α) and scanning electron microscopy (SEM). The transmission spectra were recorded by UV-Vis spectrophotometer in the wavelength range 350-1000 nm. The luminescence properties were investigated by fluoro Max-4 Spectrofluorometer (HORIBA TOBIN YVON) with a 450 xenon lamp at room temperature in rang of 550–750 nm.

3. Results and discussion

The DTA curve of parent glass using heating rate of 5 °C/min is illustrated in Figure 1. The glass transition temperature (T_g) was observed at 845 °C. In addition, the crystallization temperature (T_c) was observed at 925 °C. The exothermic peak is correspondent to the precipitation of the main crystalline phases from glass matrix. Therefore, four temperatures such as 875, 890, 905 and 920 °C were chosen for determining the crystallization behavior of the glass-ceramic materials.

Figure 2 shows the XRD patterns of glass and glass-ceramic samples obtained by different heat treatment temperature. The as-quenched glass consists of only broad peak

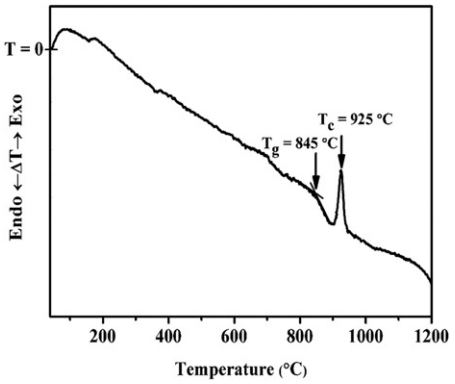

Figure 1. DTA curve of the as-quenched of CaO-MgO-Al_2O_3-SiO_2-ZnO glass doped with Sm_2O_3.

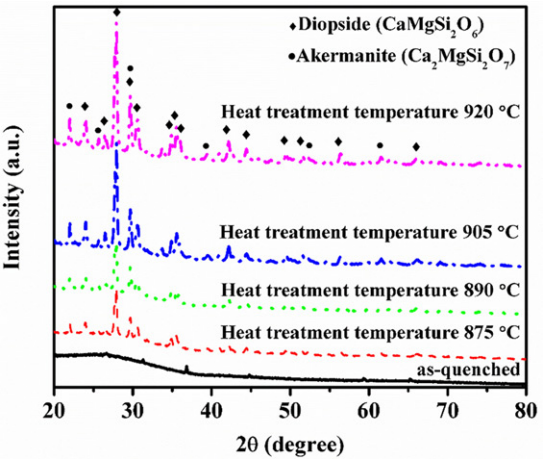

Figure 2. XRD patterns of glass and glass-ceramic samples of as-quenched and heat treated at 875, 890, 905 and 920 °C, respectively for 2 h.

centering at about $2\theta \approx 27$ degree confirming amorphous phase in this glass system. When the initial glass was heat treated at 875 °C for 2 h, a few diffraction peaks existed on the curve, ascribing to the formation of some small crystalline particles in glass matrix. The small particles can also be noticed in Figure 3a. The well-pronounced diffraction peaks related to the better crystallinity in these glass-ceramic after heat treatment at high temperature from 890 °C to 920 °C for 2 h. It can be noticed that all of the glass-ceramic samples compose of the diopside ($CaMgSi_2O_6$) phase, having a monoclinic structure c2/p space group (JCPDS file No. 17-0318) and akermanite ($Ca_2MgSi_2O_7$) phase with a tetragonal structure P-421m space group (JCPDS file No. 02.0824), respectively. No change in the shape and position of XRD patterns, with increasing heat treatment temperature but the slight increases in intensity were observed, meaning that the main crystal phase is slightly effected by heat treatment temperature in calcium magnesium silicate glass-ceramics. At the same time, these results of glasses heat treated at 920 °C and 875 °C are significant different in intensity.

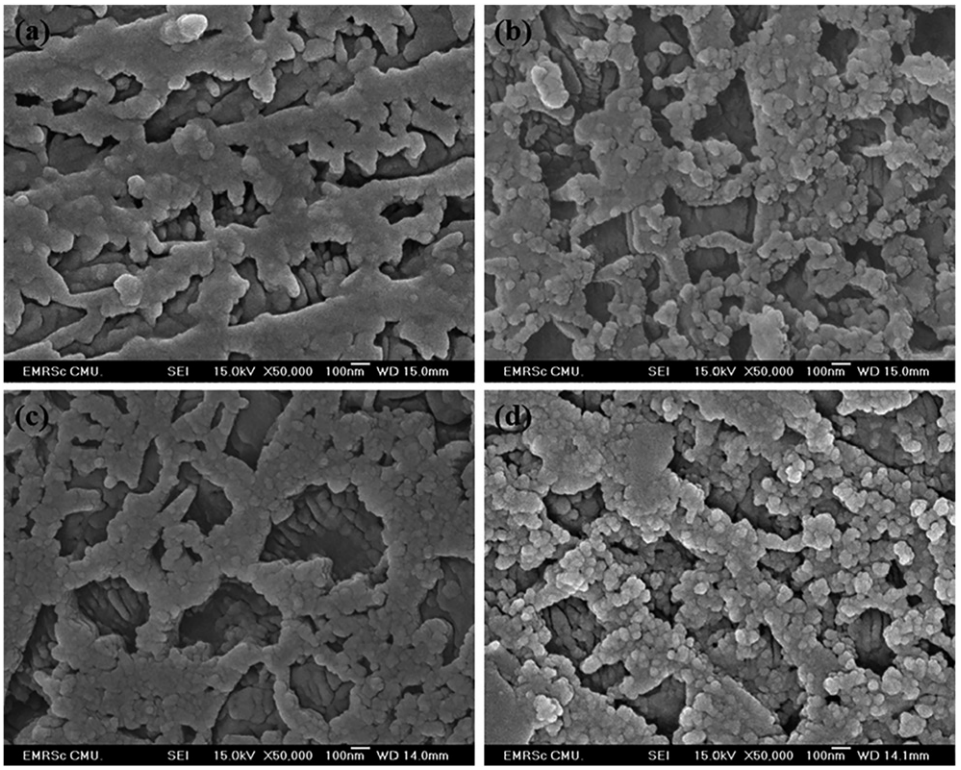

Figure 3. SEM micrographs of glass-ceramic heat treated at different temperatures at (a) 875 °C, (b) 890 °C, (c) 905 °C, and (d) 920 ° for 2 h.

This may be caused by the increasing of crystallinity of glass samples with increasing heat treatment temperature as confirmed by SEM results.

The SEM results of the prepared glass-ceramics with different heat treatment temperatures are shown in Figure 3. The microstructure of the samples heat treated at 875 °C in Figure 3a exhibited the nano crystallite size as about 100 nm which randomly distributed in the notice glass. The noticeable crystals exhibited both spherical and dendrite shape, which can be identified as diopside ($CaMgSi_2O_6$) and akermanite ($Ca_2MgSi_2O_7$) phase. When using higher heat treatment temperatures of 890 to 920 °C, it can be found that the amount of both phase increased. On the other hand, we found that the glass-ceramic sample heat treated at 905 °C exhibited higher amount of dendrite shape crystals that of spherical one. This may answer the higher intensity of the luminescence spectra of the glass-ceramic heat treated at 905 °C than other glass-ceramics heat treated at 890 to 920 °C as seen Figure 6.

The transmission spectra of Sm^{3+} doped with calcium magnesium silicate glass and glass-ceramics measured at room temperature in range of 350-1000 nm are shown in Figure 4. The as-quenched glass sample and samples heat treated at 875 °C and 890 °C are transparent as seen Figure 5a–c, respectively. Absorption peaks of the glass and glass-ceramics were observed at 373, 402 and 475 nm. The peak at 402 nm exhibited high absorption band, corresponding to the exited state $^6P_{3/2}$. These there absorption peaks corresponds to transition of Sm^{3+} $^6H_{5/2}\rightarrow{}^6P_{7/2}$, $^6H_{5/2}\rightarrow{}^6P_{3/2}$ and $^4I_{13/2}\rightarrow{}^4M_{15/}$

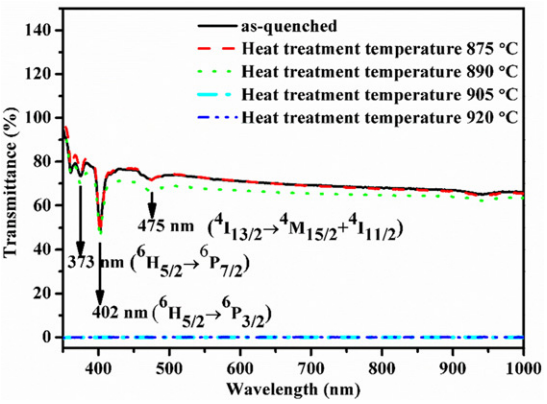

Figure 4. Percent transmittance of glass and glass-ceramic samples of as-quenched and heat treated at 875, 890, 905 and 920 °C, respectively for 2 h.

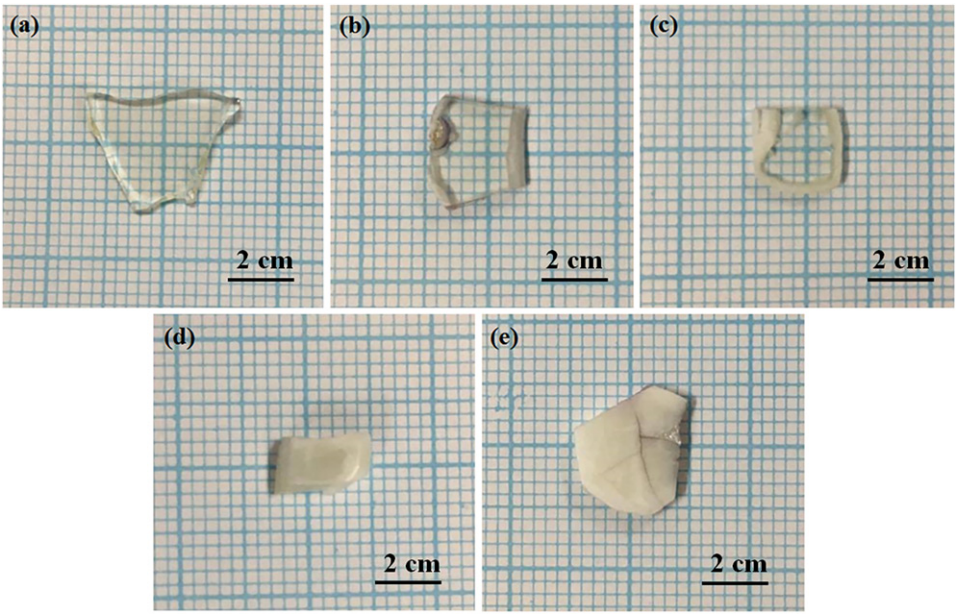

Figure 5. Physical appearance of glass and glass-ceramic samples at different heat treatment temperatures at (a) as-quenched, (b) 875 °C, (c) 890 °C, (d) 905 °C, and (e) 920 °C.

$_2+{}^4I_{11/2}$. In general, the rare earth ions are characterized by 4f electron transition which is shielded by $5s^2$ and $5p^6$ electrons while all of the transitions in absorption band of Sm^{3+} start with the ground state $^6H_{3/2}$ to different exited state. The majority of transition spectra begin with selection rule $\Delta J \leq 6$. Thus, the absorption band at 402 nm may be attributed to the surface defect in the glass-ceramic doped with Sm^{3+} phosphors. This may correspond to the oxygen to silicon (O-Si) ligand-to-metal charge transfer (LMCT) in the $Si_3{}^{2-}$group [9,10]. The overall transmittance of the glass-ceramics decreased with increasing heat treatment temperature (905 °C and 920 °C). These may be caused by the light scattering due to the occurrence of crystals in the glass-ceramic

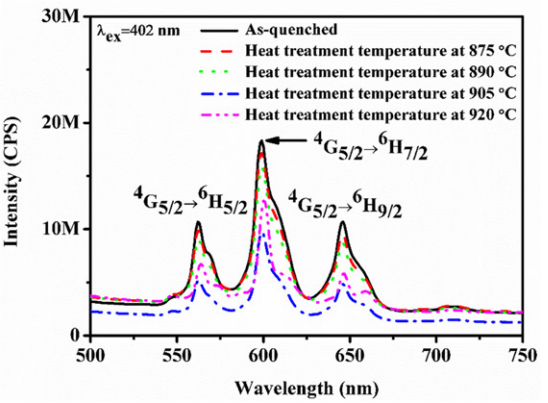

Figure 6. Emission spectra of glass and glass-ceramic samples at glass-ceramic samples of as-quenched and heat treated at 875, 890, 905 and 920 °C, respectively under 402 nm excitation.

samples with size larger than 200 nm and hence the corresponding samples should be opaque as shown in Figure 5d and e.

The luminescence of calcium magnesium silicate glass-ceramics doped with $0.5Sm^{3+}$ prepared at different heat treatment temperatures are shown in Figure 6. The red-orange emission spectra of the glass-ceramics are in the range of 500–750 nm under 402 nm excitation. There are three main emission peaks at 562, 599 and 645 nm. It may be assumed that those emission peaks are caused by f-f forbidden transition of Sm^{3+} with $4f^5$ $^4G_{5/2}\rightarrow{}^6H_{j(j\ =\ 5/2,\ 7/2,\ 9/2)}$ electron configuration of the $^4G_{5/2}\rightarrow{}^6H_{5/2}$ (562 nm), $^4G_{5/2}\rightarrow{}^6H_{7/2}$ (599 nm) and $^4G_{5/2}\rightarrow{}^6H_{9/2}$ (645 nm), respectively.

The highest emission intensity band was observed at 599 nm while that of 562 and 645 nm bands are lower. These results agree well with another report [11]. In Figure 6, it can be seen that the position of emission peaks are not affected by increasing heat treatment temperatures, because the 4f electron orbit is in the inner layer making the f-f transition. It is noticed that at 599 nm the emission intensity of all heat treated samples are nearly similar. While other emission spectra at 562 and 645 nm have different in intensity. It is observed that the varities of peak intensity. The glass-ceramic samples of the as-quenched and heated at 875 and 890 °C exhibit hight emission intensity, while glass-ceramic sample heat treated at 905 and 920 °C exhibits low emission intensity. This may be due to different in crystallite size, crystallite distribution and the fluctuation in transparency of the measured glass-ceramic samples. This is the strong proof of association between heat treatment temperatures and embedded crystalline phase as confirmed by SEM results.

The existence of Sm^{3+} ions improve the glass structure of network former due to their large ionic radius and high coordination numbers. After heat treatment, crystals were precipitated in glass matrices, and then Sm^{3+} should substitute in their lattice sites. It is assumed that phonon energy can be decreased, giving rise to the higher luminescent intensity. Comparing between the as-quenched sample and the heated sample at 875 °C in Figure 6, small decrease of emission intensity in the heated sample was observed even though this heated sample has diopside crystals for substitution of Sm^{3+} ions and the transmission spectra of these two samples are significantly similar as seen in Figure 4. This may be due to the thermal quenching process which could be either

of a phonon relaxation process or thermal ionization of the interaction between dopant ion and vibration lattice of host materials [12,13]. However, with the increase of heat treatment temperature from 890 to 920 °C the decrease in transparency of the related glass-ceramics is dominated, resulting in the decrease in their luminescent intensity.

4. Conclusions

The glass-ceramics from CaO-MgO-Al_2O_3-SiO_2-ZnO system doped with Sm^{3+} ions were successfully prepared by conventional melt-quenching method following by heat treatment process. The XRD results show that the diopside ($CaMgSi_2O_6$) and akermanite ($Ca_2MgSi_2O_7$) phase are two major crystalline phase. The transmittance spectra of glass and glass-ceramics in range of 350-1000 nm are varied with heat treatment temperature. The luminescence spectra of glass-ceramics contain three possible emission peaks of 562, 599 and 654 nm under 402 nm excitation. The strongest emission peak was found at 599 nm. The increase in heat treatment temperature has significant effect on transparency of the glass-ceramic but has little effect on the color of emission spectra.

Acknowledgement

W. Senanon would like to thank the Science Achievement Scholarship of Thailand (SAST). We would also like to thank the Thailand Research Fund (BRG5780015 and IRG5780013) for financial support.

Funding

This work was supported by the Research and Researchers for Industries-RRI, the National Research University Project under Thailand's Office of the Higher Education Commission for financial support and National Research Council of Thailand and the Faculty of Science and the Graduate School of Chiang Mai University.

References

1. Z. Luxian *et al.*, Structure and luminescence properties of Sm^{3+} doped SrO-MgO-SiO_2. *J. Wuhan Univ. Technol.-Master. Sc. Ed.* **30**, 282 (2015).
2. E. Caponetti, D. C. Martino, and M. L. Saladino, Preparation of Nd:YAG nanopowder in a confined environment. *J. Chem. Master*. **18**, 947 (2006).
3. S. C. Prahatha, B. N. Lakshminarasappa, and B. M. Nagabhushana, Photoluminescence and thermoluminescence studies of Mg_2SiO_4:Eu^{3+} nanon phosphor. *J. Alloy. Compd*. **509**, 10185 (2011). DOI: 10.1016/j.jallcom.2011.03.148.
4. T. Peijing, C. Jinshu, and Z. Gaoke, X-Ray photoelectron spectroscopy of Sm^{3+} -doped CaO-MgO-Al_2O_3-SiO_2 glasses and glass ceramics. *Appl. Surf. Sci*. **257**, 4896 (2011).
5. F. Kuei-Chih *et al.*, Zirconia nucleating agent on microstructural and electrical properties of a $CaMgSi_2O_6$diopside glass-ceramics for microwave dielectric. *Meter. Res. Bull*. **47**, 2851 (2012). DOI: 10.1016/j.materresbull.2012.04.046.
6. F. Qin, C. Chengkang, and M. Dali, Luminescent properties of $Sr_2MgSi_2O_7$ and $Ca_2MgSi_2O_7$ long lasting phosphors activated by Eu^{2+}, Dy^{3+}. *J. Alloy. Comp*. **390**, 133 (2005).

7. Y. H. Won *et al.*, Red-emitting $LiLa_2O_2BO_3:Sm^{3+}$, Eu^{3+} phosphor for near-ultraviolet light-emitting diopsides-based solid-state lighting. *J. Electrochem. Soc.* **155** (9), J226–J229 (2008).DOI: 10.1149/1.2946482.
8. C. Srinivasa Rao, and C. K. Jayasankar, Spectroscopic and radiative properties of Sm^{3+} -doped K-Mg-Al phosphate glasses. *Opt Commun.* **286**, 204 (2013). DOI: 10.1016/j.optcom.2012.08.042.
9. S. Arunkumar, and K. Marimuthu, Concentration effect of Sm^{3+} ion in B_2O_3-ZnO-PbO-PbF_2-Bi_2O_3-ZnO glasses-structural and luminescence investigation [j]. *J. Alloys. Comp.* **565**, 104 (2013). DOI: 10.1016/j.jallcom.2013.02.151.
10. G. Lakshminarayana, and S. Buddhudu, Spectral analysis of Sm^{3+} and Dy^{3+}: B_2O_3-ZnO-PbO glasses. *Physica B.* **373** (1), 100 (2006). DOI: 10.1016/j.physb.2005.11.143.
11. M. Seshadri *et al.*, Effect of ZnO on spectroscopic properties of Sm^{3+}doped zinc phosphate glasses. *Physica B.* **459**, 97 (2015).
12. A. Hussain, and K. Kontis, Thermographic phosphors for high temperature measurements: Principles, current state of the art and recent applications. *MDPI.* **8** (9), 5673 (2008). DOI: 10.3390/s8095673.
13. A. R. West, *Solid State Chemistry and its Application* (John Wiley & Son Ltd., New York 1984).

Materials Letters 249 (2019) 160–164

Contents lists available at ScienceDirect

Materials Letters

journal homepage: www.elsevier.com/locate/mlblue

Comparison between incorporation and conventional fabrication techniques of diopside-based glass-ceramics

Wipada Senanon [a,b], Ploypailin Yongsiri [c], Sukum Eitssayeam [a], Tawee Tunkasiri [a], Kamonpan Pengpat [a,d,*]

[a] Department of Physics and Materials Science, Faculty of Science, Chiang Mai University, Chiang Mai 50200, Thailand
[b] Graduate School, Chiang Mai University, Chiang Mai, 50200, Thailand
[c] Department of Applied Physics, Faculty of Science and Technology, Valaya Alongkorn Rajabhat University under Royal Patronage Pathum, Thani 13180, Thailand
[d] Research Center of Physics and Astronomy, Faculty of Science, Chiang Mai University, Chiang Mai 50200, Thailand

ARTICLE INFO

Article history:
Received 9 November 2018
Received in revised form 5 March 2019
Accepted 19 April 2019
Available online 20 April 2019

Keywords:
Crystal growth
Microstructure
Thermal analysis

ABSTRACT

Crystallization kinetics was widely used for studying nucleation and crystallization mechanism in the materials. In this study, the crystallization kinetics via non-isothermal method of diopside glass-ceramics prepared by incorporation and conventional techniques, have been investigated. The difference between incorporation and conventional method is the use of a simple mixed-oxide technique for producing diopside powder and the powder is then mixed with a glass batch while that of conventional one uses only simple oxides as starting precursors. Therefore, in this work, the diopside powder was calcined at 1200 °C for 4 h and subsequently mixed with SiO_2, Al_2O_3 and ZnO in the $30CaMgSi_2O_6$:$40SiO_2$ + $20Al_2O_3$ + 10ZnO (mol%). For, the conventional method, the simple oxide powders of $CaMgSi_2O_6$ (stoichiometric composition) were used instead of the calcined $CaMgSi_2O_6$ powders, in similar glass formula. From the heating rate dependence on crystallization temperature, the activation energy (E_a) of crystallization and Avrami parameter (n) were calculated by Kissinger and Ozawa equation, respectively. It was found that these two methods show similar crystallization mechanism but the incorporation method tends to crystallize easier than that of conventional one.

1. Introduction

Glass-ceramics are crystalline materials consisting of crystalline phase and residual glass phase. Glass-ceramics have several advantages such as chemical stability, low thermal expansion and reproducible microstructure [1]. The properties of glass-ceramics are mostly dependent on two important effects which are crystalline phase and microstructure [2]. These two effects can be improved by chemical composition [3], heat treatment and even the use of nucleating agents. Therefore, to understand the nucleation mechanism and crystal growth in materials especially glasses, consideration crystallization kinetics are the best choice to start. Crystallization kinetics parameters of a glass, consisting of the activation energy (E_a), Avrami parameter (n) and the morphology index (m) should be carefully studied in order to optimize the properties of the glass-ceramics for the relevant best use in each application.

The diopside based glass-ceramics are of interest due to their excellent responses in both mechanical and optical properties [4–6]. Many researchers have reported that the optical property of the diopside quenched glass was worse than that of diopside glass-ceramic as the order structure of the diopside crystal in the glass matrices help to increase luminesce property of these glass-ceramics [7–9]. The size of the diopside crystal is also important to the transparency of the glass-ceramics. So it is important to study crystallization mechanism and crystal growth of diopside glass-ceramics to optimize the property of these materials.

Guo et al., [10] reported that crystallization and microstructure of CaO-MgO-Al_2O_3-SiO_2 glass-ceramics containing complex nucleation agents by body crystallization process showed strip-like shape; one-dimensional crystal growth and sheet shape; three-dimensional crystal growth respectively, with irregular distribution of crystals growth occurred in their glass-ceramics. Tian et al. [11], reported that the effect of reactant on crystallization of diopside glass with $C_{12}H_{22}O_{11}$ doping was prepared by conventional method. The observed microstructure contained two-dimensional dendritic crystal growth on surface with regular arrangement.

In this study, the different methods between conventional and incorporation have investigated for first time. The crystallization kinetics parameters were defined by differential thermal analysis (DTA) under non-isothermal conditions. The crystalline phase

* Corresponding author at: Department of Physics and Materials Science, Faculty of Science, Chiang Mai University, Chiang Mai 50200, Thailand.
E-mail address: kamonpan.p@cmu.ac.th (K. Pengpat).

https://doi.org/10.1016/j.matlet.2019.04.077
0167-577X/

was identified by X-ray diffraction (XRD) and the continuous nucleation and crystal growth were recognized by scanning electron microscopy (SEM).

2. Experiment

All commercial starting powders were used for the preparation of the compositions in this study consisting of $CaCO_3$ (Sigma-Aldrich, 99% purity), MgO (Riedel-dehaen, 98–100.5% purity), Al_2O_3 (Fluka-Guarantee, 99% purity), SiO_2 (CERAC Incorporation, 99.5% purity) and ZnO (Fluka-Guarantee, 99% purity), respectively. The diopside ($CaMgSi_2O_6$) glass-ceramic from $25CaO + 20MgO + 55SiO_2$ system was prepared by incorporation method. This method was started with the preparation of $CaMgSi_2O_6$ powders. All compositions were mixed for 24 h. Then, the powders were dried for 24 h and calcined at 1200 °C for 4 h. The phase formation was analyzed by XRD. Then, the prepared $CaMgSi_2O_6$ powders were mixed with glass-forming powders in a ratio of $30CaMgSi_2O_6$: $40SiO_2 + 20Al_2O_3 + 10ZnO$ (mol%), while the conventional method used all simple oxides with $20CaO + 15MgO + 50SiO_2 + 10Al_2O_3 + 5ZnO$ (mol%) as seen in Table 1. Both techniques were mixed and melted in a platinum crucible using an electric furnace at 1500 °C for 4 h. The study of crystallization kinetics was carried out by DTA under non-isothermal conduction with various heating rates of 5, 10, 15 and 20 °C/min. The DTA data were collected using ground powder samples with the same particle size as about 77 μm. To study the mechanism of crystal growth, the obtained glasses were subjected to the heat treatment at 978 °C for 4 h, this temperature was selected by DTA results as the suitable temperature for crystals growth in glass matrices of those two methods, at various heating rates from 5 to 15 °C/min. To determine the phase formation of the prepared glass–ceramic samples, XRD was performed. The continuous nucleation and crystal growth were confirmed by SEM analysis.

3. Results and discussion

The thermal parameters of the parent glass using different heating rates of 5, 10, 15 and 20 °C/min prepared by incorporation and conventional methods are shown in Table 2. It is clearly seen that the T_p (crystallization peak temperature) increases with increasing heating rate. The glass stability ($\Delta T = T_p - T_g$) of conventional method significantly higher than that of incorporation method, implying that the conventional method provide more stable glass which has the reduced trend to form crystallization. Therefore the glass produced by incorporation method may tend to crystallize easier than that of the conventional method.

The crystallization fraction (x) as a function of temperature at the different heating rates for the conventional and incorporation methods are shown in Fig. 1(a) and (b), respectively. This result shows the beginning of crystallization process of diopside crystals starting from fraction of saturated nuclei until the final state of complete crystallization. It can be seen that the s-type curves shift to higher temperature with increasing heating rates. It can be assumed that the low heating rate has certain amount of energy and enough time to generate crystals which is in contrast to that of high heating rate.

Table 1
Chemical composition of glasses from different techniques.

Incorporation technique $30CaMgSi_2O_6$: $40SiO_2 + 20Al_2O_3 + 10ZnO$		Conventional technique $20CaO + 15MgO + 50SiO_2 + 10Al_2O_3 + 5ZnO$	
Oxide Powders	Weight (%)	Oxide Powders	Weight (%)
$CaMgSi_2O_6$	55.27	CaO	18.21
SiO_2	20.45	MgO	9.82
Al_2O_3	17.36	SiO_2	48.80
ZnO	6.92	Al_2O_3	16.56
Total	**100**	ZnO	6.61
		Total	**100**

Table 2
The T_g, T_p and ΔT of parent glasses were prepared by incorporation and conventional methods.

Method	Rate (°C/min)	T_g	T_p	ΔT
Incorporation method	5	853	912	59
	10	874	931	57
	15	890	947	57
	20	900	952	52
Conventional method	5	854	948	94
	10	859	973	114
	15	865	991	126
	20	887	1002	115

Fig. 1(c) shows a plot of $\ln[-\ln(1-x)]$ versus $\ln \alpha$ for all heating rates prepared by conventional and incorporation methods. Where x is the volume fraction of crystal and α is each heating rate. The slopes exhibit the Avrami parameter (n) values of conventional and incorporation methods which are closely similar as 3.16 and 3.04, respectively. Due to the domination about non-integer value of Avrami parameter, the n values in this study can be inferred as 3, (m = 2). It can be used to determine the crystallization mechanism in the glass-ceramics which in this case the two-dimensional crystal growth was dominated mechanism during the crystallization process of the parent glasses [11] that can be confirmed by SEM results.

The E_a was determinate by the plot of $ln\left(T_p^2/\alpha^n\right)$ versus $100/T_p$ as shown in Fig. 1(d). A linear line exhibits the right of the Kissinger method as seen in Eq. (1).

$$ln\left(T_p^2/\alpha^n\right) = mE_a/RT_p \quad (1)$$

where T_p is crystallization peak temperature for a heating rate (α), E_a is activation energy, R is gas constant (8.314 J/mol.K), n is Avrami parameter and m is crystallization mechanism. The E_a for the formation of conventional and incorporation methods are 293 and 241 kJ/mol, respectively. It clearly seen that the E_a of the incorporation method is lower than that of the glass-ceramics prepared by conventional method. It may be assumed that crystallization in the glass prepared by incorporation method is easier than that prepared by conventional method. Moreover, the E_a values of those two methods are less than that found by Wu et al. (463.81 kJ/mol) [12]. Therefore, it may be implied that the crystallization of diopside crystals on our glass system is easier than that prepared by other conventional glass-ceramics methods [13].

Fig. 2 shows the XRD patterns of glass-ceramics prepared by incorporation and conventional methods, heat treated at 978 °C for 4 h with different heating rates of 5, 10, 15 and 20 °C/min. These contained the monoclinic phase of diopside ($CaMgSi_2O_6$), as a main phase and tetragonal phase of akermanite ($Ca_2MgSi_2O_7$) as a second phase. The second phase may have been occurred from compositional fluctuation during firing. This result is similar to the result reported by Jiang et al. [14]. This compositional fluctuation may have been caused by the first approximation of multi-component system such as a ternary glass formation of SiO_2-MgO-CaO system which has been revealed that both $CaMgSi_2O_6$ and $Ca_2MgSi_2O_7$ are thermodynamic equilibrium phases. It can be clearly seen that the intensity of $2\theta = 27.60$ degree of incorporation method is more dominated than that found in conventional method. It may be assumed that an incorporation method offers the preferred orientation on (2 2 0) phase in the resulting glass-ceramics. Furthermore, it was found that the

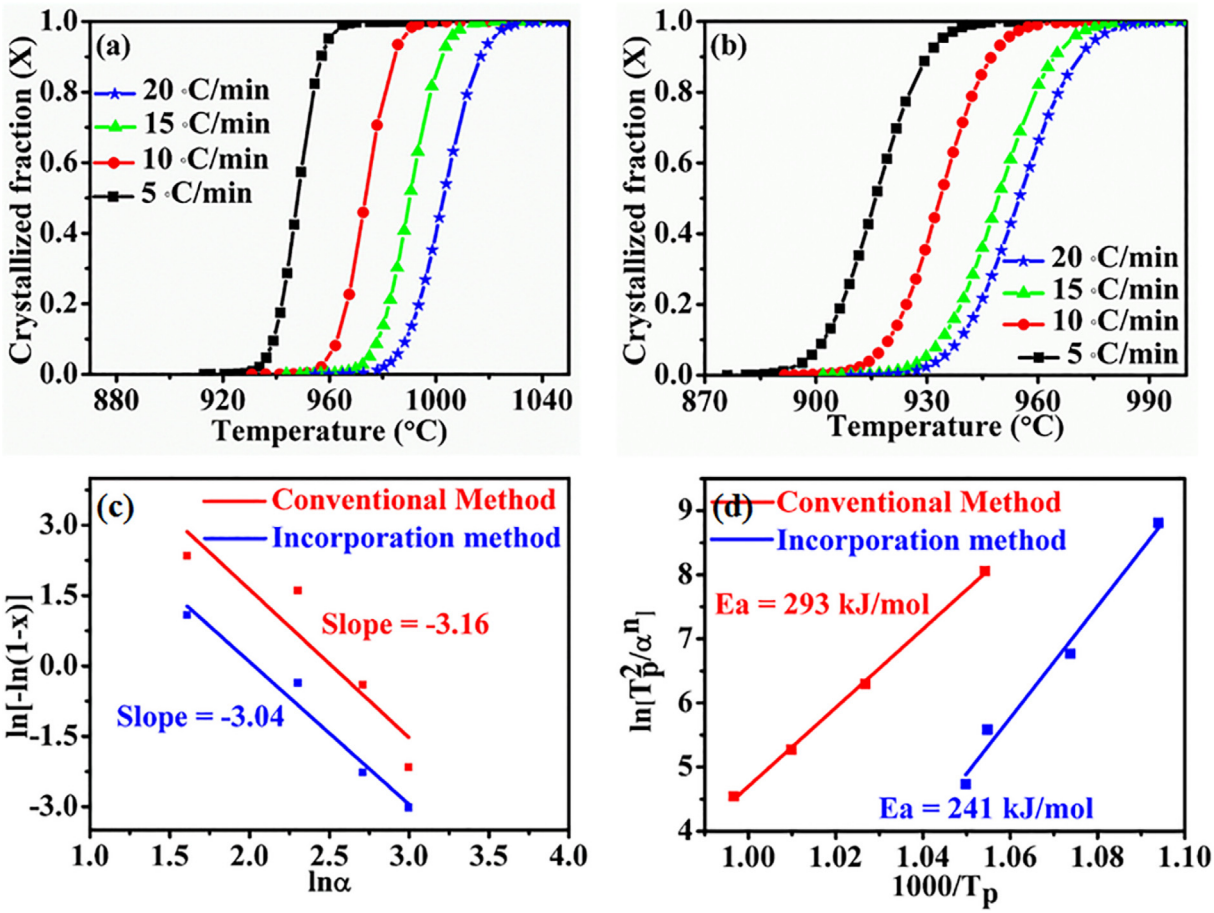

Fig. 1. Evolution of crystallization fraction (x) of diopside glasses prepared by (a) conventional, (b) incorporation method, (c) the Avrami parameter and (d) the E_a combined with the exothermic with different heating rates.

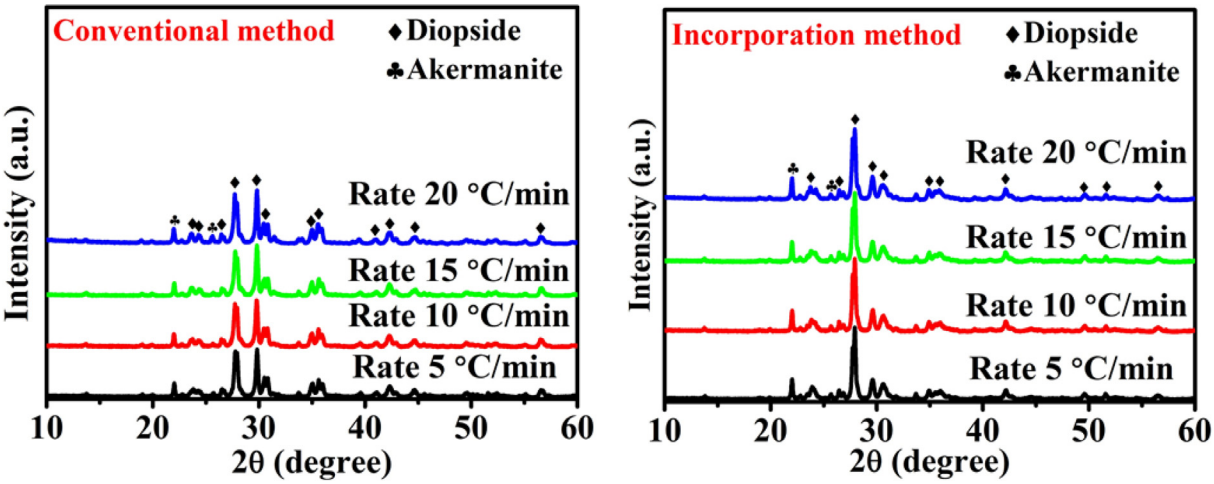

Fig. 2. XRD patterns of glass-ceramics prepared by incorporation and conventional methods, heat treated at 978 °C for 4 h with different heating rates.

increasing of heating rate was shown no effect on peak intensity and phase change. The proportions of each phase can be calculated by GSAS-II (Crystallography Data Analysis Software) with the collection codes: 9000331 ($CaMgSi_2O_6$ phase) and 4124694 ($Ca_2MgSi_2O_7$ phase). The calculated values of the weight fraction of $CaMgSi_2O_6$: $Ca_2MgSi_2O_7$ ratio, equals to 0.434:0.566 or about (2:3) for conventional method, while that of incorporation method is 0.978:0.022 or about (50:1). From this result, it may be assumed that the glass-ceramic obtained by incorporation method contains a lot higher amount of diopside crystals than that obtained by conventional one.

The SEM micrographs (Fig. 3(a-f)) show the morphology of the clearly revealed two-dimensional dendrite growth of crystals spreading in the glass matrices, however, it is difficult to distinguish between diopside and akermanite phases. Further investigation such as TEM may be needed to solve this problem.

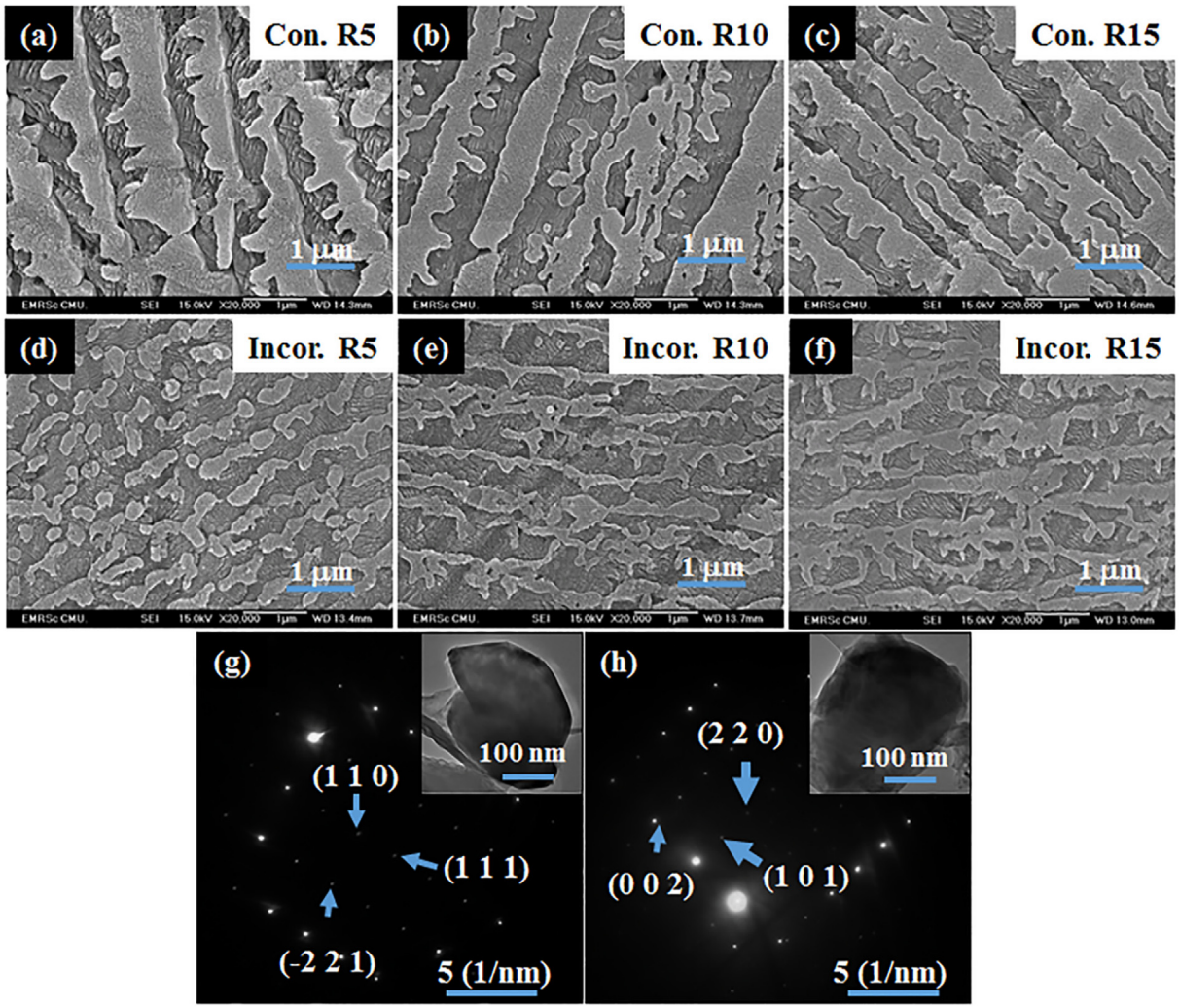

Fig. 3. (a-f). SEM images of glass-ceramics prepared by conventional and incorporation method, heat treated at 978 °C for 4 h with different heating rates and TEM images of (g) tetragonal structure and (h) monoclinic structure. (Conventional = Con., Incorporation = Incor. and Rate = R).

Nevertheless, the particle size of the crystals prepared by the incorporation method was found to be slightly smaller than that of conventional one. Moreover, it can be seen that the crystal orientation of the glass-ceramics prepared by incorporation method was more orderly in it preferred direction.

The insets are TEM micrographs of the revealed TED (transmission electron diffraction) as shown in Fig. 3(g-h). These pictures revealed the monoclinic phase of diopside ($CaMgSi_2O_6$) as seen in Fig. 3(g) and tetragonal phase of akermanite ($Ca_2MgSi_2O_7$) as seen in Fig. 3(h). These results confirmed the co-existing phases in the glass-ceramics. However, it is difficult to use this TEM result for determining between the two phases in the related SEM micrographs, as the shape and size of these two crystals are closely similar.

4. Conclusion

In this study, the crystallization kinetics via non-isothermal method of diopside glass-ceramics have been performed, in order to compare between the incorporation and conventional fabrication techniques. The Avrami parameter of the parent glass was determined as 3.16 and 3.04 for conventional and incorporation methods, respectively. This is indicated that two-dimensional crystallites morphology occurred during the crystallization process, which is well corresponded to the dendritic-growth crystals observed in the related SEM micrographs. The activation energy of conventional method is slightly higher than that of incorporation method, referring to the easier process of crystallization for that of the incorporation method. This incorporation method may be utilized in the preparation of the diopside glass-ceramics for improving their optical properties.

Acknowledgements

The authors would like to express their sincere gratitude to Faculty of Science, and the Graduate School, Chiang Mai University for financial support. Wipada Senanon also expresses her thanks to the Science Achievement Scholarship of Thailand (SAST).

Declaration of interests

The authors declare that they have no known competing financial interests or personal relationships that could have appeared to influence the work reported in this paper.

Appendix A. Supplementary data

Supplementary data to this article can be found online at https://doi.org/10.1016/j.matlet.2019.04.077.

References

[1] X. Guo, H. Yang, M. Cao, C. Han, et al., Nonferrous Met. Soc. Chaina. 16 (2006) 593–597.
[2] L.A. Zhunia, V.N. Shara, V.F. Tsitko, et al., New York, 1964.
[3] M. Kang, S. Kang, Ceram. Int. 38 (2012) S551–S555.
[4] A. Arora, E.R. Shaaban, K. Singh, et al., J. Non-Cryst. Solids 354 (2008) 3944–3951.
[5] J. Kim, S. Hwang, W. Sung, et al., J. Electroceram. 23 (2009) 209–213.
[6] A.A. Reddy, D.U. Tulyaganov, G.C. Mather, et al., J. Phys. Chem. C 119 (2015) 11482–11492.
[7] L. Zhang, F. He, J. Xie, et al., J. Wuhan Univ. Technol. Mater. Sci. Ed. 30 (2015) 282–287.
[8] M. Rezvani, V. Marghussian, B. Eftehari Yekta, Int. J. Appl. Ceram. Technol. 8 (2011) 152–162.
[9] L. Jiang, C. Chang, D. Mao, et al., J. Alloys. Compd. 377 (2004) 211–215.
[10] X. Guo, X. Cai, J. Song, G. Yang, H. Yang, J. Non-Cryst. Solids 405 (2014) 63–67.
[11] P. Tian, J. Cheng, W. Zheng, et al., Thermochim. Acta 494 (2009) 30.
[12] J. Wu, Z. Li, Y. Huang, et al., Ceram. Int. 39 (2003) 7743–7750.
[13] M.M. Kržmanc, U. Došler, D. Suvorov, et al., J. Am. Ceram. Soc. 95 (2012) 1920–1926.
[14] L. Jiang, Ch. Chang, D. Mao, J. Alloy. Comp. 360 (2003) 193–197.